PB85-152973

Particulate Emissions and Control in Fluidized-Bed Combustion Modeling and Parametric Performance

Westinghouse Research and Development Center
Pittsburgh, PA

Prepared for

Environmental Protection Agency
Research Triangle Park, NC

Jan 85

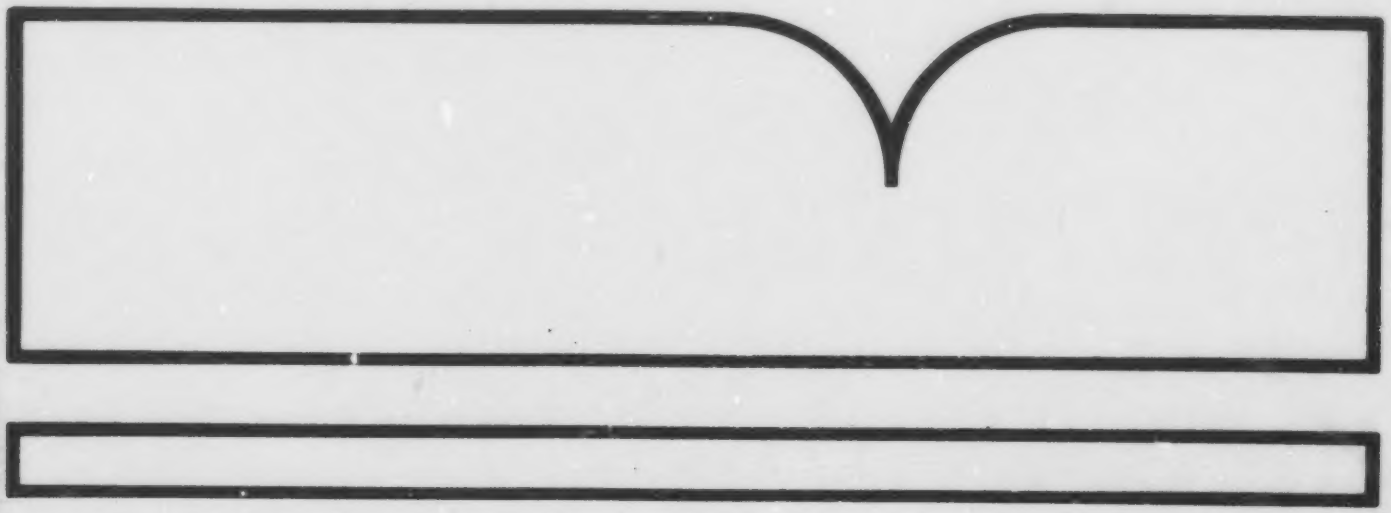

U.S. Department of Commerce
National Technical Information Service
NTIS

PB85-152973

EPA/600/7-85/002
January 1985

PARTICULATE EMISSIONS AND CONTROL IN FLUIDIZED-BED COMBUSTION: MODELING AND PARAMETRIC PERFORMANCE

by

A. Y. Ranadive, R. A. Newby, D. F. Ciliberti
Westinghouse Research & Development Center
1310 Beulah Road
Pittsburgh, PA 15235

Contract No. 68-02-3110

EPA Project Officer: John O. Milliken
Air and Energy Engineering Research Laboratory
Office of Environmental Engineering and Technology
Research Triangle Park, NC 27711

AIR AND ENERGY ENGINEERING RESEARCH LABORATORY
OFFICE OF RESEARCH AND DEVELOPMENT
U.S. ENVIRONMENTAL PROTECTION AGENCY
RESEARCH TRIANGLE PARK, NC 27711

REPRODUCED BY
NATIONAL TECHNICAL
INFORMATION SERVICE
U.S. DEPARTMENT OF COMMERCE
SPRINGFIELD, VA. 22161

TECHNICAL REPORT DATA
(Please read Instructions on the reverse before completing)

1. REPORT NO.	2.	3. RECIPIENT'S ACCESSION NO.
EPA/600/7-85/002		PB85 152973/AS

4. TITLE AND SUBTITLE	5. REPORT DATE
Particulate Emissions and Control in Fluidized-Bed Combustion: Modeling and Parametric Performance	January 1985
	6. PERFORMING ORGANIZATION CODE
7. AUTHOR(S)	8. PERFORMING ORGANIZATION REPORT NO.
A. Y. Ranadive, R. A. Newby, and D. F. Ciliberti	
9. PERFORMING ORGANIZATION NAME AND ADDRESS	10. PROGRAM ELEMENT NO.
Westinghouse Research and Development Center 1310 Beulah Road Pittsburgh, Pennsylvania 15235	11. CONTRACT/GRANT NO. 68-02-3110
12. SPONSORING AGENCY NAME AND ADDRESS	13. TYPE OF REPORT AND PERIOD COVERED
EPA, Office of Research and Development Air and Energy Engineering Research Laboratory Research Triangle Park, NC 27711	Final; 14. SPONSORING AGENCY CODE EPA/600/13

15. SUPPLEMENTARY NOTES IERL-RTP project officer is John O. Milliken, Mail Drop 61; 919/541-7716.

16. ABSTRACT The report discusses a model, developed to describe the physical characteristics of the particulates emitted from fluidized-bed combustion (FBC) systems and to evaluate data on FBC particulate control systems. The model, which describes the particulate emissions profile from FBC, considers the attrition of the bed material and the recycling of the elutriated fines in addition to other FBC phenomena. For a given combustor design and set of operating conditions, the particle profile program projects the mass rate and size distribution of the solids in the bed draw-off and carry-over streams, as well as those emitted from particle removal devices of any given configuration. Examples of particulate emission and control are given for both atmospheric-pressure and pressurized FBC systems. The effect of calcium-to-sulfur ratio, rate of sorbent attrition, superficial gas velocity, and recycle cyclone efficiency was examined by using the model. A manual for the particle profiles program comprising a quick-reference user's section, as well as a more detailed descriptive section, is provided in the full report.

17. KEY WORDS AND DOCUMENT ANALYSIS

a. DESCRIPTORS	b. IDENTIFIERS/OPEN ENDED TERMS	c. COSATI Field/Group
Pollution Particles Dust Fluidized Bed Processing Combustion Mathematical Models Physical Properties Coal	Pollution Control Stationary Sources	13B 14G 11G 21D 13H, 07A 21B 12A

18. DISTRIBUTION STATEMENT	19. SECURITY CLASS (This Report)	21. NO. OF PAGES
Release to Public	Unclassified	147
	20. SECURITY CLASS (This page)	22. PRICE
	Unclassified	

EPA Form 2220-1 (9-73)

NOTICE

This document has been reviewed in accordance with U.S. Environmental Protection Agency policy and approved for publication. Mention of trade names or commercial products does not constitute endorsement or recommendation for use.

ABSTRACT

The work described in this report was performed by the Westinghouse Electric Corporation R&D Center for the United States Environmental Protection Agency in order to develop a modeling tool to enhance the understanding of the physical characteristics of the particulates emitted from fluidized-bed combustion (FBC) systems and to assess FBC particulate control systems.

A particle profile model incorporating the fluidized-bed combustor and particle control subsystems has been developed. The model considers the attrition of the bed material and the recycling of the elutriated fines in addition to other FBC phenomena. For a given combustor design and set of operating conditions, the particle profile program will project the mass rate and size distribution of the solids in the bed draw-off and carry-over streams as well as those emitted from any given configuration of particle removal devices.

The particle profile program is illustrated by some preliminary assessments of particulate emission and control for atmospheric pressure fluidized-bed combustion (AFBC) and pressurized fluidized-bed combustion (PFBC) systems. The results of parametric studies with respect to calcium-to-sulfur ratio, rate of sorbent attrition, superficial gas velocity, and recycle cyclone efficiency are described. A manual for the particle profile program comprising a quick-reference users' section, as well as a more detailed descriptive section, is provided.

TABLE OF CONTENTS

	Page
ABSTRACT	iii
SUMMARY	xiii
1. INTRODUCTION	1
2. CONCLUSIONS AND RECOMMENDATIONS	4
3. THE PARTICLE PROFILE MODEL	6
The Carry-over Model-Development for a One-Species System	6
Extension to a Two-Species System	10
Particle Removal Equipment Simulation	14
Illustrative Problem	16
4. EVALUATION OF PARTICULATE EMISSIONS FROM FBC SYSTEMS	25
Projected Emissions and Particulate Control Device Performance for PFBC	25
Design and Operating Conditions and Feed Materials	25
Sensitivity to Calcium-to-Sulfur Ratio	30
Performance of Particle Removal Devices	36
New Source Performance Standards (NSPS) and Turbine Protection Requirements	43
Projected Emissions and Particulate Control Device Performance for AFBC	44
Design and Operating Conditions and Feed Materials	44
Sensitivity to Calcium-to-Sulfur Ratio	45

Preceding page blank

TABLE OF CONTENTS (Continued)

	Page
Performance of Particle Removal Devices	51
Compliance with New Source Performance Standards (NSPS)	52
5. PARAMETRIC STUDIES	57
Recycle Cyclone	57
Superficial Velocity	59
Attrition Rate	68
6. REFERENCES	72
APPENDIX A	73
APPENDIX B	89

LIST OF TABLES

		Page
1.	Example Problem Results	20
2.	PFBC Combustor Operating and Design Conditions Selected for Study	25
3.	Composition of a Deep-Mined Illinois Coal	26
4.	Composition of a Plum Run Dolomite	26
5.	Sorbent Feed and Attrition Rates Corresponding to Various Calcium-to-Sulfur Ratios	30
6.	PFBC Particulate Emission Projections for a Calcium-to-Sulfur Ratio of 1	31
7.	PFBC Particulate Emission Projections for a Calcium-to-Sulfur Ratio of 2	32
8.	PFBC Particulate Emission Projections for a Calcium-to-Sulfur Ratio of 3	33
9.	PFBC Particulate Emission Projections for a Calcium-to-Sulfur Ratio of 4	34
10.	PFBC Particulate Emission Projections for a Calcium-to-Sulfur Ratio of 5	38
11.	AFBC Combustor Operating and Design Conditions Selected for Study	45
12.	Sorbent Feed and Attrition Rates Corresponding to Various Calcium-to-Sulfur Ratios	46
13.	AFBC Particulate Emission Projections for a Calcium-to-Sulfur Ratio of 2	48
14.	AFBC Particulate Emission Projections for a Calcium-to-Sulfur Ratio of 3	49

LIST OF TABLES (Continued)

		Page
15.	AFBC Particulate Emission Projections for Calcium-to-Sulfur Ratio of 4	50
16.	AFBC Particulate Emission Projections for a Calcium-to-Sulfur Ratio of 5.	51
17.	Parameters Input to the Program for the Base Case	58
18.	Base Case Results	58
19.	Results with Different Recycle Cyclones	63
20.	Results with Different Superficial Velocities	66
21.	Results with Different Rates of Sorbent Attrition	71

LIST OF FIGURES

		Page
1.	Fluidized-Bed Combustion Processes Applications Perspective	2
2.	Schematic of Solids Flow System	8
3.	Schematic of Two-Species Solids Flow System	8
4.	Flow Schematic for Illustrative Example	17
5.	Size Distributions of Feed and Attrited Material	18
6.	Grade Efficiency Curves for Ducon High-Efficiency Cyclone	19
7.	Theoretical Size Distribution Profiles for Sorbent	21
8.	Theoretical Size Distribution Profiles for Ash	22
9.	Comparison of Theoretically Predicted and Experimentally Reported Size Distribution Profiles	23
10.	Calculated and Assumed Ash Size Distributions	24
11.	Size Distributions for Feed and Attrited Sorbent and Generated and Attrited Ash	27
12.	Flow Scheme Assumed for PFBC System	28
13.	Grade Efficiency Curves for Ducon High-Efficiency Cyclone	29
14.	Grade Efficiency for Granular-Bed Filter	29
15.	Increase in Solids Grain Loading with Calcium-to-Sulfur Ratio	36
16.	Size Distributions and Loadings for a Calcium-to-Sulfur Ratio of 1	37
17.	Size Distributions and Loadings for a Calcium-to Sulfur Ratio of 5	38

LIST OF FIGURES (Continued)

		Page
18.	Flow Scheme for Parametric Studies	39
19.	Size Distributions and Loadings at Various Points of the PFBC System for a Calcium-to-Sulfur Ratio of 2	40
20.	Grade Efficiency Curve for Sunbury Fabric Filter	41
21.	Results of Using Different Final (PFBC) Stage Devices	42
22.	Summary of Woven Ceramic-Bag Filter Test Results at Air-to-Cloth Ratio of 1.7 m/min (5.6 ft/min)	43
23.	Flow Scheme Assumed for AFBC System	46
24.	Increase in Solids Grain Loading with Calcium-Sulfur Ratio	52
25.	Size Distributions and Loadings for a Calcium-to-Sulfur Ratio of 2 (AFBC)	52
26.	Size Distributions and Loadings for a Calcium-to-Sulfur Ratio of 5 (AFBC)	54
27.	Grade Efficiency for a Cold-Side Electrostatic Precipitator	55
28.	Results of Using Different Final-Stage Cleaning Devices	56
29.	Flow Scheme for Parametric Studies	59
30.	Typical Feed and Attrited Size Distributions	60
31.	Grade Efficiencies of Recycle Cyclone	61
32.	Base Case Results	62
33.	Results without Fines Recycle	64
34.	Results with a More Efficient Recycle Cyclone	65
35.	Results Using a Velocity Reduced by 50% over Base Case	67
36.	Increase in Recycle Rate with Gas Velocity	69
37.	Results with a Tenfold Reduction in Sorbent Attrition Rate	70

NOMENCLATURE

A = rate constant in expression for shrinkage of solid particles, sec^{-1}

A_2 = mass flow rate of attrited solids, g/s

$A_{2,i}$ = mass flow rate of attrited solids of i^{th} species of a two-species system, g/s

D = physical diameter of solids, μm (see *)

D_m = smallest solids diameter, μm

D_M = largest solids diameter, μm

F_o = mass flow of solids in feed, g/s

$F_{o,i}$ = mass flow of solids of i^{th} species in feed, g/s

F_1 = mass flow of solids in draw-off, g/s

$F_{1,i}$ = mass flow of i^{th} component in draw-off, g/s

F_2 = mass flow of solids in carry-over, g/s

$F_{2,i}$ = mass flow of i^{th} component in the carry-over

k = rate constant in expression for shrinkage of solid particles, sec^{-1}

K = elutriation constant, sec^{-1}

m = mass of an individual solids particle, G

p_a = population density function of attrited solids, cm^{-1}

$p_{a,i}$ = population density function for the attrited solids of the i^{th} species, cm^{-1}

p_b = population density function of bed solids, cm^{-1}

$p_{b,i}$ = population density function of the bed solids of the i^{th} species, cm^{-1}

p_o = population density function of feed solids, cm^{-1}

$p_{o,i}$ = population density function of feed solids of the i^{th} species, cm^{-1}

p_1 = population density function of draw-off solids, cm^{-1}

* D is the particle size used in graphical presentation of results

$p_{1,i}$ = population density function of draw-off solids of the i^{th} species, cm^{-1}

p_2 = population density function of carry-over solids, cm^{-1}

$p_{2,i}$ = population density function of the carry-over solids of the i_{th} species, cm^{-1}

$R = \frac{dD}{dt}$ = rate of shrinkage (attrition) of a solid particle of size D, cm/s

t = time, s

U_o = superficial velocity, cm/s

W = total mass of solids in bed, g

Z = cumulative size distribution function

Z_c = cumulative size distribution of the combined $(A_2 + F_2)$ stream

$Z_{c,i}$ = cumulative size distribution of the combined $(A_2 + F_2)$ stream for the i^{th} species

Δ = difference

$\eta(D)$ = grade efficiency of particle removal device

ρ_s = solid density, g/cm^3

ε = bed porosity

Σ = summation

AFBC = atmospheric pressure fluidized-bed combustion

CURL = Coal Utilization Research Laboratory

NCB = National Coal Board

PFBC = pressurized fluidized-bed combustion

SUMMARY

The particulate control problem as it relates to fluidized-bed combustion (FBC) is threefold. First, the particle emission characteristics of fluidized-bed combustors need to be determined. Secondly, acceptable levels of particle loadings and size distributions, from the standpoint both of environmental constraints and, for PFBC, of the requirements for reliable gas turbine operation, need to be established. Finally, an appropriate train of particulate control devices needs to be identified for reducing the particle emissions to levels deemed acceptable.

The present work addresses two of the aforementioned areas of concern. A particle profile model incorporating the fluidized-bed combustor and particulate control subsystems has been developed that permits rational and consistent projections of solid sizes and loadings from the fluidized-bed combustor and throughout the FBC system. The model considers particle attrition and the recycling of elutriated fines, in addition to other FBC phenomena, and is able to simulate any desired configuration of gas cleaning equipment.

The particle profile model is illustrated by some initial perspective on particle emission and control for atmospheric pressure (AFBC) and pressurized fluidized-bed combustion (PFBC) systems. The results of parametric studies with respect to calcium-to-sulfur (Ca/S) ratio, rate of sorbent attrition, superficial gas velocity, and recycle cyclone efficiency are described.

Commercial final-stage particulate control devices (i.e., fabric filter and electrostatic precipitators) are available that will perform satisfactorily to meet environmental standards with AFBC. Some technical problems remain to be dealt with for both fabric filters and electrostatic precipitators. Staged cyclones will be insufficient for meeting environmental standards, except in cases of unusual coals and sorbents.

A host of technical and economic considerations can result in either the environmental standards or the turbine protection requirements being the most stringent and controlling in the selection and design of the particulate control system with PFBC. Final-stage particulate control devices are being developed for this application, but their performance and economic feasibility are not yet established.

The particle profile model developed represents a highly useful tool for the evaluation of FBC design and operating conditions relating to particulate emissions from the combustor. Particulate control devices and systems integrated with fluidized-bed combustors can be assessed for their ability to satisfy environmental standards and/or gas turbine protection requirements. Particle attrition (sorbent and ash) represents the greatest uncertainty in the model. We recommend that:

- Further studies be conducted to develop increased understanding of attrition and elutriation
- The model projections be compared with available plant data to establish their validity and to identify and characterize controlling phenomena.

1. INTRODUCTION

The fluidized-bed combustion (FBC) of coal offers the potential for a thermally more efficient, environmentally superior, and more economical way to utilize coal resources for the generation of electric power and the production of industrial steam than do conventional methods for coal utilization.

Many different FBC concepts have been proposed having significantly different emission behavior and control requirements. Characterized by the technique selected for controlling the bed temperature, these various concepts fall into three general classes:

- Excess air: Adiabatic combustors use excess air to generate heat and control temperature.
- Heat transfer surface: In-bed surfaces use water/steam, air, or process fluids to remove heat.
- Circulating solids: Recirculating solids remove heat to control temperature.

Fluidized-bed combustion concepts based on each of these techniques can be used for atmospheric (AFBC) or pressurized (PFBC) operation and for industrial or utility applications. Figure 1 illustrates how these areas interrelate.

The conventional FBC boiler concept integrates coal combustion, sulfur control, and temperature control in a single component. In both AFBC and PFBC boilers, coal and sulfur sorbent (limestone or dolomite) are fed into a fluidized-bed reactor, where the combustion of coal occurs, accompanied by the release of heat, ash, and sulfur as sulfur oxides. The sorbent in the bed reacts with the sulfur to form a solid product, thereby reducing the release of the sulfur pollutant to the atmosphere. Most of the ash,

Dwg. 1697845

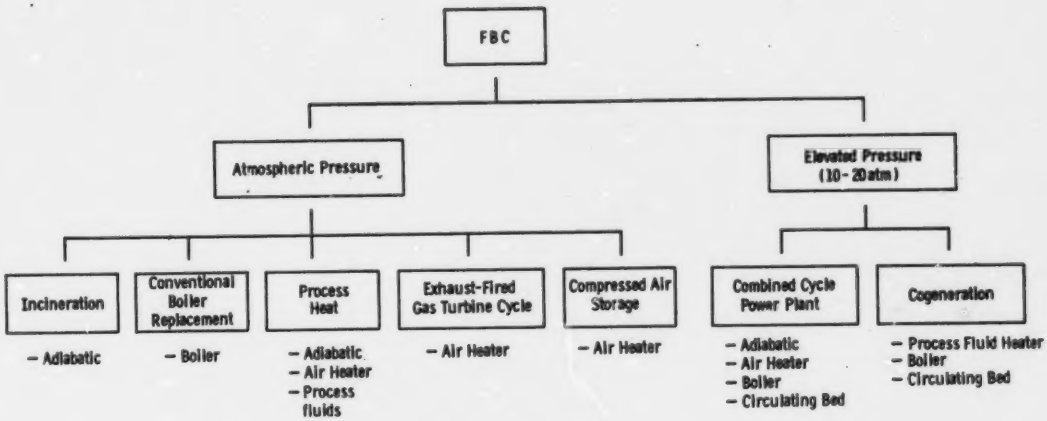

Figure 1 - Fluidized-Bed Combustion Processes Applications Perspective

together with some sorbent and char, is carried overhead and out of the reactor with the off-gas. The bulk of these particulate emissions may be captured in a cyclone and recycled to the bed in order to achieve higher carbon and sorbent utilization if desired. Heat is extracted from the reactor by immersing heat transfer surface in the bed to generate steam. For industrial applications the steam so generated finds use as process heat or as process feedstock. For utility applications the steam is expanded through a steam turbine for power generation. Additionally, in the case of PFBC for utility applications, the hot, pressurized gas from the reactor is cleaned of particulate matter by passing it through a train of particle removal devices and then expanding it through a gas turbine for power generation.

Environmental regulations impose constraints on the particulate that can be emitted to the atmosphere. Particle emissions from PFBC processes utilizing gas turbine expanders for power generation must also conform to particulate levels deemed to be acceptable for reliable turbine operation. Particulate control is, therefore, a vital aspect of FBC technology.

The particulate control problem associated with FBC processes is threefold. First, the characteristics of the particle emissions from fluidized-bed combustors need to be determined. Secondly, acceptable levels of particulate loadings and size distributions from the standpoint of both environmental constraints and, for PFBC, gas turbine protection requirements need to be established. Finally, an appropriate configuration of particle removal devices for reducing the level of particle emissions to those deemed acceptable needs to be identified.

The work described in this report addresses the first and third of the aforementioned areas of concern. A particle profile model and computer program incorporating the fluidized-bed combustor and particulate control subsystems have been developed. The model considers the attrition of the bed material and the recycle of elutriated fines, in addition to other FBC phenomena, and can simulate the performance of any given configuration of particle removal device. For a given combustor design and set of operating conditions, the particle profile program can project the mass rate and size distribution of the solids in the bed draw-off and carry-over, as well as those emitted subsequently from any given particle removal device(s).

The particle profile program is illustrated by providing some initial perspective on particle emission and control for AFBC and PFBC systems. The results of parametric studies with respect to calcium-to-sulfur (Ca/S) ratio, rate of sorbent attrition, superficial gas velocity, and recycle cyclone efficiency are described. Finally, a manual for the particle profile program comprising a quick-reference users' section, as well as a more detailed descriptive section, is provided.

2. CONCLUSIONS AND RECOMMENDATIONS

The particle profile model developed represents a highly useful tool for evaluating FBC design and operating conditions that relate to particulate emissions from the combustor. Particulate control devices and systems integrated with fluidized-bed combustors can be assessed for their ability to satisfy environmental standards and/or gas-turbine protection requirements. Particle attrition (sorbent and ash) represents the greatest uncertainty in the model. We recommend that:

- Further studies be conducted to develop increased understanding of attrition and elutriation
- The model projections be compared with available plant data to establish their validity and to identify and characterize controlling phenomena.

The application of the particle program to particle emission and control for AFBC and PFBC systems, with parametrically conducted studies on Ca/S ratio, rate of sorbent attrition, superficial gas velocity, and recycle cyclone efficiency, result in the following conclusions:

- The final particulate control device is of primary importance, since this filter stage determines the particle size distribution and loading released to the environment or presented to the turbine
- FBC design and operating conditions (and resulting Ca/S ratio) have little effect on the size distribution of particles emitted for the final-stage control devices examined here.
- The selection of coal and sorbent and the FBC design will significantly affect the particle loading to the environment or to the turbine for a given final-stage device performance. The coal-ash particle size distribution, the sorbent attrition

rate, and the attrited sorbent particle size distribution are important performance factors.

- The design of the FBC to minimize sorbent consumption (Ca/S) and particle attrition is important for minimizing the quantity of particles emitted to the environment or turbine.
- The recycle cyclone performance strongly influences the rate of solids recycling. The use of a high-efficiency recycle cyclone results in high solid recycle rates while leaving the particulate emission from the final cleaning device unaffected. The relation between recycle rate and FBC combustion and sulfur removal performance is not generally predictable. To minimize the recycled solids handling requirement and minimize the erosion of convective heat transfer surface above the bed, a medium-efficiency, rather than a high-efficiency, recycle cyclone should be used.
- For AFBC, commercial final-stage particulate control devices (i.e., fabric filters and electrostatic precipitators) are available that will satisfactorily perform to meet environmental standards. Some technical problems remain to be dealt with for both fabric filters and electrostatic precipitators. Staged cyclones will be insufficient for meeting environmental standards, except in cases of unusual coals and sorbents.
- For PFBC, a host of technical and economic considerations can result in either the environmental standards or the turbine protection requirements being the most stringent and controlling the selection and design of the particulate control system. Final-stage particulate control devices are being developed for this application, but their performance and economic feasibility are not yet established.

3. THE PARTICLE PROFILE MODEL

BACKGROUND

The particle profile model is comprised of two subsystems. In the first subsystem, called the carry-over model, Kunii and Levenspiel's general development[1] for the solids balance in a back-mixed, fluidized-bed reactor with continuous solid feed, overflow, and elutriation is incorporated into a scheme for two species, e.g., sorbent and coal ash. The second subsystem models and synthesizes the performance of any given configuration of particle removal devices. Thus, the carry-over estimates for each species from the first subsystem can be entered into the second subsystem to obtain the corresponding solid loadings and particle size distributions throughout the FBC system. This section reviews the derivation of the main equations of the particle profile model.

THE CARRY-OVER MODEL - DEVELOPMENT FOR A ONE-SPECIES SYSTEM

The model employed to describe particle carry-over from the bed (Figure 2) is based on a mass balance of particles in a certain size range. The method used to estimate the rate at which particles are carried out of the bed requires that a correlation for the elutriation rate constant be available. We define this elutriation rate constant by asserting that the mass of particles of size D in the overhead is proportional to the mass of particles of size D in the bed, or that

$$K(D) = \frac{F_2 P_2(D)}{W p_b(D)} \quad . \qquad (1)\ *$$

Many such correlations are available in the literature,[2,3] but none appears to be applicable to all systems.

The model treats attrition as if the surface of the large particles were gradually abraded away so that the large particle slowly shrinks in

* Terms in equation (1) are defined on page 11.

size according to some rate expression of the general form:

$$\frac{dD}{dt} = R(D) \quad . \tag{2}$$

The fines ground from the large particle are considered to pass out of the system as if in the gas phase. The mass of these particles can be calculated, but their size distribution must be assumed and they are not included in the recycle stream.

The general performance equation arises from a mass balance on particles sized between D and D + ΔD. In unit time,

$$\begin{pmatrix}\text{Solids entering}\\ \text{in feed}\end{pmatrix} - \begin{pmatrix}\text{Solids leaving}\\ \text{in overflow}\end{pmatrix} - \begin{pmatrix}\text{Solids leaving}\\ \text{in carry-over}\end{pmatrix} +$$

$$\begin{pmatrix}\text{Solids growing}\\ \text{into interval}\\ \text{from larger size}\end{pmatrix} - \begin{pmatrix}\text{Solids growing}\\ \text{out of interval}\\ \text{to smaller size}\end{pmatrix} - \begin{pmatrix}\text{loss of mass}\\ \text{due to shrinking}\\ \text{within interval}\end{pmatrix} = 0 \ , \tag{3}$$

or

$$\int_D^{D+\Delta D} F_o p_o dD - \int_D^{D+\Delta D} F_1 p_1 dD - \int_D^{D+\Delta D} F_2 p_2 dD + \left(W p_b R\right)_{D+\Delta D}$$

$$- \left(W p_b R\right)_D - \int_D^{D+\Delta D} \frac{3\, W p_b R dD}{D} = 0 \quad . \tag{4}$$

If we divide by ΔD and take limits as ΔD → 0, using equation (1) and assuming back-mix flow, i.e., $p_1 = p_b$, we obtain the following differential equation:

$$F_o p_o - F_1 p_1 - W K p_1 + W \frac{d(p_1 R)}{dD} - \frac{3\, W P_1 R}{D} = 0 \quad . \tag{5}$$

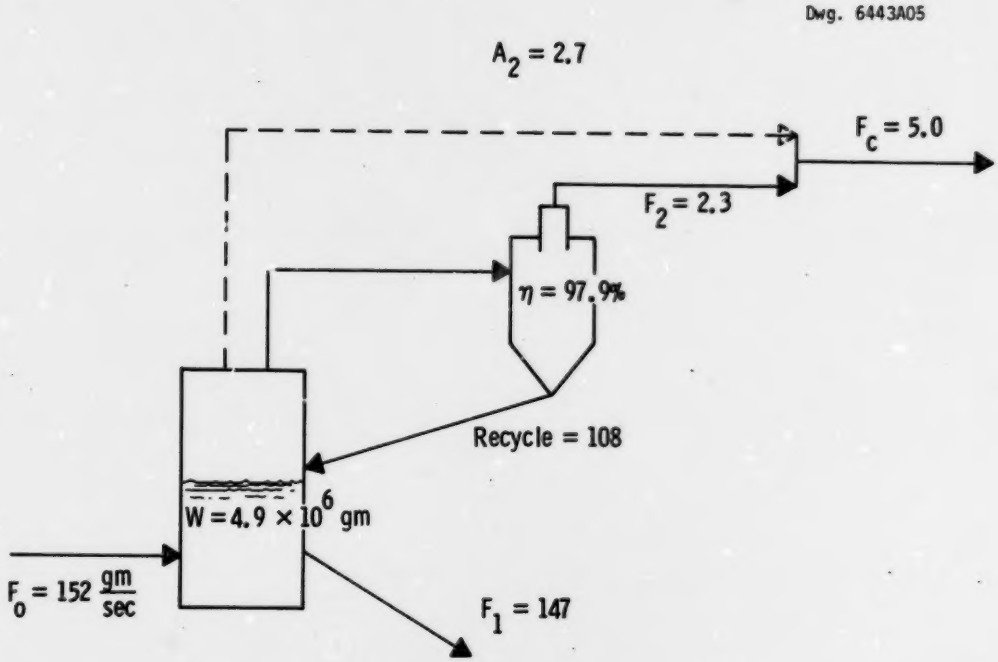

Figure 2 - Schematic of Solids Flow System

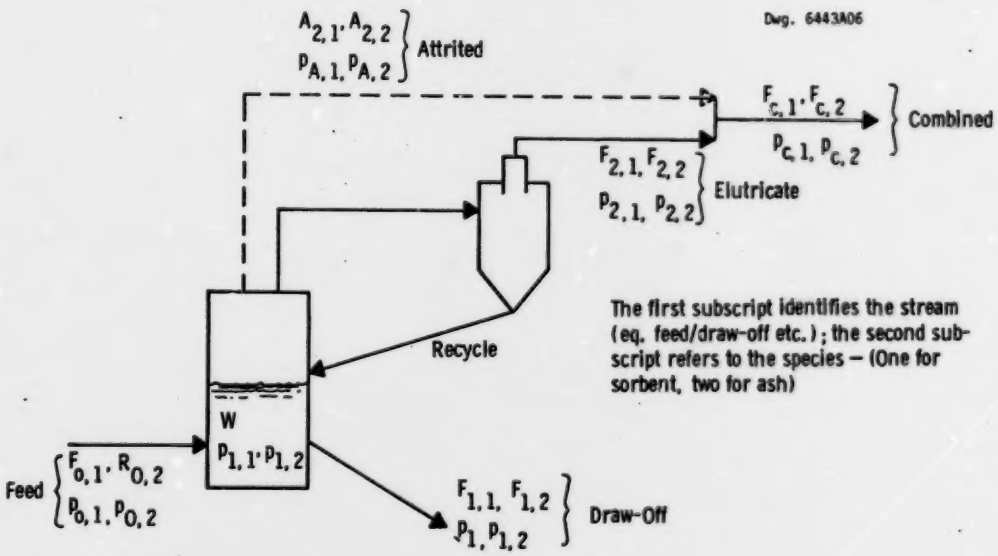

Figure 3 - Schematic of Two-Species Solids Flow System

Further manipulation of this basic balance leads to the general performance equation of the model, which is given as:

$$\frac{W}{F_o} = \int_{D_m}^{D_M} \frac{\hat{D}^3 I(\hat{D},D_M)}{|R(\hat{D})|} \int_{D=\hat{D}}^{D=D_M} \frac{p_o(D)dD}{D^3 I(D,D_M)} d\hat{D} \quad , \tag{6}$$

where the $I(D,D_M)$ term is defined as

$$I(D,D_M) = \exp\left[- \int_{D_M}^{D} \frac{\frac{F_1}{W} + K}{R} dD \right] . \tag{7}$$

The final form of the performance equation is that of the triple integral expressed in equation (6). To include the effect of a cyclone recycling coarse material to the bed, one needs only to modify the elutriation rate constant, K, by multiplying it by the cyclone penetration (1-efficiency) so that the K term of equation (7) is replaced by $k(1-\eta)$. With a recycle cyclone the $I(D,D_M)$ term is, therefore, defined as

$$I(D,D_M) = \exp\left[- \int_{D_M}^{D} \frac{\frac{F_1}{W} + K(1-\eta)}{R} dD \right] . \tag{8}$$

Use of equations (6) and (7) (or equations (6) and (8)) requires an iterative procedure, since usually F_o and W are specified but F is not. The solution algorithm proceeds as follows:

1. For given F_o and W, pick F_1.
2. Calculate the triple integral of equation (6).
3. Compare the result with W/F_o; if not sufficiently close, update the F_1 value and iterate.

4. Once convergence to F_1 is achieved, p_1 can be calculated from the expression:

$$p_1(D) = \frac{F_o D^3 I(D,D_M)}{W|R|} \int_D^{D_M} \frac{p_o(\hat{D})d\hat{D}}{\hat{D}^3 I(\hat{D},D_M)} \quad . \tag{9}$$

5. Knowing p_1, one can calculate F_2 as follows:

$$\int_{D_m}^{D_M} F_2 p_2 dD = F_2 = \int_{D_m}^{D_M} WK(1-\eta)p_1 dD \quad . \tag{10}$$

6. The size distribution of F_2 can be obtained directly from the elutriation rate expression:

$$p_2 = (W/F_2)K(1-\eta)p_1 \quad . \tag{11}$$

7. The mass of the attrited material A_2 can be calculated by integration of the rate equation over the bed size distribution or, more simply, by an overall mass balance:

$$A_2 = F_o - F_1 - F_2 \quad . \tag{12}$$

The loading presented to the particulate removal train is obtained as the sum of the A_2 and F_2. The size distribution of F_2 is known, but the size distribution of A_2 (p_A) must be assumed. The cumulative size distribution of the combined stream is then obtained as:

$$Z_C(D) = \int_{D_m}^{D} \frac{F_2 p_2 + A_2 p_A}{F_2 + A_2} dD \quad . \tag{13}$$

EXTENSION TO A TWO-SPECIES SYSTEM

Thus far our development has pertained to a single-species (e.g., sorbent only) system. To include the effects of a second component, we shall assume that the single-component solid balances, as presented above,

hold for each of the two individual species, and the coupling for the two-species extension occurs in the elutriation from the bed surface. This effect is presumed to manifest itself by reducing the elutriation rate of each species in proportion to its mass fraction in the bed. Recall that the elutriation rate constant is given by

$$K(D) = \frac{F_2 p_2(D)}{W p_b(D)} \quad , \tag{1}$$

where

$K(D)$ = elutriation rate constant

F_2 = mass rate of elutriate

$p_2(D)$ = population density function for elutriate

$p_b(D)$ = population density function for bed (or equivalently the draw-off) material

W = weight of bed.

Let

α_1 = mass fraction of species one in the bed

α_2 = mass fraction of species two in the bed.

Then, the weight of species one in the bed = $\alpha_1 W$, (14)

and the weight of species two in the bed = $\alpha_2 W$.

The modified elutriation rate constant for species one of a two-species system is therefore given by:

$$K_1(D) = \frac{F_{2,1} p_{2,1}(D)}{\alpha_1 W p_{b,1}(D)} \quad , \tag{15A}$$

where

$K_1(D)$ = elutriation rate constant for species one of a two-species system

$F_{2,1}$ = mass rate of species one in the elutriate

$p_{2,1}$ = population density function for species one in the elutriate

α_1 = mass fraction of species one in the bed

W = bed weight

$p_{b,1}(D)$ = population density function for species one in the bed or equivalently in the draw-off.

Using the same nomenclature, the modified elutriation rate constant for species two of a two-species system is:

$$K_2(D) = \frac{F_{2,2}p_{2,2}(D)}{\alpha_2 W p_{b,2}(D)} \quad . \tag{15B}$$

Figure 3 shows the flow scheme for a two-species system. The solution algorithm for such a system proceeds as follows:

(Note: In the following the second subscript refers to the species, e.g., $F_{0,1}$ is the feed rate of the sorbent, $F_{2,2}$ is the mass rate of ash in the elutriate, etc.)

1. For given $F_{0,1}$, $F_{0,2}$, pick α_1,α_2,$F_{1,1}$,$F_{1,2}$.
2. On the basis of a choice of α_1 or α_2, calculate the total bed weight.
3. Independently calculate $F_{1,1}$ and $F_{1,2}$ by solving equations (6) and (7) [or (6) and (8) if a recycle cyclone is used] individually for each species, with the exception of modifying the species elutriation rate constants as indicated by equations (15A) and (15B).
4. Use the $F_{1,1}$ and $F_{1,2}$ values to calculate the fraction of each species (α_i') in the bed:

$$\alpha_1' = \frac{F_{1,1}}{(F_{1,1} + F_{1,2})}$$

$$\alpha_2' = \frac{F_{1,2}}{(F_{1,1} + F_{1,2})} \quad . \tag{16}$$

Compare α_i' with α_i.

5. Update the α_1 and α_2 values and iterate until convergence is achieved.

6. Once convergence is achieved for α_i, $F_{1,1}$, and $F_{1,2}$, the remainder of the computations consist of relatively straightforward calculations for $p_{1,1}(D)$, $F_{2,1}(D)$, $p_{2,1}(D)$, $A_{2,1}(D)$, $p_{1,2}(D)$, $F_{2,2}$, $p_{2,2}(D)$, and $A_{2,2}(D)$. These are, of course, performed independently for each species in a fashion analogous to that indicated earlier for the one-species system.

The loading presented to the particulate removal train is:

$$\begin{aligned} \text{Loading (species 1)} &= A_{2,1} + F_{2,1} \quad ; \\ \text{Loading (species 2)} &= A_{2,2} + F_{2,2} \quad . \end{aligned} \tag{17}$$

The size distributions of $F_{2,1}$ and $F_{2,2}$ are known, but the size distributions of $A_{2,1}(p_{A,1})$ and $A_{2,2}(p_{A,2})$ must be assumed.

The cumulative size distribution of the combined* stream for each species is then obtained as:

$$\begin{aligned} Z_{C,1}(D) &= \int_{D_m}^{D} \frac{F_{2,1}p_{2,1} + A_{2,1}p_{A,1}}{F_{2,1} + A_{2,1}} \, dD \quad , \\ Z_{C,2}(D) &= \int_{D_m}^{D} \frac{F_{2,2}p_{2,2} + A_{2,2}p_{A,2}}{F_{2,2} + A_{2,2}} \, dD \quad , \end{aligned} \tag{18}$$

where

$Z_{C,i}(D)$ = cumulative size distribution of the combined stream for the i^{th} species, i = 1 or 2

*Combined is taken to mean elutriated plus attrited material.

PARTICLE REMOVAL EQUIPMENT SIMULATION

The mass rate F_E of solids escaping a collector is given by:

$$F_E = F \int_{D_{min}}^{D_{max}} p(D)(1-\eta)\, dD \quad , \tag{19}$$

where

F = mass rate of solids presented to the collector

$p(D)$ = population density function (size distribution) of solids presented to the collector

$\eta(D)$ = grade efficiency of collector

D = particle diameter.

In general, for a system of i collectors in series, the mass rate F_E of solids escaping the i^{th} collector is:

$$F_E = F \int_{D_{min}}^{D_{max}} p(D)(1-\eta_1)(1-\eta_2)\cdots\cdots(1-\eta_i)\, dD \quad , \tag{20}$$

where

F = mass rate of solids presented to the first collector

$p(D)$ = population density function (size distribution) of solids presented to the first collector

$\eta_i(D)$ = grade efficiency of the i^{th} collector

D = particle diameter.

Equations (18) and (20) used in conjunction will give the mass rate of either species escaping the i^{th} device in any given configuration of particle removal devices. Closer examination of both these equations reveals the presence of a population density term, $p_{A,L}$ or $p_{A,?}$ in equation (18) and p(D) in equation (20); $p_{A,1}$ and $p_{A,2}$ are the population density functions assumed for the attrited size distributions of species one and two, respectively. Generally, these assumed distributions

for the attrited material will be specified as cumulative size distributions $Z_{A,1}(D)$ and $Z_{A,2}(D)$. Similarly, as seen in equation (18), the distribution presented to the particulate removal train is of the cumulative form $Z_{C,1}(D)$ and $Z_{C,2}(D)$. These cumulative function values must be converted to the population density function form if one is to perform the required computations.

The population density function is the derivative of the cumulative function with respect to diameter

$$p(D) = \frac{dZ(D)}{dD} \quad , \tag{21}$$

where

$p(D)$ = population density function
$Z(D)$ = cumulative function
D = diameter.

Since most fine particles tend to be log-normally distributed, the cumulative size distributions can be conveniently fitted to the log-normal form over relatively short size intervals, typically

0.1-0.2, 0.2-0.3	0.9-1.0
1.0-2.0, 2.0-3.0	9.0-10.0
10.0-20.0	90.0-100.0.

The cumulative function of a log-normal size distribution is given by

$$Z(D) = 1/2 \left[1 + \text{erf}\left\{\frac{\text{Ln}\,\frac{D}{D_s}}{2\text{Ln}(\sigma)}\right\}\right] \quad , \tag{22}$$

where D_s, the mass median diameter, and σ, the standard deviation, are the two parameters of the log-normal form. The particle profile program determines this pair of parameters over each of the chosen intervals (D_i to D_{i+1}) by inserting the values of the cumulative function

($Z(D_i)$ and $Z(D_{i+1})$) into equation (22) and using a nonlinear root-finding technique to determine $(D_s)_i$ and $(\sigma)_i$ for this (i^{th}) interval. The value of the population density function is then obtained from

$$p\ (Di \leq D \leq D_{i+1}) = \frac{1}{\sqrt{2\pi}\ DLn(\sigma_i)}\ \exp\left(\frac{Ln\left(\frac{D}{(D_s)_i}\right)}{\sqrt{2}\ Ln(\sigma_i)}\right)^2 . \qquad (23)$$

The other parameter required by equation (20) is the penetration (1-efficiency) for each device as a function of particle size. For many particle control devices the penetration can be correlated with a function of the following form:

$$(1-\eta(D)) = \text{Penetration } (D) = Ae^{-BD} , \qquad (24)$$

where

$\eta(D)$ = device grade efficiency
D = particle diameter
A,B = constants.

Performance data for various devices such as cyclones of different design, fabric filters, electrostatic precipitators, and granular-bed filters are stored in the subroutine DEVICE of the particulate profile program. DEVICE uses the form of equation (24) to interpolate between data points to yield the penetration of any specified device at any diameter D. Each device is assigned a device number. Based on the device number and the species number (one for sorbent, two for ash) DEVICE performs the interpolation using the appropriate performance data.

ILLUSTRATIVE PROBLEM

The following operating parameters reported by the National Coal Board (NCB) Coal Utilization Research Laboratory (CURL)[4] were used to predict the solid loading and size distributions throughout the fluidized-bed combustion system shown schematically in Figure 4.

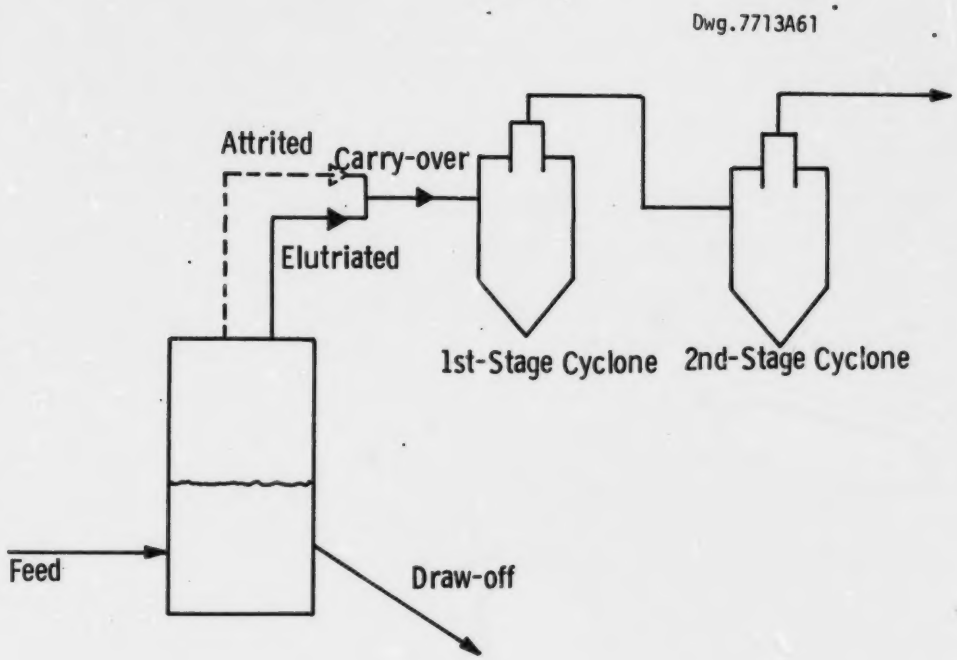

Figure 4 - Flow Schematic for Illustrative Example

Combustor Operating Data:

Pressure	607.8 kPa (6 atm)
Temperature	843°C (1550°F)
Bed depth (unexpanded)	0.44 m (8 ft)
Bed expansion ratio	1.5
Superficial velocity	0.91 m/s (3 ft/sec)

Feed Materials:

- 161 kg (354 lb)/hr of a Glenn-Brooke coal having a 13.64% ash content
- 45.4 kg (100 lb)/hr of a Plum-Run dolomite having a size distribution as shown in Figure 5.

The size distributions assumed for the attrited sorbent and ash are also shown in Figure 5. The two cleaning stages are assumed to be Ducon cyclones. Grade efficiency curves predicted by Ducon for three apparent specific gravities at 1700°F and 10 atmospheres are shown in Figure 6.

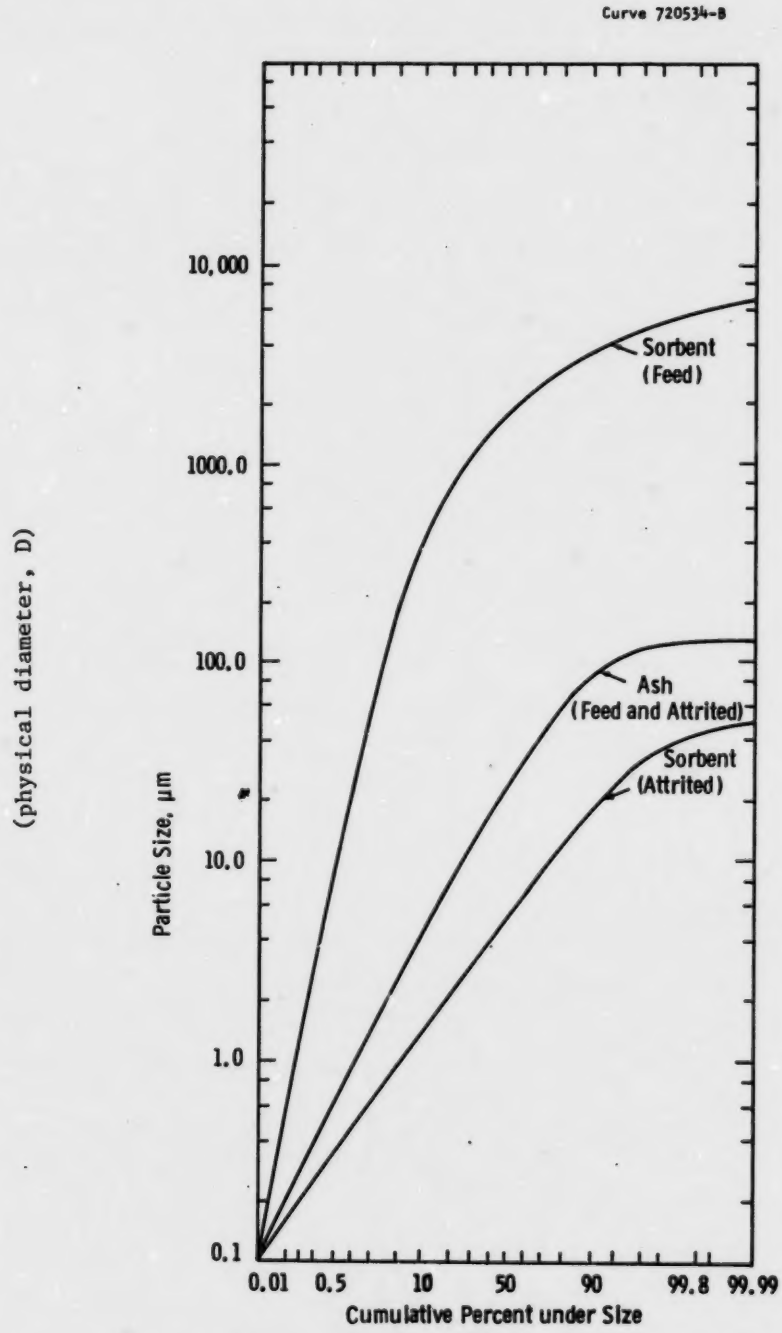

Figure 5 - Size Distributions of Feed and Attrited Material

Table 1 summarizes the results of the computation. Figures 7 and 8 show the size distribution profiles from the fluidized bed and the two cleaning cyclones individually for each species. The combined (ash and sorbent) distributions are shown in Figure 9 alongside the CURL experimentally measured curves.

The dotted curve of Figure 10 is the result of subtracting the calculated sorbent carry-over size distribution from the combined (ash plus sorbent) size distribution measured by CURL. Since the rate of attrition for each species was adjusted to force agreement between its calculated and experimental carry-over rate, the resulting curve is a truer representation of the attrited/elutriated ash than the one assumed in Figure 5. (For comparison the latter is also shown in Figure 10.)

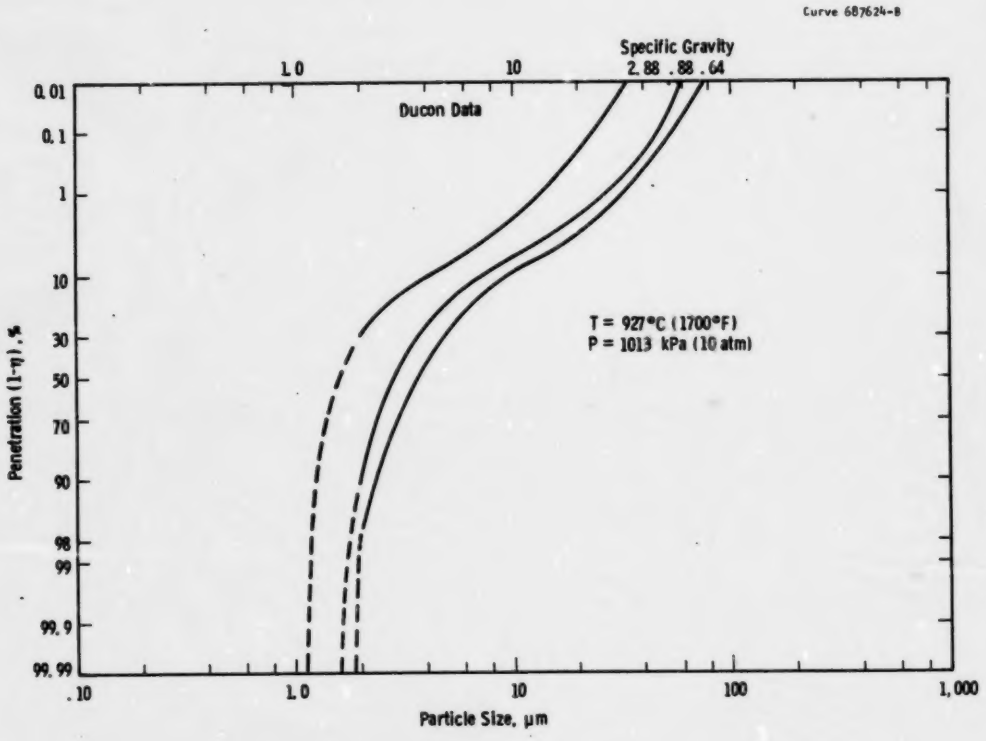

Figure 6 - Grade Efficiency Curves for Ducon High-Efficiency Cyclone

Table 1

EXAMPLE PROBLEM RESULTS

		Sorbent	Ash
Feed	Feed rate, g/s	12.61	6.09
Carry-over	Rate of carry-over, g/s	4.24	5.75
Draw-off	Rate of draw-off, g/s	8.37	0.34
Recycle Cyclone	Type Solids in cyclone Solids in recycle Overall efficiency	No recycle cyclone	No recycle cyclone
First Cleaning Device	Type Overall efficiency, % Mass rate of solids escaping, g/s	Ducon full-size cyclone 96.44 0.15	Ducon full-size cyclone 90.04 0.57
Second Cleaning Device	Type Overall efficiency, % Mass rate of solids escaping, g/s	Ducon full-size cyclone 47.87 0.08	Ducon full-size cyclone 43.08 0.33

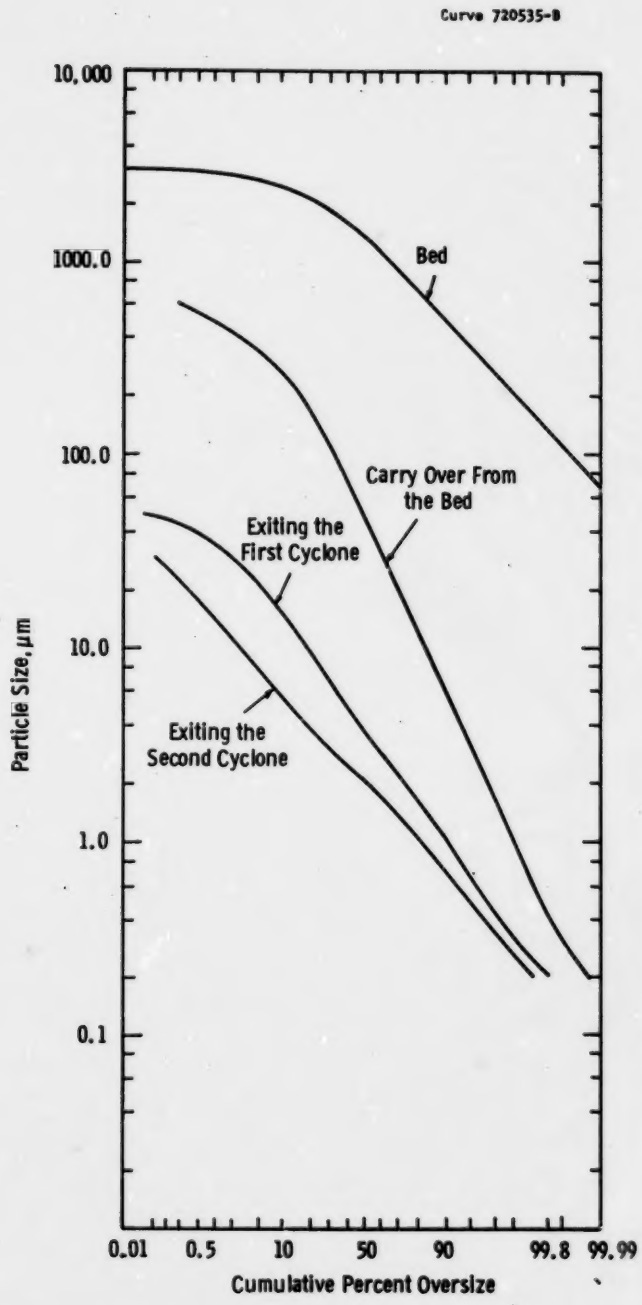

Figure 7 - Theoretical Size Distribution Profiles for Sorbent

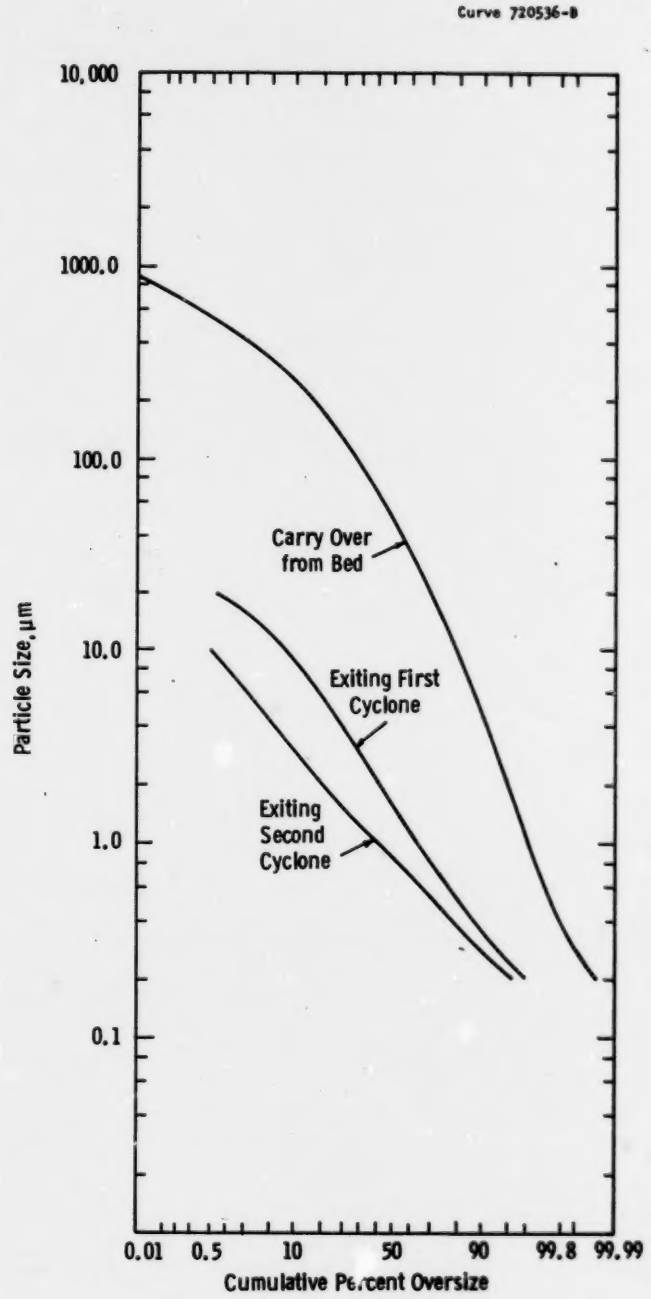

Figure 8 - Theoretical Size Distribution Profiles for Ash

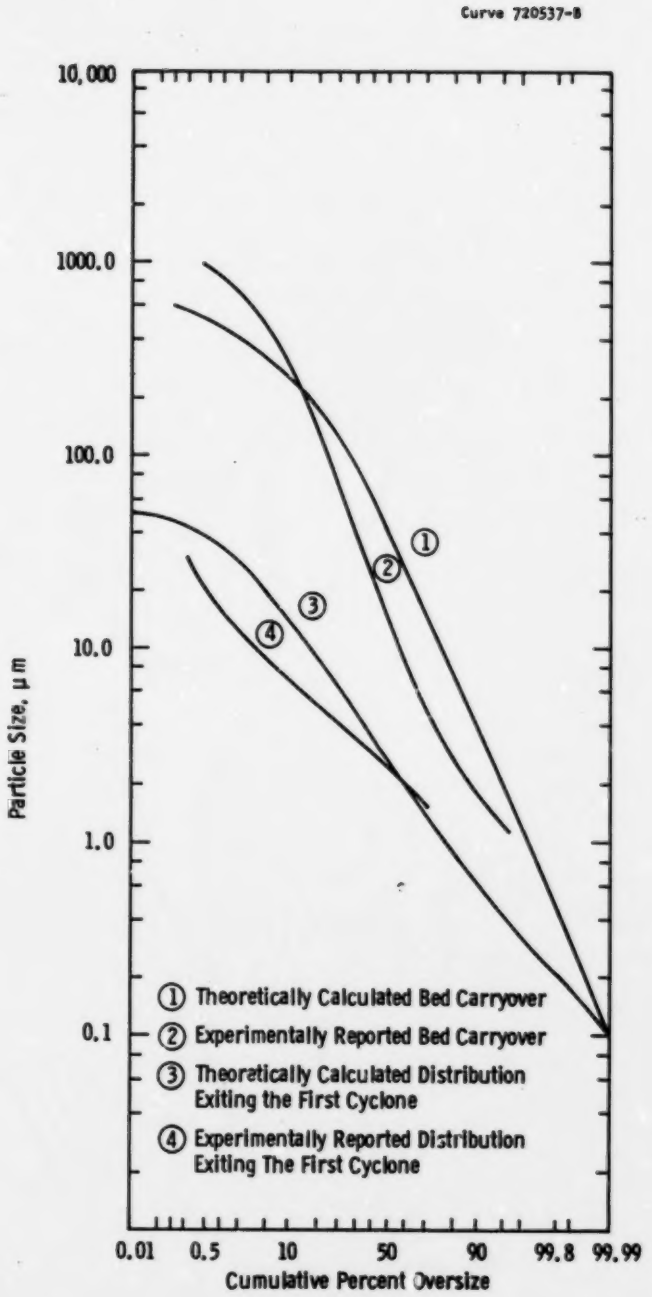

Figure 9 - Comparison of Theoretically Predicted and Experimentally Reported Size Distribution Profiles

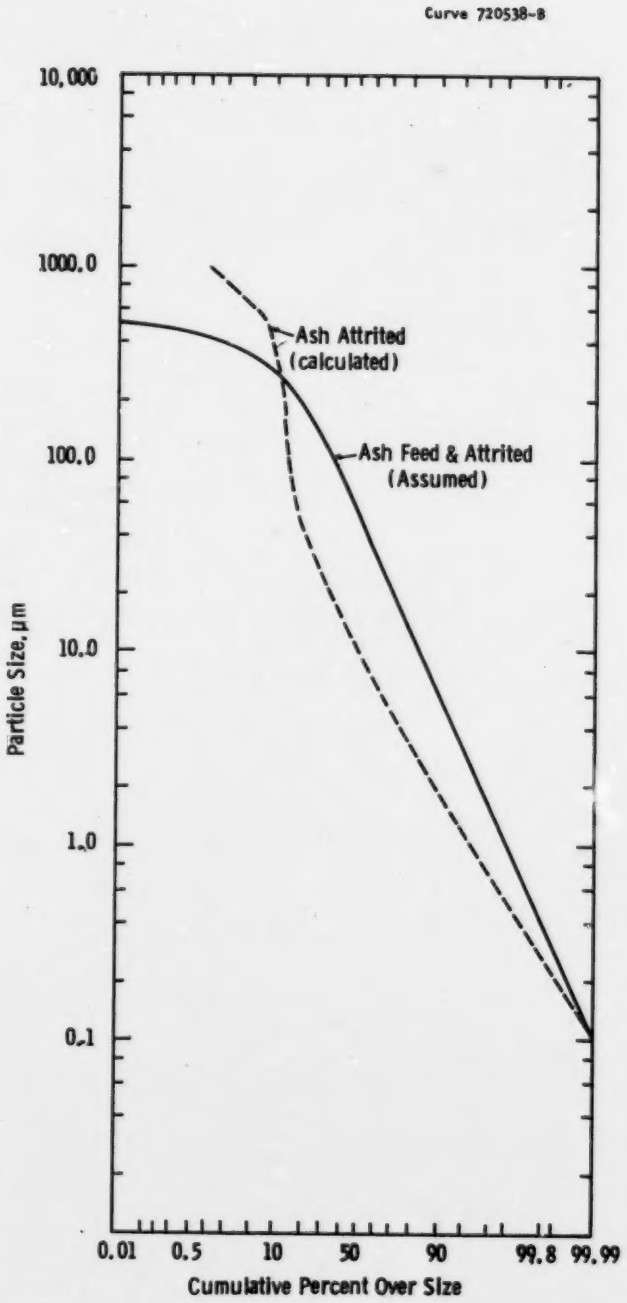

Figure 10 - Calculated and Assumed Ash Size Distributions

4. EVALUATION OF PARTICULATE EMISSIONS FROM FBC SYSTEMS

PROJECTED EMISSIONS AND PARTICULATE CONTROL DEVICE PERFORMANCE FOR PFBC

Projections to illustrate the particle profile model and to indicate the current state of PFBC information are reported. They are not intended to represent a complete engineering evaluation of this developing technology.

Design and Operating Conditions and Feed Materials

The combustor operating conditions (Table 2) that Westinghouse[5] selected for a 180 MW_e combined-cycle power plant have been used for this evaluation. The feed materials are assumed to be a deep-mined Illinois coal and Plum Run dolomite whose compositions are as shown in Tables 3 and 4. One hundred percent excess air is assumed for calculating the combustion gas rate per unit coal feed rate. The sorbent feed and generated ash mass rates have been calculated on the basis of a gas turbine inlet rate of 277 kg/s (611 lb/sec) specified by Westinghouse for the 180 MW_e power plant.

Table 2

PFBC COMBUSTOR OPERATING AND DESIGN CONDITIONS SELECTED FOR STUDY

Temperature	= 900°C (1652°F)
Pressure	= 1013 kPa (10 atm)
Superficial Gas Velocity	= 152.4 cm/s (5 ft/s)
Expanded Bed Height	= 457.2 cm (15 ft)
Bed Expansion Ratio	= 1.5
Excess Air Level	= 100%
Bed Cross-Sectional Area	= 6.04×10^5 cm^2 (650 ft^2)
Gas Inlet Rate to Turbine	= 277 kg/s (611 lb/s)

Figure 11 shows the size distributions assumed for the feed sorbent, the attrited sorbent, and the generated and attrited coal ash. The sorbent size distribution is based on a screen analysis of a single-screened Greer limestone. The fines from the screen analysis were further analyzed

Table 3

COMPOSITION OF A DEEP-MINED ILLINOIS COAL

Ultimate Analysis	Weight %
Moisture	12.0
Carbon	57.5
Hydrogen	3.7
Nitrogen	0.9
Chlorine	0.1
Sulfur	4.0
Ash	16.0
Oxygen (by difference)	5.8

Table 4

COMPOSITION OF PLUM RUN DOLOMITE

	Weight %
Calcium Carbonate ($CACO_3$)	51.3
Magnesium Carbonate ($MgCO_3$)	52.6
Aluminum Oxide (Al_2O_3)	2.1
Ferric Oxide (Fe_2O_3)	1.5
Silicon Dioxide (SiO_2)	2.35
Sodium Oxide (Na_2O)	0.067
Potassium Oxide (K_2O)	0.43

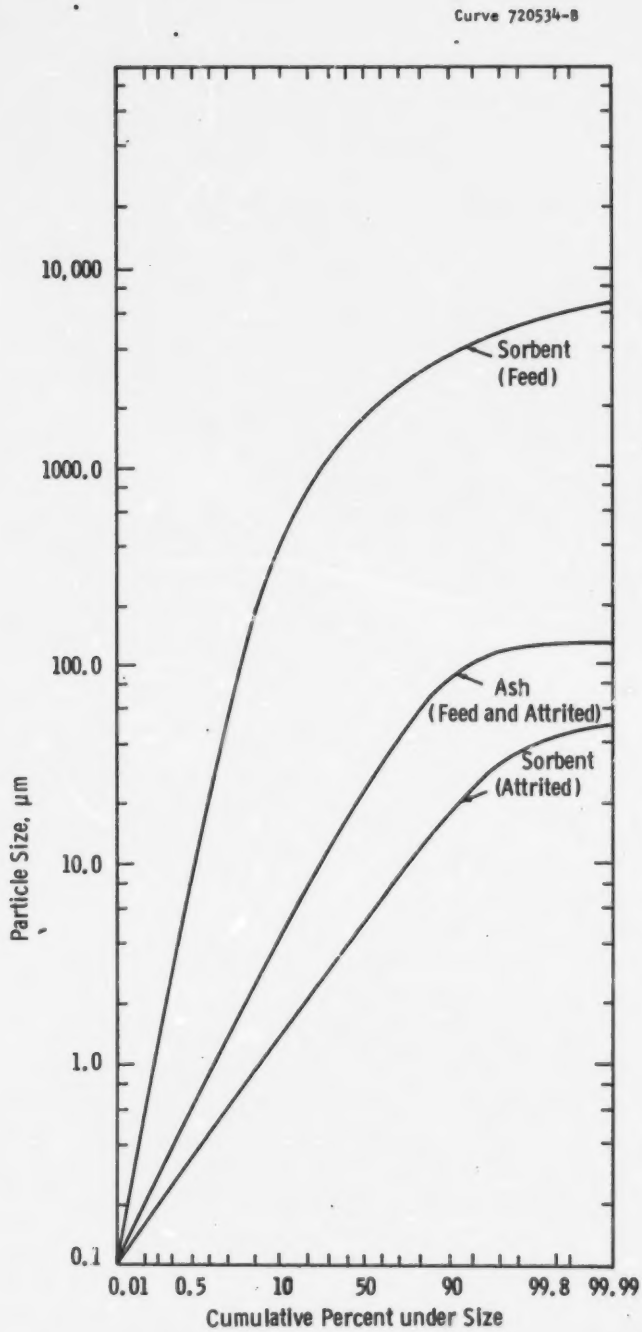

Figure 11 - Size Distributions for Feed and Attrited Sorbent and Generated and Attrited Ash

with a Coulter Counter™ for obtaining a better definition at the fines end of the size distribution. The size distribution of the attrited ash is based on experimental data reported for bed operation with coal only.[6] Since in practice most of the ash generated in the bed is instantaneously elutriated, we have assumed here that the size distributions of the feed and attrited ash are the same.

As seen in Figure 12, the particulate control train is comprised of two cyclone stages followed by a final-stage granular-bed filter. The grade efficiency curve assumed for the recycle cyclone is shown in Figure 13. The second-stage cyclone is assumed to be a conventional, high-efficiency, Ducon cyclone. Grade efficiency curves supplied by Ducon for this unit at three apparent specific gravities at 954°C (1700°F) and 1013 KPa (10 atm) are shown in Figure 13. The grade efficiency curve for the granular-bed filter shown in Figure 14 has been generated from the results of bench-scale tests conducted at Westinghouse.

Dwg.7737A52

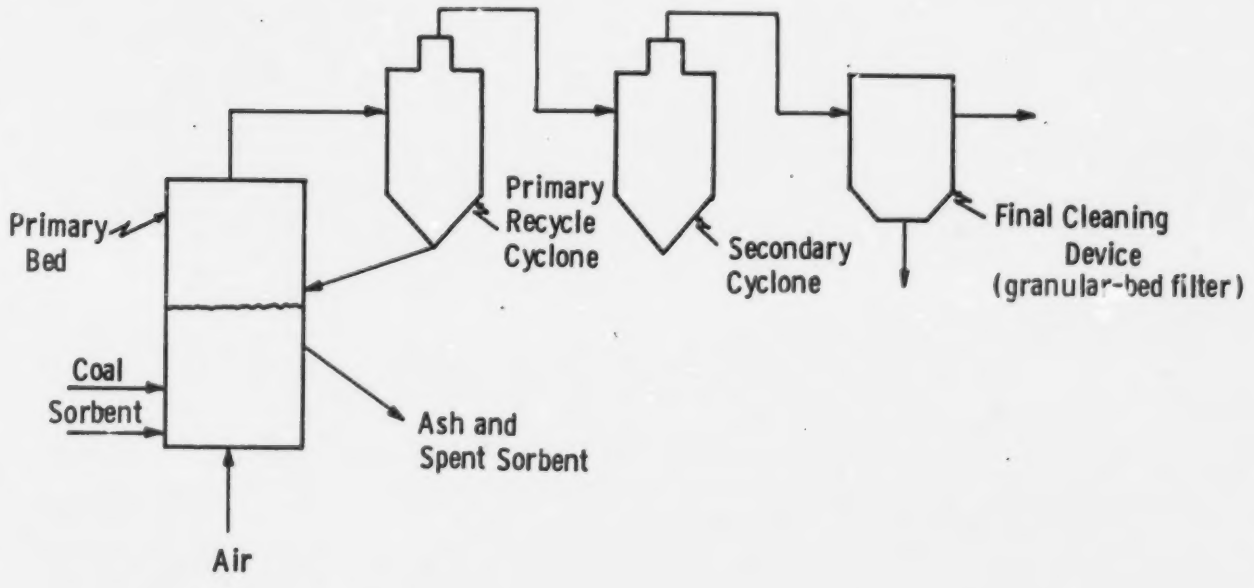

Figure 12 - Flow Scheme Assumed for PFBC System

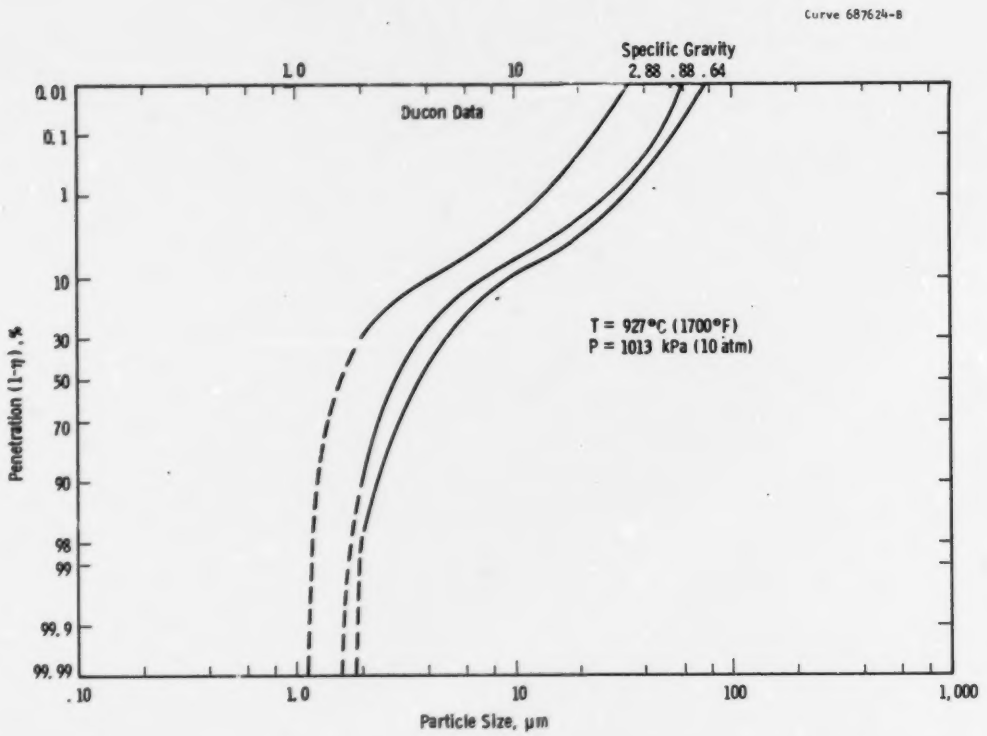

Figure 13 - Grade Efficiency Curves for Ducon High-Efficiency Cyclone

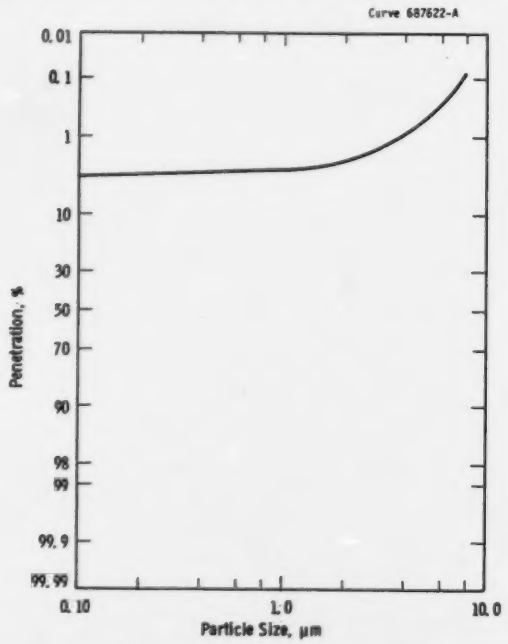

Figure 14 - Grade Efficiency Curve for Granular-Bed Filter

Sensitivity to Calcium-to-Sulfur Ratio

This section examines the effect of increasing the Ca/S ratio on the particulate emissions from the fluidized-bed combustion system. Sorbent feed and attrition rates corresponding to Ca/S ratios in the range of 1 to 5 are shown in Table 5. A sorbent attrition rate of 2.5 percent of the bed weight per hour is assumed for the case of a Ca/S ratio of 2. For estimating the sorbent attrition rates for the other four cases examined, we have assumed that the rate of sorbent attrition is directly proportional to the sorbent feed rate.

Table 5

SORBENT FEED AND ATTRITION RATES CORRESPONDING TO VARIOUS CALCIUM-TO-SULFUR RATIOS

Calcium-to-Sulfur Ratio	Sorbent Feed Rate, g/s	Sorbent Attrition Rate, % of bed weight/hr
1	4126	1.25
2	8252	2.5
3	12378	3.75
4	16504	5.0
5	20630	6.25

Tables 6 through 10 show that the most pronounced effect of increasing the Ca/S ratio is to increase the particulate emissions from the fluidized-bed system. This effect is more conveniently viewed in Figure 15. Increasing the Ca/S ratio also causes the recycle rates through the primary cyclone to increase. For instance, increasing the Ca/S ratio from 1 to 5 causes the recycle rate to increase by approximately 20 percent. The particle size distributions at various points of the fluidized-bed system are shown in Figures 16 and 17 for Ca/S ratios of 1 and 5, respectively. While the bed size distribution remains unchanged, the effect of increasing the Ca/S ratio is to slightly shift the size distributions of the particulate emitted from each of the particle removal stages towards finer sizes.

Table 6

PFBC PARTICULATE EMISSION PROJECTIONS FOR A CALCIUM-TO-SULFUR RATIO OF 1

		Sorbent	Ash	Total
Feed to Bed, g/s		4125.5	2709.2	6834.7
Bed Draw-off, g/s		2314.5	196.5	2511.0
Overhead from Bed, g/s		39282.1	4135.1	43417.2
Primary Cyclone Recycle Rate, g/s		37471.1	1622.4	39093.5
Primary Cyclone Emission				
Mass rate, g/s		1811.0	2512.7	4323.7
Grain loading,	g/m^3	8.40	11.66	20.06
	(gr/scf)	(3.674)	(5.09)	(8.77)
Secondary Cyclone Emission				
Mass rate, g/s		429.0	269.0	698.0
Grain loading,	g/m^3	1.99	1.25	3.24
	(gr/scf)	(0.87)	(0.55)	(1.42)
Secondary Cyclone Overall Efficiency		76.31	89.29	83.85
Final-Stage Device Emission				
Mass rate, g/s		8.69	4.74	13.43
Grain loading,	g/m^3	0.04	0.022	0.062
	(gr/scf)	(0.018)	(0.0096)	(0.027)
Final-Stage Overall Efficiency		97.97	98.24	98.08

Table 7

PFBC PARTICULATE EMISSION PROJECTIONS FOR A CALCIUM-TO-SULFUR RATIO OF 2

		Sorbent	Ash	Total
Feed to Bed, g/s		8251.1	2709.2	10960.3
Bed Draw-off, g/s		4633.1	373.4	5006.5
Overhead from Bed, g/s		43917.8	3804.5	47722.3
Primary Cyclone Recycle Rate, g/s		40299.8	1468.7	41768.5
Primary Cyclone Emission				
Mass rate, g/s		3618.0	2335.8	5953.8
Grain loading,	g/m^3	16.79	10.84	27.63
	(gr/scf)	(7.34)	(4.74)	(12.07)
Secondary Cyclone Emission				
Mass rate, g/s		864.2	255.1	1119.3
Grain loading,	g/m^3	4.01	1.18	5.19
	(gr/scf)	(1.75)	(0.52)	(2.27)
Secondary Cyclone Overall Efficiency		76.12	89.08	81.2
Final-Stage Device Emission				
Mass rate, g/s		17.51	4.52	22.03
Grain loading,	g/m^3	0.081	0.021	0.102
	(gr/scf)	(0.036)	(0.0092)	(0.045)
Final-Stage Overall Efficiency		97.97	98.23	98.03

Table 8

PFBC PARTICULATE EMISSION PROJECTIONS FOR A CALCIUM-TO-SULFUR RATIO OF 3

	Sorbent	Ash	Total
Feed to Bed, g/s	12377.0	2709.2	15086.2
Bed Draw-off, g/s	6944.6	536.1	7480.7
Overhead from Bed, g/s	47623.1	3504.6	51127.7
Primary Cyclone Recycle Rate, g/s	42190.6	1331.5	43522.1
Primary Cyclone Emission			
Mass rate, g/s	5432.4	2173.1	7605.5
Grain loading, g/m^3	25.21	10.08	35.29
Grain loading, (gr/scf)	(11.01)	(4.41)	(15.42)
Secondary Cyclone Emission			
Mass rate, g/s	1305.0	241.6	1546.6
Grain loading, g/m^3	6.06	1.12	7.18
Grain loading, (gr/scf)	(2.65)	(0.49)	(3.14)
Secondary Cyclone Overall Efficiency	75.98	88.88	79.66
Final-Stage Device Emission			
Mass rate, g/s	26.44	4.30	30.74
Grain loading, g/m^3	0.12	0.020	0.14
Grain loading, (gr/scf)	(0.054)	(0.0087)	(0.062)
Final-Stage Overall Efficiency	97.97	98.22	98.01

Table 9

PFBC PARTICULATE EMISSION PROJECTIONS FOR A CALCIUM-TO-SULFUR RATIO OF 4

		Sorbent	Ash	Total
Feed to Bed, g/s		16502.0	2709.2	19211.2
Bed Draw-off, g/s		9247.8	678.4	9926.2
Overhead from Bed, g/s		50897.8	3245.8	54143.6
Primary Cyclone Recycle Rate, g/s		43643.6	1214.9	44858.5
Primary Cyclone Emission				
Mass rate, g/s		7254.2	2030.9	9285.1
Grain loading,	g/m^3	33.66	9.42	43.08
	(gr/scf)	(14.71)	(4.12)	(18.83)
Secondary Cyclone Emission				
Mass rate, g/s		1750.0	229.3	1979.3
Grain loading,	g/m^3	8.12	1.06	9.18
	(gr/scf)	(3.55)	(0.47)	(4.02)
Secondary Cyclone Overall Efficiency		75.88	88.71	78.68
Final-Stage Device Emission				
Mass rate, g/s		35.46	4.10	39.56
Grain loading,	g/m^3	0.16	0.019	0.18
	(gr/scf)	(0.072)	(0.0083)	(0.08)
Final-Stage Overall Efficiency		97.97	98.21	98.0

Table 10

PFBC PARTICULATE EMISSION PROJECTIONS FOR A CALCIUM-TO-SULFUR RATIO OF 5

		Sorbent	Ash	Total
Feed to Bed, g/s		20628.0	2709.2	23337.2
Bed Draw-off, g/s		11543.0	808.2	12351.2
Overhead from bed, g/s		53933.8	3012.3	56946.1
Primary Cyclone Recycle Rate, g/s		44849.2	1111.4	45960.6
Primary Cyclone Emission				
Mass rate, g/s		9084.6	1901.0	10985.6
Grain loading,	g/m^3	42.15	17.64	59.79
	(gr/scf)	(18.42)	(7.71)	(26.13)
Secondary Cyclone Emission				
Mass rate, g/s		2199.0	217.6	2416.6
Grain loading,	g/m^3	10.2	1.01	11.21
	(gr/scf)	(4.46)	(0.44)	(4.9)
Secondary Cyclone Overall Efficiency		75.8	88.55	81.2
Final-Stage Device Emission				
Mass rate, g/s		44.56	3.91	48.47
Grain loading,	g/m^3	0.21	0.018	0.22
	(gr/scf)	(0.09)	(0.0079)	(0.098)
Final-Stage Overall Efficiency		97.97	98.20	97.99

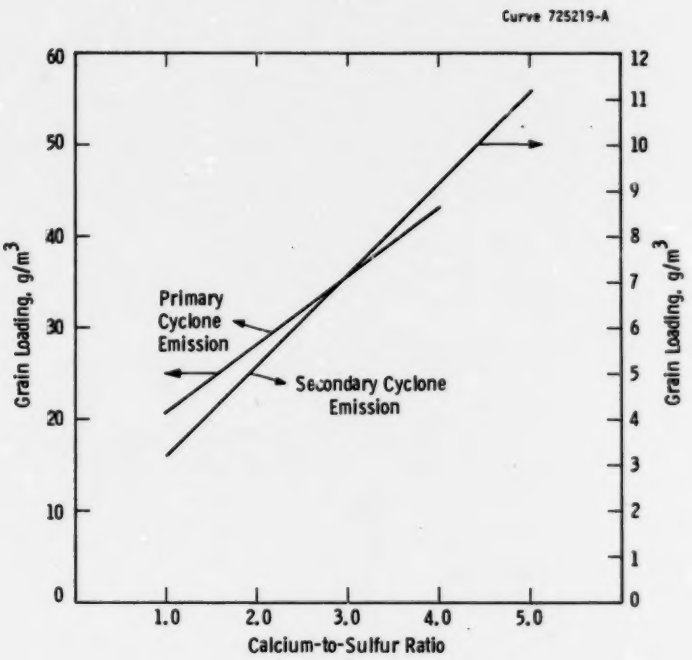

Figure 15 - Increase in Solids Grain Loading with Calcium-to-Sulfur

Performance of Particle Removal Devices

Figure 18 shows the configuration of particle removal devices that we envision for the PFBC system.

The first-stage recycle cyclone enhances combustion efficiency and sulfur capture while decreasing the particulate emissions from the bed and also offering the advantages of low cost and simple maintenance. On the basis of the results of parametric studies we conducted (see Section 4), we believe that a medium-efficiency recycle cyclone has greater merit than a high-efficiency one. As we shall see in Section 4, the recycle rates through the recycle cyclone are very high, typically up to five or six times the solids feed rate. A high-efficiency recycle cyclone further boosts the recycle rate, perhaps by as much as 20 percent.

Curve 726911-B

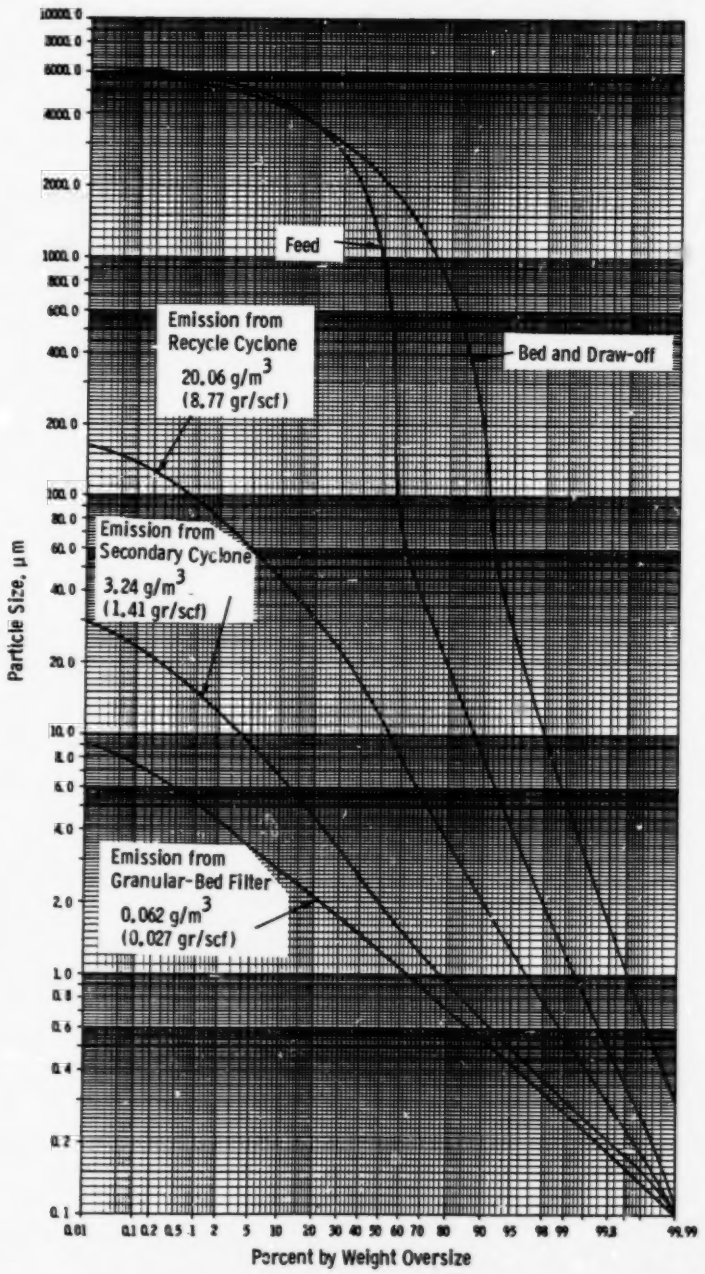

Figure 16 - Size Distributions and Loadings for a Calcium-to-Sulfur Ratio of 1

Reproduced from best available copy.

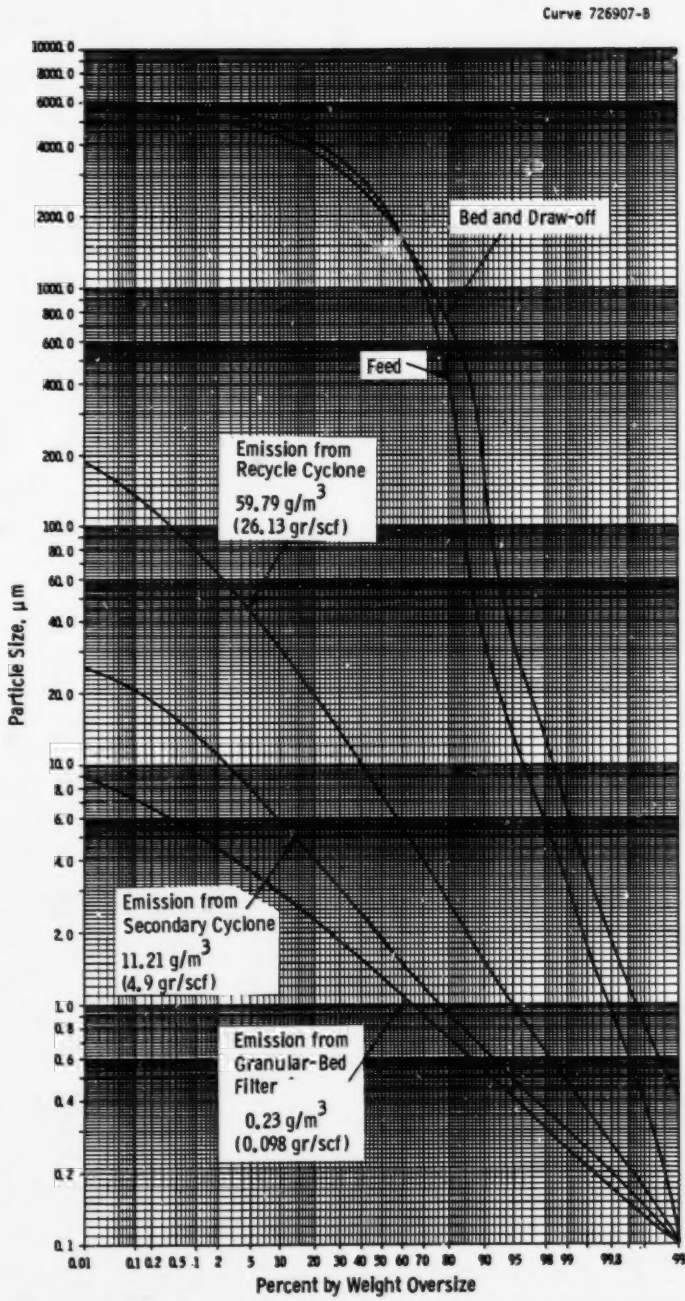

Figure 17 - Size Distributions and Loadings for a Calcium-to-Sulfur Ratio of 5

Reproduced from best available copy.

Dwg.7737A54

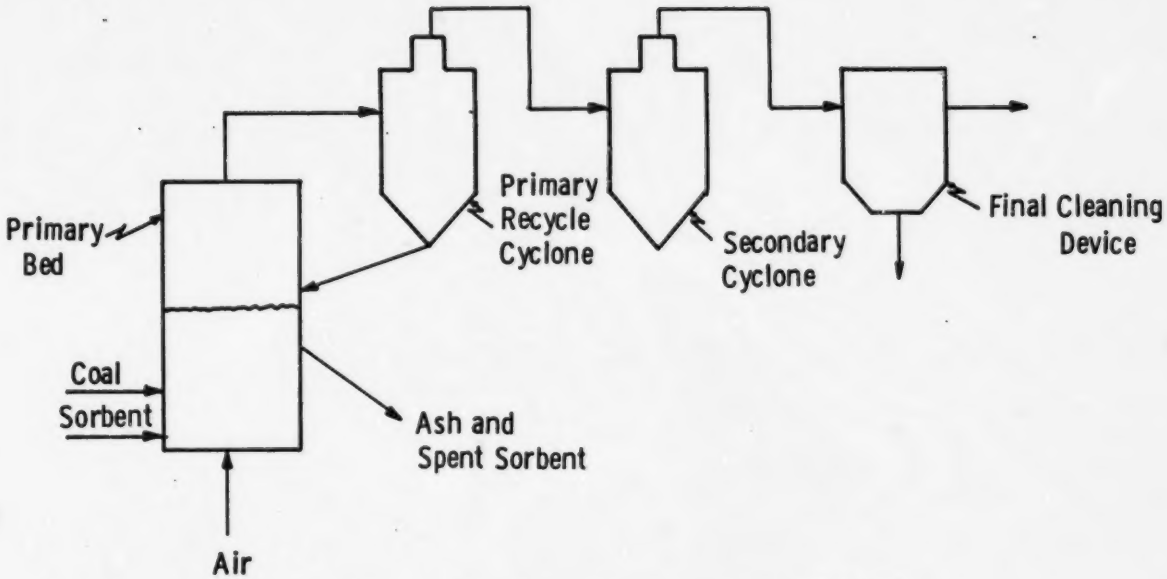

Figure 18 - Flow Scheme for Parametric Studies

The purpose of the second-stage cyclone is to reduce the grain loading presented to the final cleaning stage by collecting the larger particles that escape the recycle cyclone. A high-efficiency cyclone, therefore, is favored for this stage.

The final stage of particle cleanup must reduce the particulate emissions to levels that conform to the dictates of environmental and gas turbine protection constraints. Since hot, pressurized, fine particle control is not as yet state-of-the-art practice, the final particle removal stage is not well defined for PFBC. Possible candidates are granular-bed filters, ceramic bag filters, and ceramic membrane filters.

Since a Ca/S ratio of 2 is fairly well established for achieving adequate sulfur dioxide (SO_2) retention (90% SO_2 removal) in PFBC using high-sulfur coals, we may refer to the projections made in Table 7 and Figure 19 to gain a perspective on the particulate emissions that may

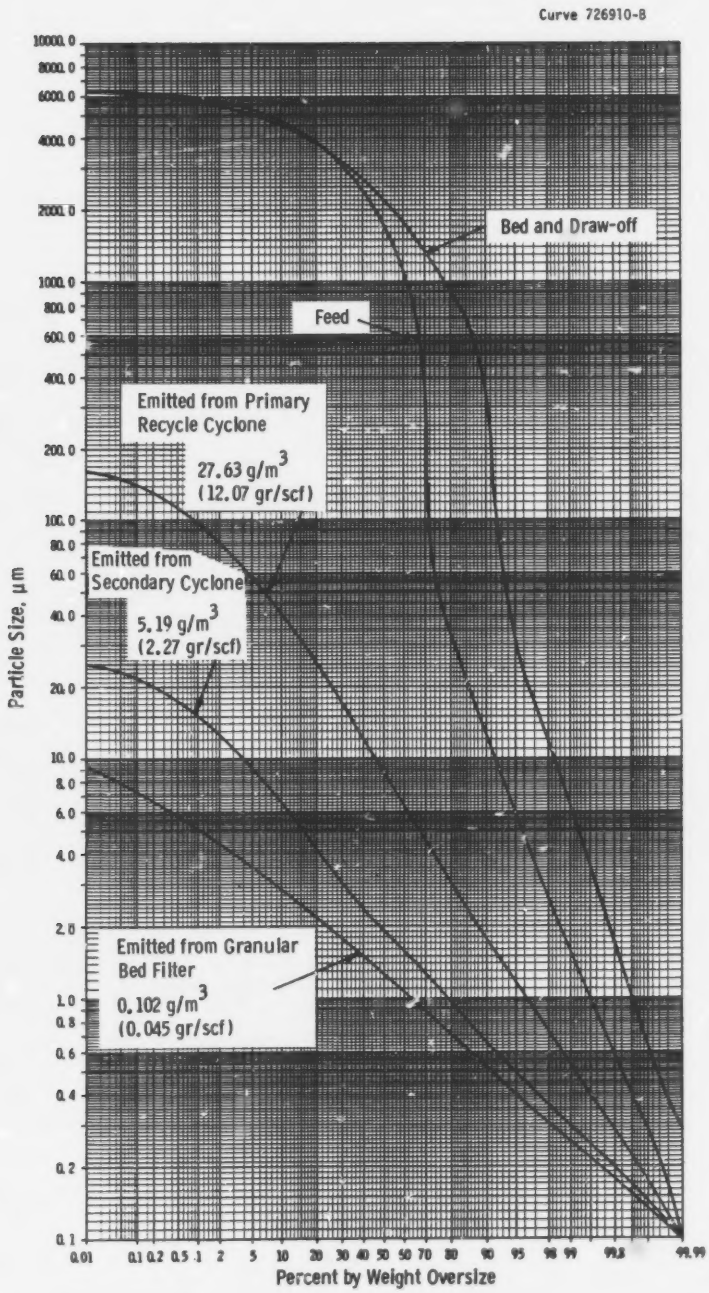

Figure 19 - Size Distributions and Loadings at Various Points of the PFBC System for a Calcium-to-Sulfur Ratio of 2

Reproduced from best available copy.

typically be expected from PFBC systems. In Figure 19 we have assumed that the final cleaning stage is a granular-bed filter. (Note that the grade efficiency assumed for the granular bed is based on tests Westinghouse[7] conducted on a small, experimental unit. The data from these tests are more optimistic than those realized from larger units.) The effect of substituting for the granular-bed filter a final stage having the performance of (a) a fabric filter (Figure 20) and (b) a high efficiency cyclone (Figure 13) is shown in Figure 21. While the size distribution of the particulate emitted from the final stage is not significantly altered, note the marked difference in the emitted grain loadings.

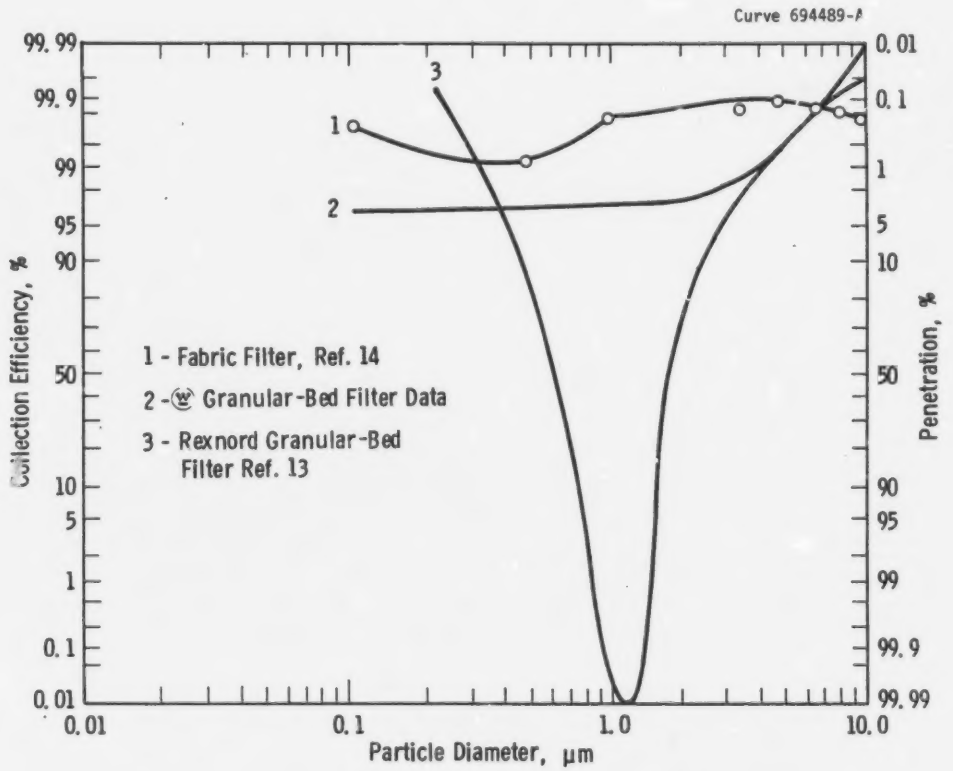

Figure 20 - Grade Efficiency Curve for Sunbury Fabric Filter

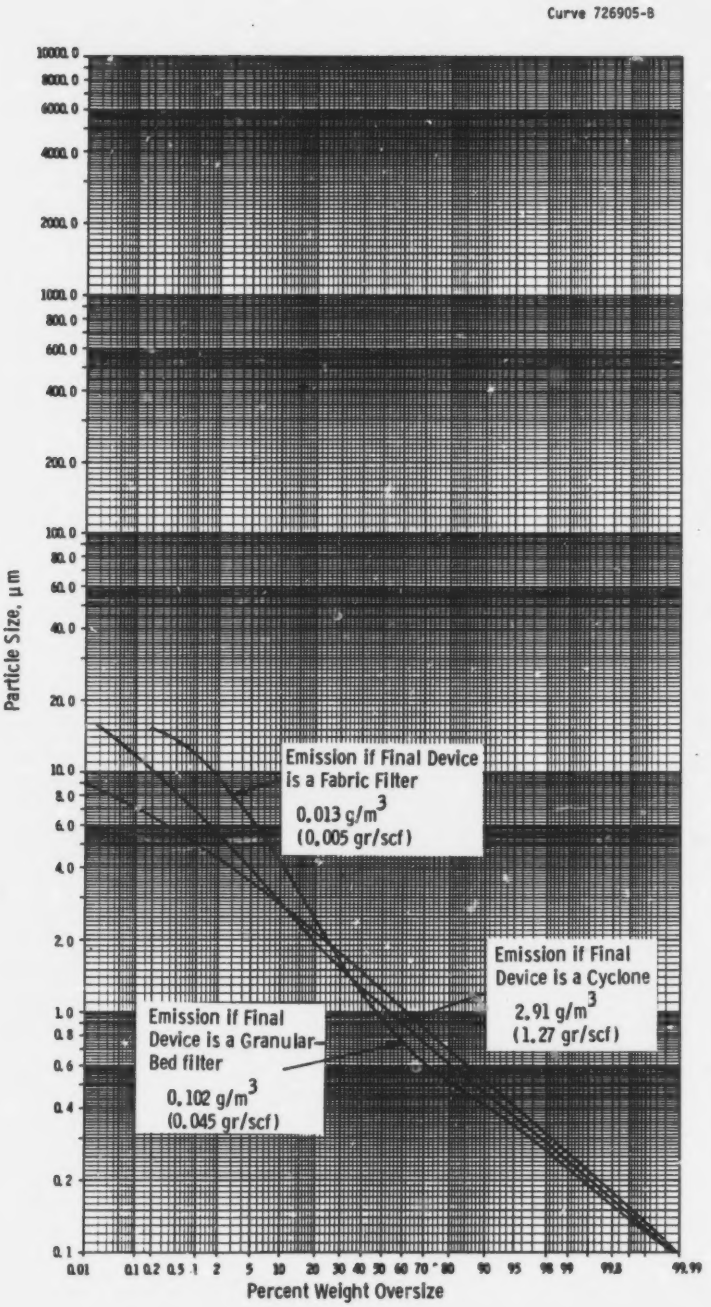

Figure 21 - Results of Using Different Final (PFBC) Stage Devices

Reproduced from best available copy.

New Source Performance Standards and Turbine Protection Requirements

The New Source Performance Standard (NSPS) of 12.9 ng/J (0.03 lb/MBtu) applicable to particulates translates to approximately 0.028 g/m^3 (0.012 gr/scf) for the 100% excess air PFBC case considered. Particulate loadings and size distributions as they relate to turbine protection are not precisely known.

Using its turbine erosion and deposition models, Westinghouse has evaluated turbine tolerances and gas cleanup requirements for large utility turbines operating with PFBC power plants. The particulate loading and size distribution requirements to achieve a desired turbine life or economic objective will depend on many factors. Illustrations of these requirements as a function of turbine life are available.[5,8] Preliminary assessments have been carried out to project the impact of particle deposition in the turbine, which is directly related to the particulate loading and distribution.[5]

On the basis of the performance of different final-stage devices projected earlier, we see that neither a high-efficiency cyclone nor a granular-bed filter appears to be adequate for meeting the NSPS. A fabric filter, however, appears to do a sufficient job of controlling particulate emissions to levels well below even the more stringent gas turbine protection requirements. Note that the grade efficiency assumed for the fabric filter in this study is based on performance data reported for a baghouse in commercial use at a power station.[9] While this particular baghouse is unsuitable for use at elevated pressures and temperatures, ceramic bag filters being developed for such use are expected to have similar performance. Preliminary high-pressure and -temperature tests conducted by Westinghouse on a pilot-scale 3M/Buell ceramic bag filter have produced the grade efficiency curve shown in Figure 22, which may be compared to the grade efficiency curve of Figure 20 assumed for

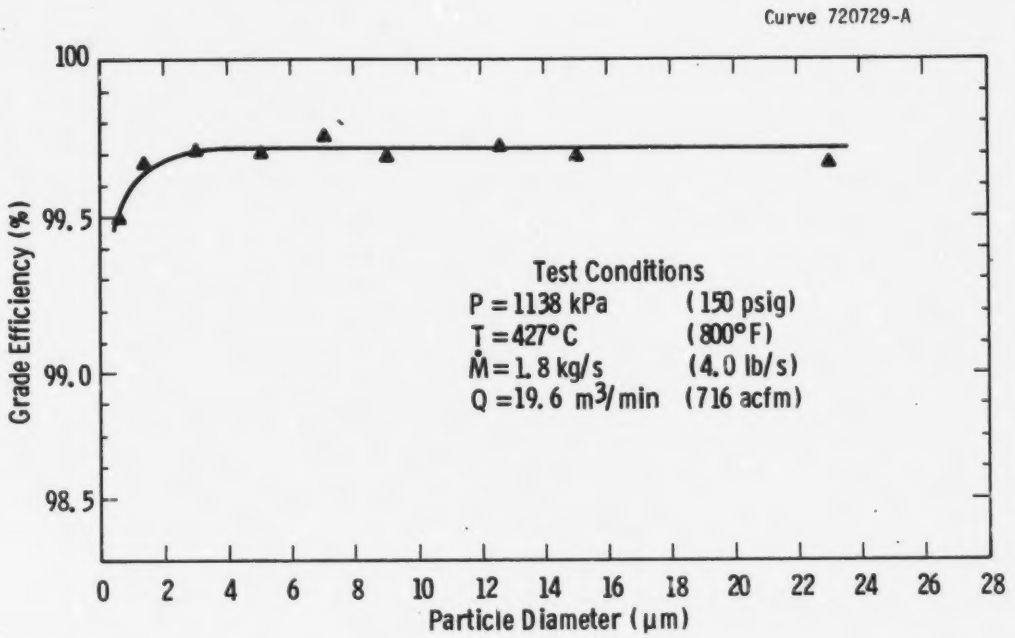

Figure 22 - Summary of Woven Ceramic-Bag Filter Test Results at Air-to-Cloth Ratio of 1.7 m/min (5.6 ft/min)

this study. Finally, note that the size distributions of the particulates penetrating the final stage for all three cases examined (a high efficiency cyclone, a granular-bed filter, and a baghouse fabric filter) are very similar and have mass median diameters of around 1 μm.

PROJECTED EMISSIONS AND PARTICULATE CONTROL PERFORMANCE FOR AFBC

This section is not presented as an engineering evaluation of final-stage control devices. It only illustrates how the model can be used and indicates the current state of information for AFBC.

Design and Operating Conditions and Feed Materials

The design and operating conditions selected for this evaluation are summarized in Table 11. For effecting a comparison with the PFBC projections made above, the coal feed rate assumed pertains to the requirement of a 180 MW_e power plant operating with a 34 percent efficiency. A deep-mined Illinois coal (Table 3) and a 20 percent excess-air level are assumed for estimating the combustion gas rate.

Table 11

AFBC COMBUSTOR OPERATING AND DESIGN CONDITIONS
SELECTED FOR STUDY

Temperature	= 871°C (1600°F)
Pressure	= 101.3 kPa (1 atm)
Superficial Gas Velocity	= 243.8 cm/s (8 ft/s)
Expanded Bed Height	= 121.9 cm (4 ft)
Bed Expansion Ratio	= 1.3
Excess Air Level	= 20%
Bed Cross-Sectional Area	= 2.67×10^6 cm^2 (2865 ft^2)

The feed materials are assumed to be the same as those selected for the PFBC study (see PFBC section for the coal and sorbent compositions and the size distributions of the feed and attrited sorbent, as well as the generated and attrited coal ash).

The particulate control device arrangement shown in Figure 23 is essentially the same as that assumed for the PFBC study except for the final cleaning stage here, a baghouse fabric filter. The grade efficiency curve assumed for the fabric filter (Figure 20) is based on performance data from a baghouse at the Sunbury Steam Electric Station.[9]

Sensitivity to Calcium-to-Sulfur Rates

This section examines the effect of increasing the Ca/S ratio of the particulate emissions from the AFBC system. Sorbent feed and attrition rates corresponding to Ca/S ratios ranging from 2 to 5 are shown in Table 12. The attrition rate for a Ca/S ratio of 2 was estimated using Rittinger's Crushing Law as follows:

Rittinger's Law is:

$$A = KW\ (U-U_{mf}),$$

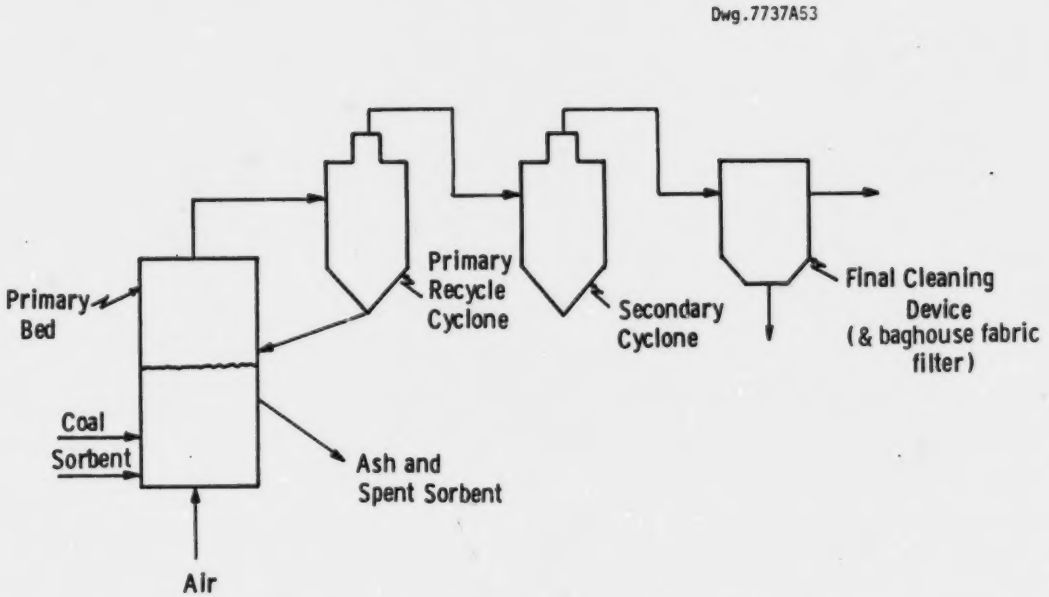

Figure 23 - Flow Scheme Assumed for AFBC System

where

A = rate of attrition

W = bed weight

U = gas superficial velocity

U_{mf} = minimum fluidizing velocity

K = constant.

Table 12

SORBENT FEED AND ATTRITION RATES CORRESPONDING TO VARIOUS CALCIUM-TO-SULFUR RATIOS

Calcium-to-Sulfur Ratio	Sorbent Feed Rate/g/s	Sorbent Attrition Rate, % of Bed Weight/hr
2	9697	3.72
3	14545	5.58
4	19393	7.44
5	24241	9.30

The constant K was evaluated by using the attrition rate assumed for a Ca/S ratio of 2 in the PFBC evaluations above, i.e.:

$$K = \frac{A_{PFBC}}{W(U-U_{mf})} \quad .$$

The assumption that the rate of sorbent attrition is directly proportional to the sorbent feed rate was made to estimate the sorbent attrition rates for the other cases examined, i.e., for Ca/S ratios of 3, 4, and 5.

As in Tables 13 through 16, the most pronounced effect of increasing the Ca/S ratio is to increase the particulate emissions from the AFBC system. Figure 24 shows the increase in the solid grain loading with increased Ca/S ratio. A higher Ca/S ratio also causes the recycle rate through the primary cyclone to increase slightly. For instance, an increase in the Ca/S ratio from 2 to 5 causes the primary cyclone recycle rate to increase by approximately 10 percent. The particle size distributions at various points of the AFBC system are shown in Figures 25 and 26 for Ca/S ratios of 2 and 5, respectively. Note that while the bed size distributions are essentially the same in both cases, the effect of increasing the Ca/S ratio is to slightly shift the size distribution of the particulate emitted from each of the particle removal devices toward finer sizes.

Performance of Particle Removal Devices (AFBC)

The configuration of particle control devices envisioned for the AFBC system is shown in Figure 23. Device type and arrangement are essentially the same as envisioned for the PFBC system, and the same rationale applies for recycling bed fines and selecting a medium-efficiency primary recycle cyclone and a high-efficiency secondary cyclone. Because of the relatively lower temperatures and the ambient pressure, a wider choice of final-stage cleaning devices exists for the AFBC system. Possible candidates are a fabric filter, an electrostatic precipitator, and a granular-bed filter.

Table 13

AFBC PARTICULATE EMISSION PROJECTIONS FOR A CALCIUM-TO-SULFUR RATIO OF 2

		Sorbent	Ash	Total
Feed to Bed, g/s		9696.5	3183.7	12880.2
Bed Draw-off, g/s		2978.5	247.9	3226.4
Overhead from bed, g/s		47446.7	6129.1	53575.8
Primary Cyclone Recycle Rate, g/s		40728.8	3193.3	43922.1
Primary Cyclone Emission				
Mass rate, g/s		6718.0	2935.8	9653.8
Grain loading,	g/m^3	46.36	20.26	66.62
	(gr/scf)	(20.26)	(8.85)	(29.11)
Secondary Cyclone Emission				
Mass rate, g/s		1648.0	278.3	1926.3
Grain loading,	g/m^3	11.37	1.92	13.29
	(gr/scf)	(4.97)	(0.84)	(5.81)
Secondary Cyclone Overall Efficiency		75.46	90.52	80.0
Final-Stage Device Emission				
Mass rate, g/s		4.03	0.62	4.65
Grain loading,	g/m^3	0.028	0.0043	0.032
	(gr/scf)	(0.012)	(0.0019)	(0.014)
Final-Stage Overall Efficiency		99.76	99.78	99.77

Table 14

AFBC PARTICULATE EMISSION PROJECTIONS FOR A CALCIUM-TO-SULFUR RATIO OF 3

	Sorbent	Ash	Total
Feed to Bed, g/s	14545.0	3183.7	17728.7
Bed Draw-off, g/s	4462.4	360.9	4823.3
Overhead from Bed, g/s	52619.6	5816.6	58436.2
Primary Cyclone Recycle Rate, g/s	42536.9	2993.8	45530.7
Primary Cyclone Emission			
Mass rate, g/s	10082.6	28228.0	12905.4
Grain loading, g/m^3	69.58	19.48	89.05
Grain loading, (gr/scf)	(30.40)	(8.51)	(38.92)
Secondary Cyclone Emission			
Mass rate, g/s	24.83	274.3	2757.3
Grain loading, g/m^3	17.13	1.89	19.03
Grain loading, (gr/scf)	(7.49)	(0.83)	(8.31)
Secondary Cyclone Overall Efficiency	75.37	90.28	78.6
Final-Stage Device Emission			
Mass rate, g/s	6.07	0.61	6.68
Grain loading, g/m^3	0.042	0.0042	0.046
Grain loading, (gr/scf)	(0.018)	(0.0019)	(0.020)
Final-Stage Overall Efficiency	99.76	99.78	99.77

Table 15

PFBC PARTICULATE EMISSION PROJECTIONS FOR A CALCIUM-TO-SULFUR RATIO OF 4

		Sorbent	Ash	Total
Feed to Bed, g/s		19393.0	3183.7	22576.7
Bed Draw-off, g/s		5935.5	464.0	6399.5
Overhead from Bed, g/s		57360.8	5535.6	62896.4
Primary Cyclone Recycle Rate, g/s		43903.3	2816.8	46720.1
Primary Cyclone Emission				
Mass rate, g/s		13457.5	2718.8	16176.3
Grain loading,	g/m^3	92.86	18.76	111.62
	(gr/scf)	(40.58)	(8.19)	(48.78)
Secondary Cyclone Emission				
Mass rate, g/s		3323.0	270.3	3593.3
Grain loading,	g/m^3	22.93	1.87	24.80
	(gr/scf)	(10.02)	(0.82)	(10.84)
Secondary Cyclone Overall Efficiency		75.31	90.06	77.79
Final-Stage Device Emission				
Mass rate, g/s		8.13	0.61	8.74
Grain loading,	g/m^3	0.056	0.0042	0.062
	(gr/scf)	(0.025)	(0.0018)	0.027
Final-Stage Overall Efficiency		99.76	99.78	99.77

Table 16

PFBC PARTICULATE EMISSION PROJECTIONS FOR A CALCIUM-TO-SULFUR RATIO OF 5

		Sorbent	Ash	Total
Feed to Bed, g/s		24241.0	3183.7	27424.7
Bed Draw-off, g/s		7395.5	565.7	7961.2
Overhead from Bed, g/s		61873.5	5268.9	67142.4
Primary Cyclone Recycle Rate, g/s		45028.2	2650.9	47679.1
Primary Cyclone Emission				
Mass rate, g/s		16845.4	2618.0	19463.4
Grain loading,	g/m^3	116.24	18.07	134.3
	(gr/scf)	(50.79)	(7.89)	(58.67)
Secondary Cyclone Emission				
Mass rate, g/s		4169.0	266.3	4435.3
Grain loading,	g/m^3	28.77	1.84	30.61
	(gr/scf)	(12.57)	(0.80)	(13.37)
Secondary Cyclone Overall Efficiency		75.25	89.83	77.21
Final-Stage Device Emission				
Mass rate, g/s		10.2	0.6	10.8
Grain loading,	g/m^3	0.07	0.0041	0.0741
	(gr/scf)	(0.031)	(0.0018)	(0.033)
Final-Stage Overall Efficiency		99.76	99.78	99.77

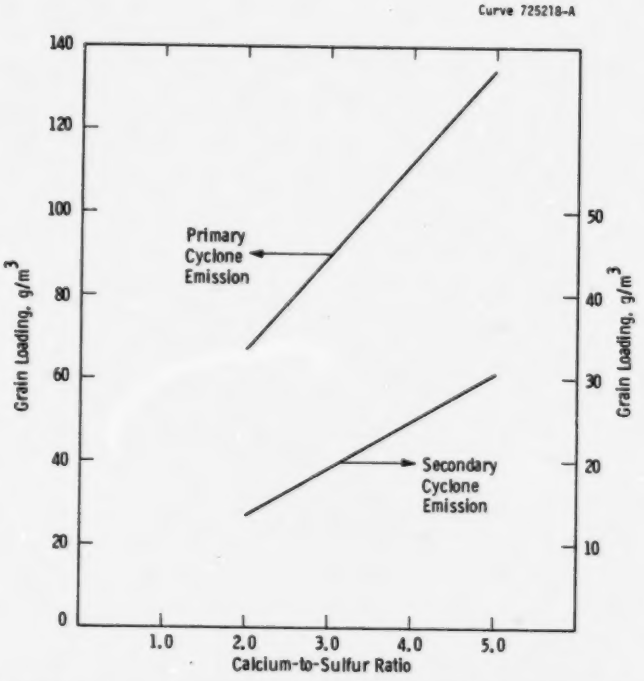

Figure 24 - Increase in Solids Grain Loading with Calcium-to-Sulfur Ratio

To gain a perspective on the particulates that may typically be emitted from an AFBC system using high-sulfur coals, refer to the projections made in Table 13 and Figure 25 for a Ca/S ratio of 2. In Figure 25 the final stage of particle removal is assumed to be a fabric filter. The effect of substituting for the final-stage fabric filter a high-efficiency cyclone (Figure 13), an electrostatic precipitator (Figure 27), and a granular-bed filter (Figure 14) is shown in Figure 28. While the size distribution of the particulate emitted using different final stages is not significantly different, note the marked difference in the emitted grain loadings for these specific final-stage control devices. This is not a general assessment of these devices.

Compliance with New Source Performance Standards

The NSPS of 12.9 ng/J (0.03 lb/MBtu) applicable to particulates translates to approximately 0.045 g/m^3 (0.02 gr/scf) for AFBC.

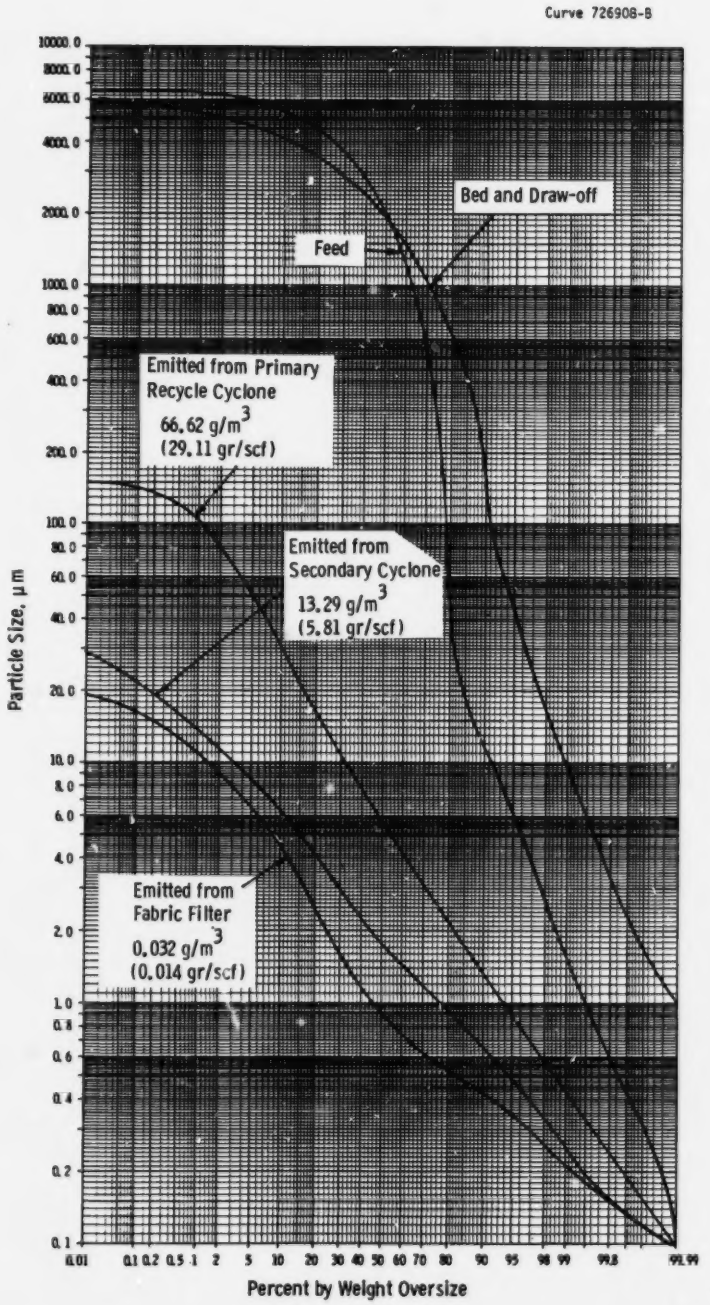

Figure 25 - Size Distributions and Loadings for a Calcium-to-Sulfur Ratio of 2 (AFBC)

Reproduced from best available copy.

On the basis of the performance of different specific final-stage devices projected earlier as examples, only the fabric filter appears to do an adequate job of controlling particulate emissions to NSPS levels. Note that the particulate emission projections pertain to a plant using a coal with a high-sulfur content (and consequently a high sorbent feed rate) and a high ash content, and are also based on an assumption of high sorbent attrition. Modifications to the design of these devices may permit them all to perform acceptably, and these examples should not be considered a general performance assessment.

A low-sulfur and a low-ash coal and a low rate of sorbent attrition will decrease the lost solid emissions, and one or all of the other third-stage devices considered could perhaps do an adequate job of controlling particulate emissions to NSPS levels.

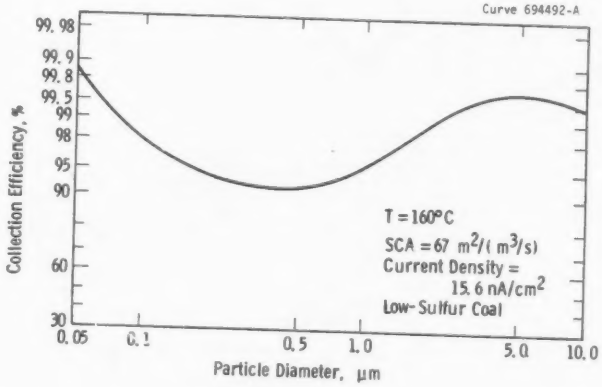

Figure 27 - Grade Efficiency for a Cold-Side Electrostatic Precipitator[10]

(Note: This grade efficiency is used as a reference and is not necessarily representative of performance on an actual AFBC plant)

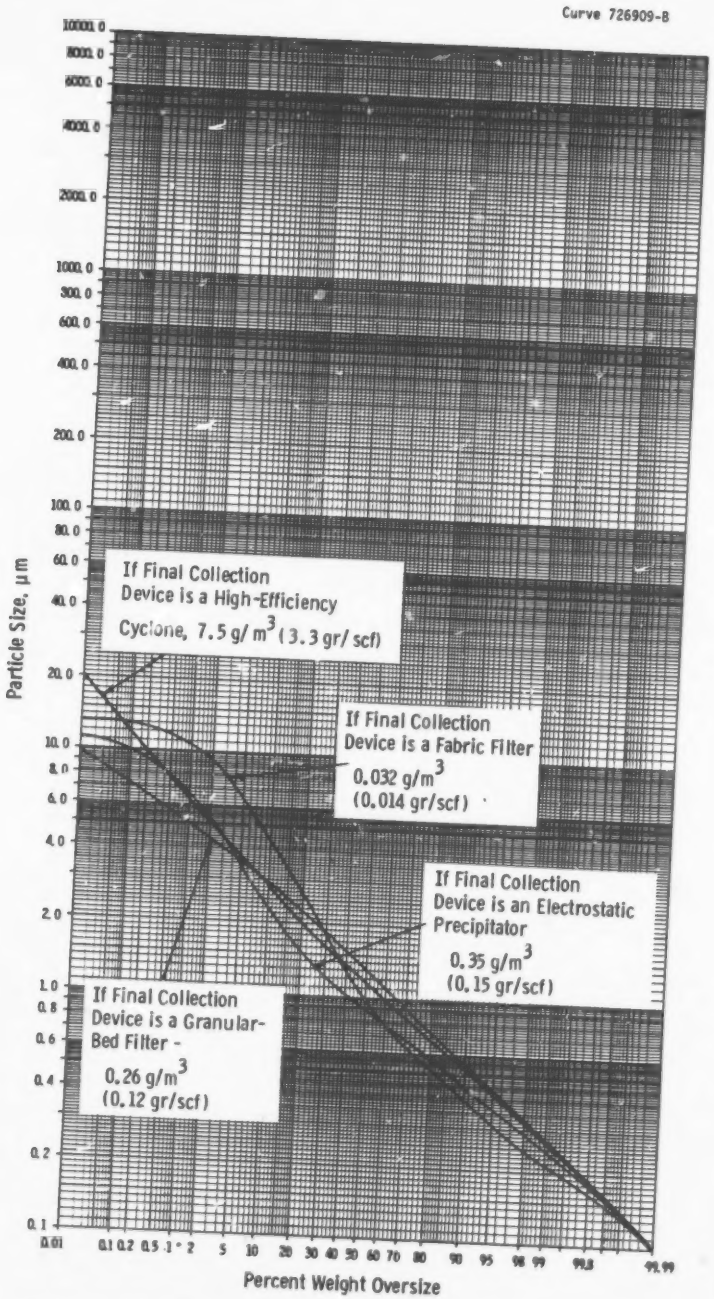
Curve 726909-B
Particle Size, µm
Percent Weight Oversize
If Final Collection Device is a High-Efficiency Cyclone, 7.5 g/m³ (3.3 gr/scf)
If Final Collection Device is a Fabric Filter 0.032 g/m³ (0.014 gr/scf)
If Final Collection Device is an Electrostatic Precipitator 0.35 g/m³ (0.15 gr/scf)
If Final Collection Device is a Granular-Bed Filter - 0.26 g/m³ (0.12 gr/scf)

Figure 28 - Results of Using Different Final-Stage Cleaning Devices

Reproduced from best available copy.

5. PARAMETRIC STUDIES

BACKGROUND

The sensitivity of a system to recycle cyclone efficiency, sulfur sorbent attrition rate, and superficial gas velocity is examined here for a PFBC case. The parameters selected for the base case are summarized in Table 17. Figure 29 shows the flow scheme assumed for the study. The size distributions assumed for the feed sorbent, for the coal ash generated in the bed, and for the attrited sorbent and ash material are the same as those selected for the PFBC and AFBC evaluations performed in Section 3. The size distributions are reproduced in Figure 30 for convenience. Grade efficiency curves for the base case recycle cyclone, as well as for another more efficient recycle cyclone, are shown in Figure 31. As seen in Figure 28, the particulate control train is comprised of a primary recycle cyclone, a secondary cyclone, and a final-stage granular-bed filter. The secondary cyclone is assumed to be a conventional, high-efficiency, Ducon cyclone (Refer to Figure 13 for the grade efficiency curve; the grade efficiency curve assumed for the granular-bed filter is shown in Figure 14). The base case results are summarized in Table 18 and Figure 32.

RECYCLE CYCLONE

Two cases were investigated. In the first case a recycle cyclone was not used. For the second case a more efficient cyclone than that employed for the base case was used. The results are shown in Table 19 and Figures 33 and 34. The primary effect of fines recycle is to decrease the lost solid emissions, to very slightly decrease the amount of 100-to-1500 μm particles in the bed, and to produce a finer distribution of emitted solids. Note that although the grain loading from the bed for the base case is lower than that for the nonrecycle case

Table 17

PARAMETERS INPUT TO THE PROGRAM FOR THE BASE CASE

Bed Area	= 7609 cm^2
Expanded Bed Height	= 257 cm
Bed Voidage	= 0.4
Superficial Gas Velocity	= 213 cm/s
Gas Density	= 0.00305 g/cm^3
Gas Viscosity	= 0.00045 g/cm-s
Sorbent Feed Rate	= 210 g/s
Ash Feed Rate	= 47 g/s
Sorbent Density	= 2.8 g/s
Ash Density	= 0.68 g/cm^3

Table 18

BASE CASE RESULTS

	Sorbent	Ash	Total
Feed F_o, g/s	210	47	257
Draw-off F_1, g/s	151.1	10.2	161.3
Draw-off as Percent of Feed, %	71.9	21.8	62.8
Attrited A_2, g/s	50.1	11.1	61.2
Elutriated F_2, g/s	8.8	25.6	34.5
Total Bed Carry-over (A_2 + F_2), g/s	58.9	36.8	95.7
Attrited A_2 as Percent of Total Carry-over, %	85	30.3	31.6
Elutriated F_2 as Percent of Total Carry-over, %	15	69.7	68.4
Overhead from Bed, g/s	1309.8	58.1	1367.9
Recycle to Bed, g/s	1251	21.3	1272.3
Total Bed Carry-over (Emission) Grain Loading, g/m^3	15.3	9.55	24.85
First Cleaning Device Emission, g/m^3	3.51	1.08	4.59
Second Cleaning Device Emission, g/m^3	0.071	0.019	0.09

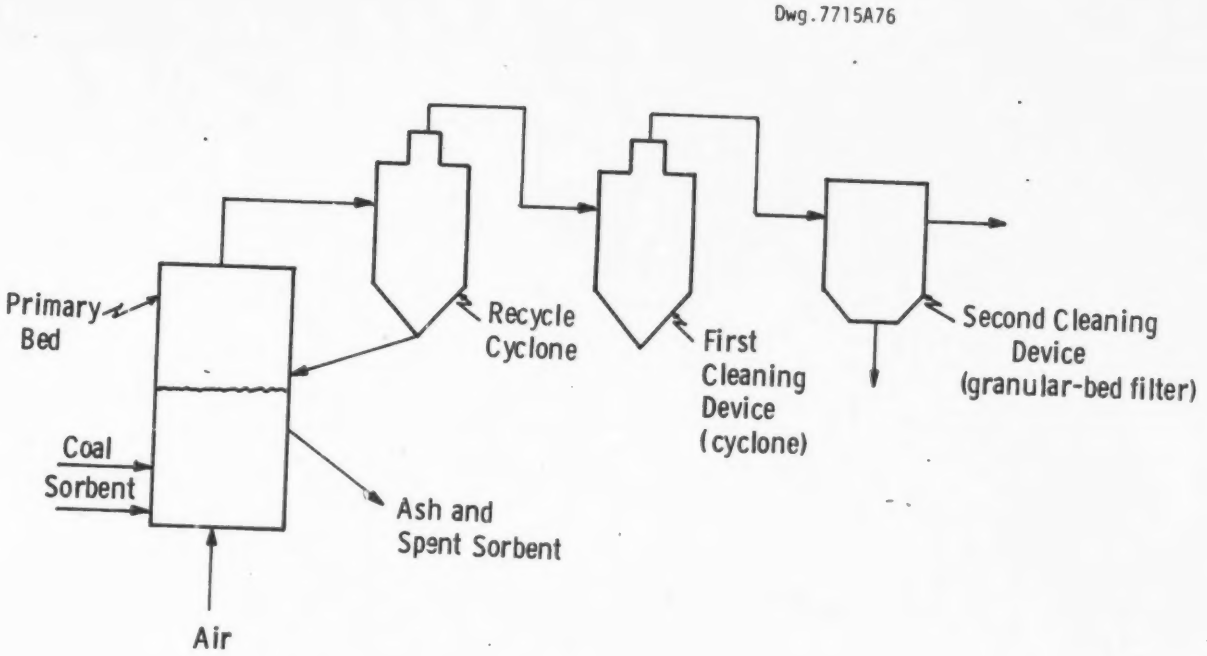

Figure 29 - Flow Scheme for Parametric Studies

(24.86 g/m^3 versus 30.61 g/m^3), the base case grain loading emitted from the first cleaning device exceeds that for the nonrecycle case. This is because the size distribution of the solids emitted from the recycle cyclone in the base case is coarser than that of the solids emitted from the bed in the nonrecycle case. Consequently, the overall efficiency of the first cleaning device is slightly higher in the nonrecycle case. As in Table 19, a higher efficiency recycle cyclone accentuates the aforementioned effects while also increasing the magnitude of the recycle stream by approximately 16 percent.

SUPERFICIAL VELOCITY

Four cases were studied for which the gas superficial velocities were 150 , 125, 75, and 50 percent of the base case velocity. The base case sorbent and ash feed rates were multiplied by factors of 3/2, 5/4, 3/4, and 1/2, respectively, to maintain the gas:solid ratio at the base

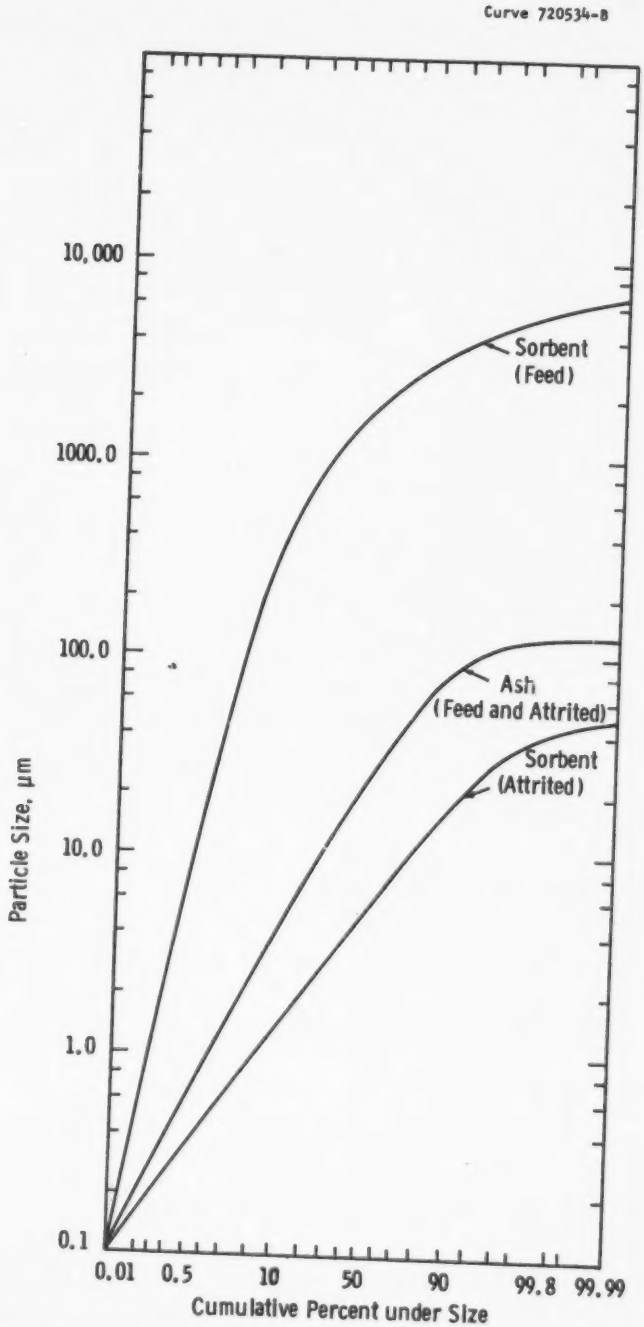

Figure 30 - Typical Feed and Attrited Size Distributions

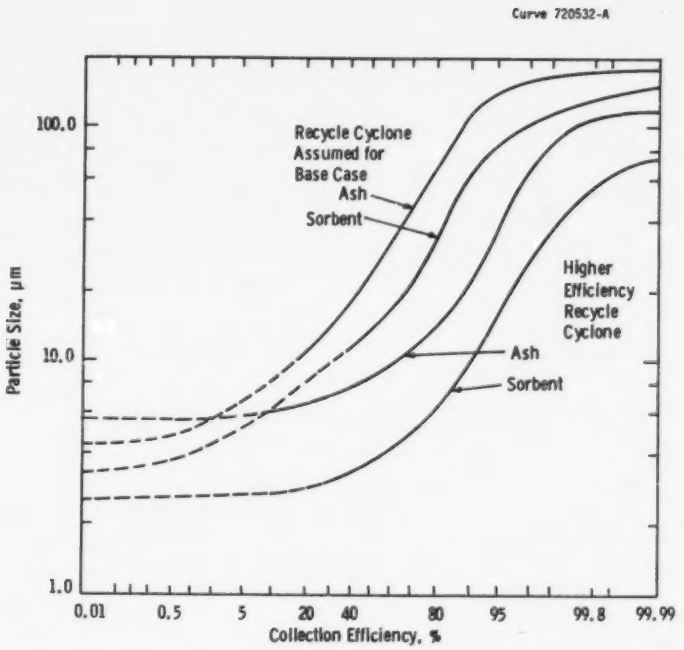

Figure 31 - Grade Efficiencies of Recycle Cyclone

case value. The following form of Rittinger's Law was used to estimate the sorbent attrition rates at the different velocities:

$$\frac{A_B}{A} = \frac{U_B - U_{mf}}{U - U_{mf}} \quad ,$$

where

A_B = rate of sorbent attrition assumed for the base case

A = rate of sorbent attrition at another gas velocity, U

U_B = base case gas velocity

U_{mf} = minimum fluidizing velocity.

The results shown in Table 20 and Figure 35 have been multiplied by factors of 2/3, 4/5, 4/3, and 2, respectively, to make them comparable to the base case flow on a per unit coal basis.

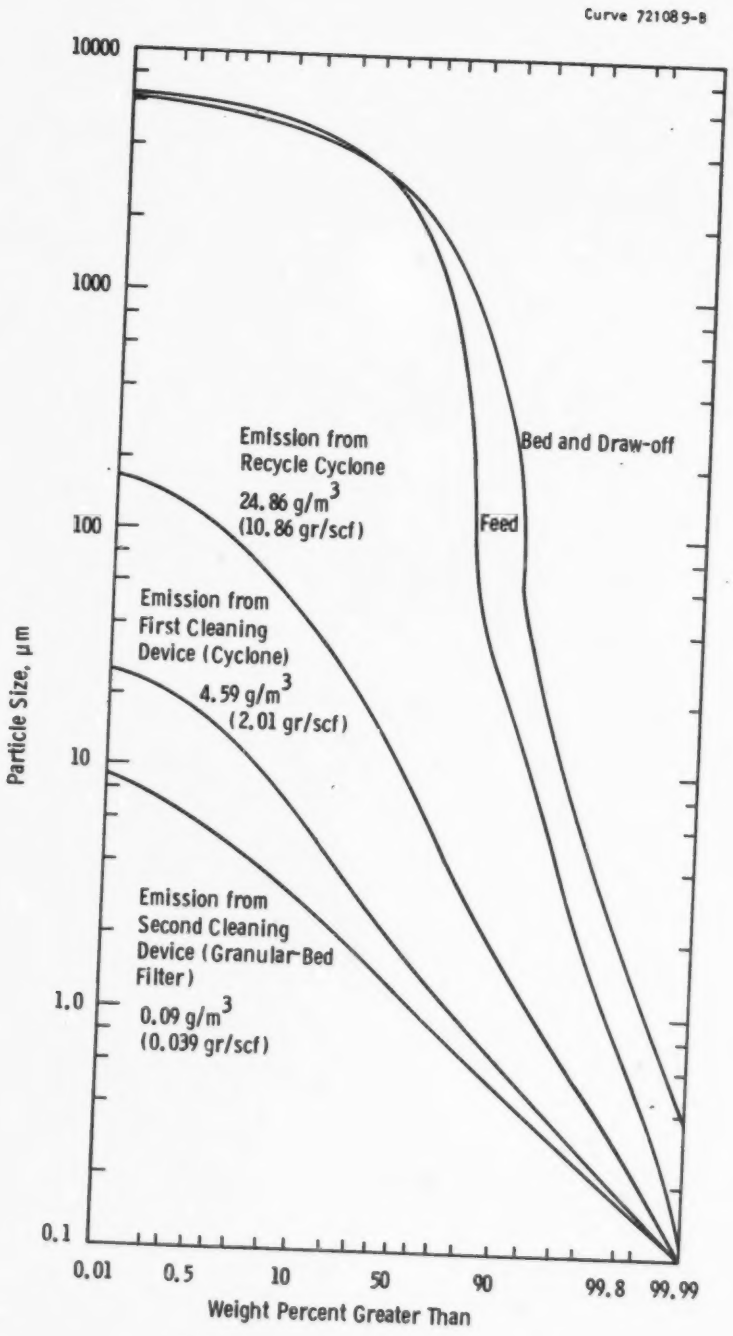

Figure 32 - Base Case Results

Table 19

RESULTS WITH DIFFERENT RECYCLE CYCLONES

Case	Fluidized-Bed Combustor							Particulate Control Train	
	Bed Draw-off		Overhead from Bed, g/s	Recycle Rate, g/s	Emission from Recycle Cyclone			Emission from Cyclone, g/m^3	Emission from Granular-Bed Filter, g/m^3
	g/s	% Feed Rate			g/s	% Feed Rate	Loading g/m^3		
Base Case	161.3	62.8	1367.9	1272.3	95.7	37.2	24.86	4.59	0.09
No Recycle Cyclone	139.2	54.2	117.84	0.0	117.84[a]	45.8[a]	30.61[a]	4.56	10.091
Higher Efficiency Recycle Cyclone	172.1	67	1557.2	1472.3	84.9	33	22.05	4.65	0.092

[a]Since there is no recycle cyclone, these refer to the bed emission.

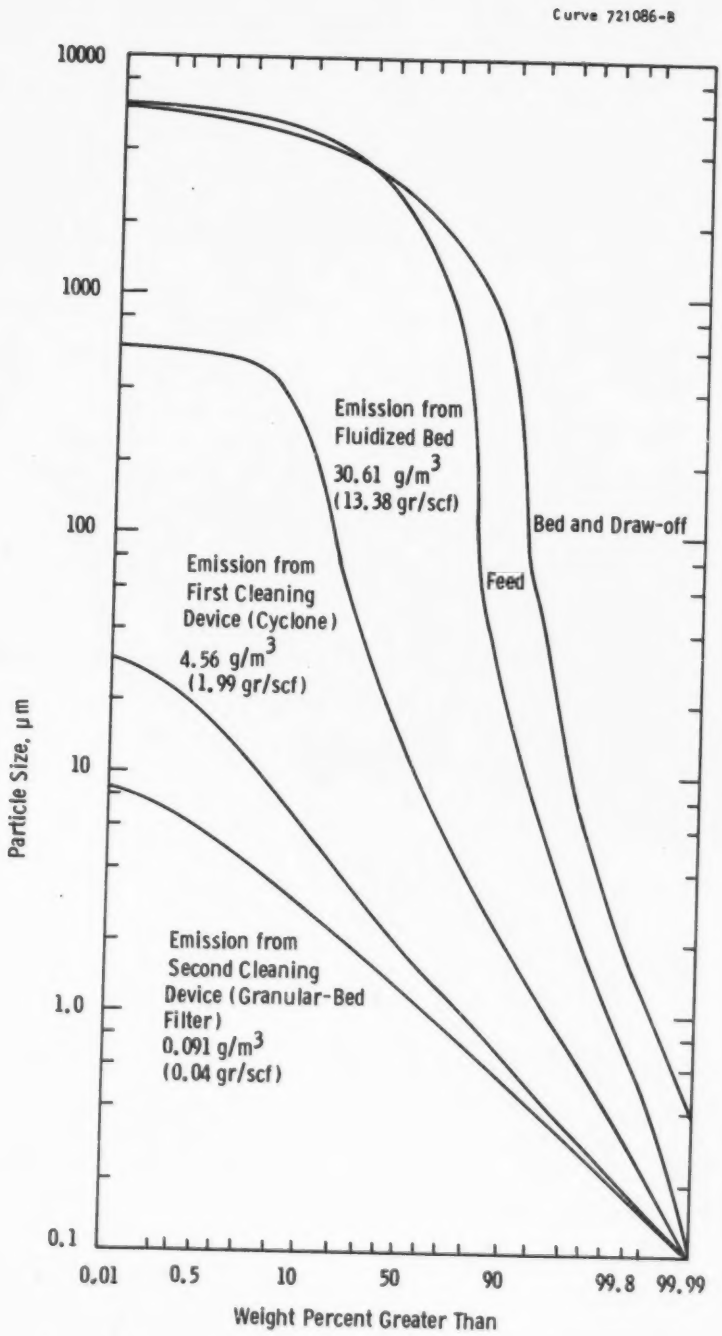

Figure 33 - Results without Fines Recycle

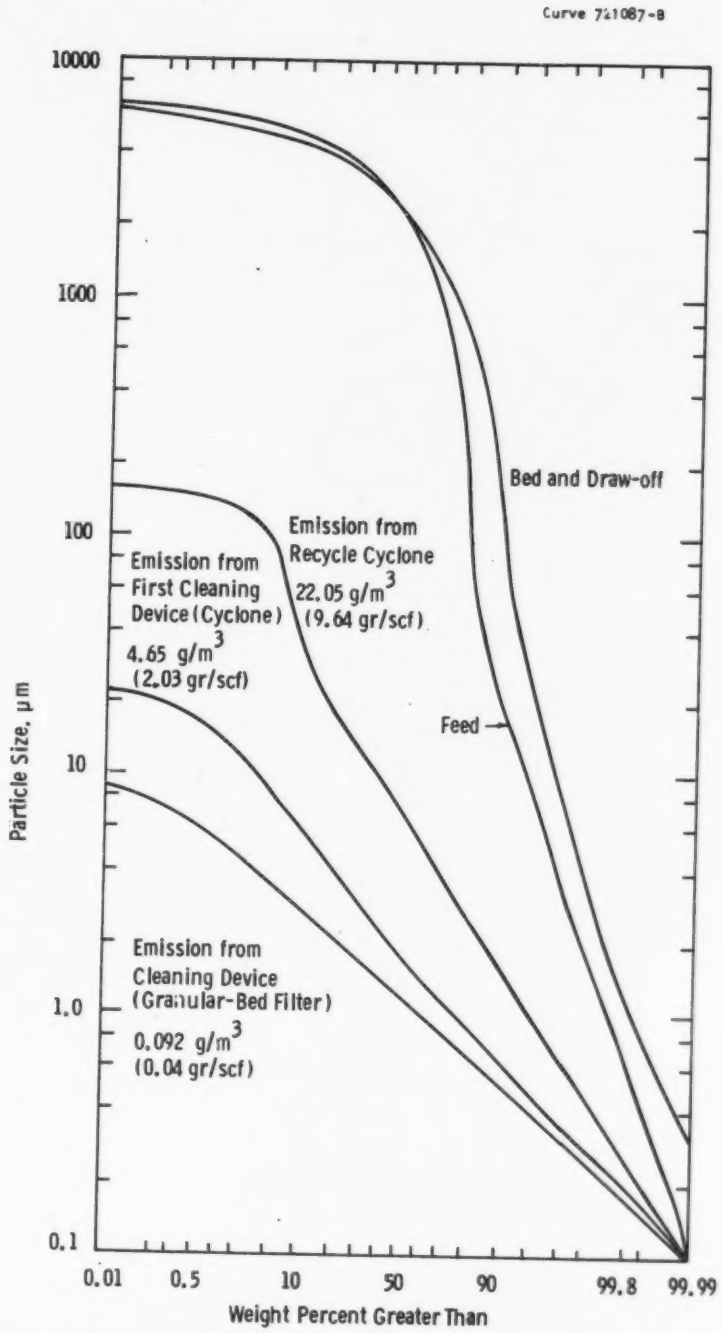

Figure 34 - Results with a More Efficient Recycle Cyclone

Table 20

RESULTS WITH DIFFERENT SUPERFICIAL VELOCITIES

Case	Fluidized-Bed Combustor							Particulate Control Train	
	Bed Draw-off		Overhead from Bed, g/s	Recycle Rate, g/s	Emission from Recycle Cyclone			Emission from Cyclone, g/m^3	Emission from Granular-Bed Filter, g/m^3
	g/s	% Feed Rate			g/s	% Feed Rate	Loading, g/m^3		
Base Case	161.3	62.8	1367.9	1272.3	95.7	37.2	24.86	4.59	0.09
Velocity 150% of Base Case Velocity	151.5	59	3789.5	3684.04	105.5	41	27.4	1.52	0.092
Velocity 125% of Base Case Velocity	157.5	61.3	2348	2248.7	99.5	38.7	25.85	1.88	0.095
Velocity 75% of Base Case Velocity	170.6	66.4	696.1	609.5	86.4	33.6	22.45	4.09	0.081
Velocity 50% of Base Case Velocity	187.7	73	285.7	216.4	69.3	27	18.0	3.149	0.062

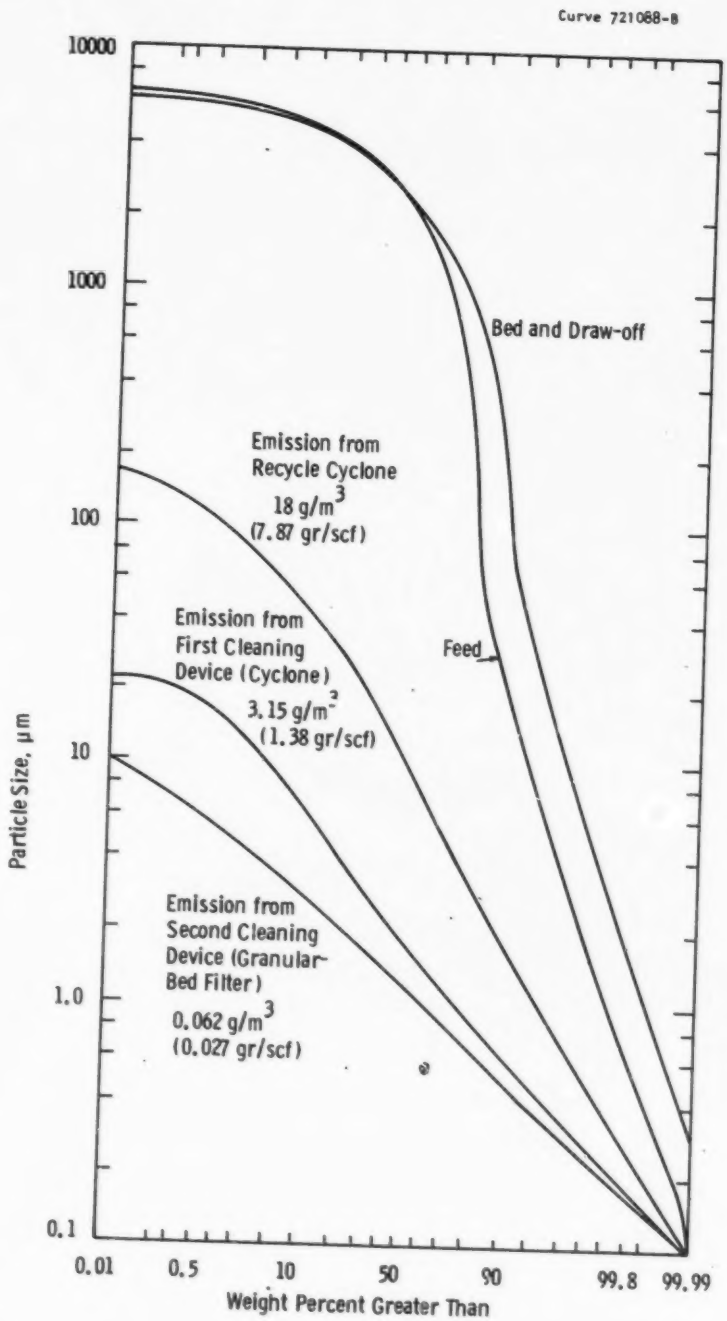

Figure 35 - Gas Velocity Used is 50% of Base Case Value

The effect of a higher gas velocity is to increase elutriation and, consequently, increase the carry-over and recycle rates through the recycle cyclone. Lower gas velocities produce the opposite effect - lower carry-over and recycle rates. While different superficial gas velocities do not significantly alter the grain loading, they very strongly influence the recycle rates, as seen in Figure 36. This result is of interest for sizing the recycle cyclone and dip leg, and also for estimating the erosion rate of the convective heat transfer surface above the bed.

ATTRITION RATE

Three cases were investigated for which the sulfur sorbent attrition rates were reduced by factors of 2, 4, and 10, respectively, of the base case attrition rate. The results are shown in Table 20 and Figure 37. Variations in the attrition rate do not significantly alter the carry-over and recycle rates. The effect of a lower attrition rate is to reduce the particulate emissions from the bed (a tenfold reduction in the attrition rate, for instance, halves the grain loading) and shift the size distribution of the emitted solids from that assumed for the attrited material to one more typical of elutriation by itself. Note that our model assumes that all the attrited fines escape the recycle cyclone. In reality, a portion of the attrited material will be captured by the recycle cyclone and recycled to the bed. If the effect of attrition is to produce fines <10 μm by abrasion, however, rather than large fragments, our assumption will model the real situation well. Finally, note that while the result of a tenfold reduction in the base case attrition rate is to approximately halve the recycle cyclone emission, the emissions from the subsequent cleaning devices (cyclone and granular-bed filter) are reduced by a factor of 3, because the size distribution of the solids escaping the recycle cyclone in the base case is much finer than that for the case for which the attrition rate was reduced tenfold. Consequently, the overall efficiencies of both

cleaning devices is larger in the latter case. This result serves to illustrate the increase in solid grain loading that may be expected from the final cleaning stage with very friable sorbent materials.

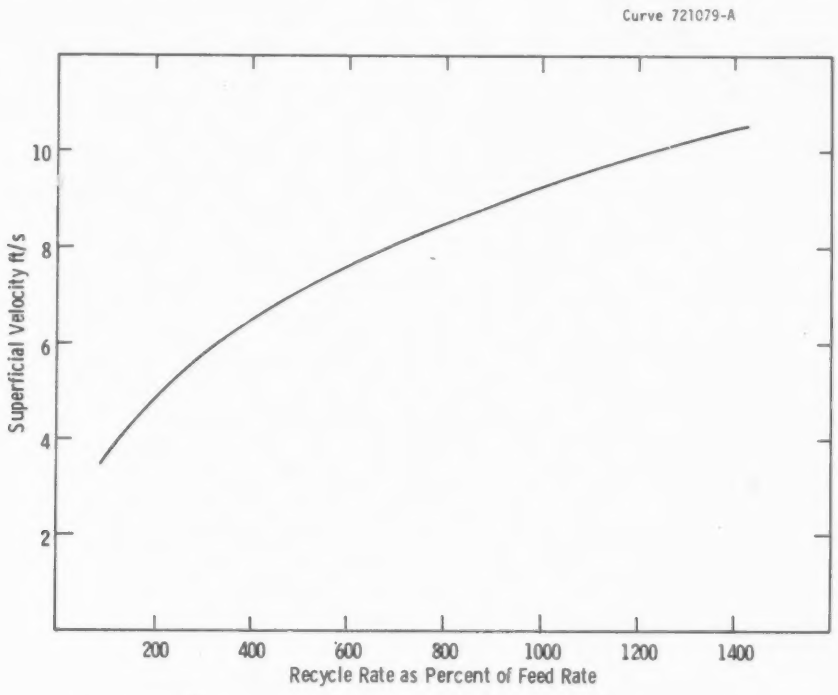

Figure 36 - Increase in Recycle Rate with Gas Velocity

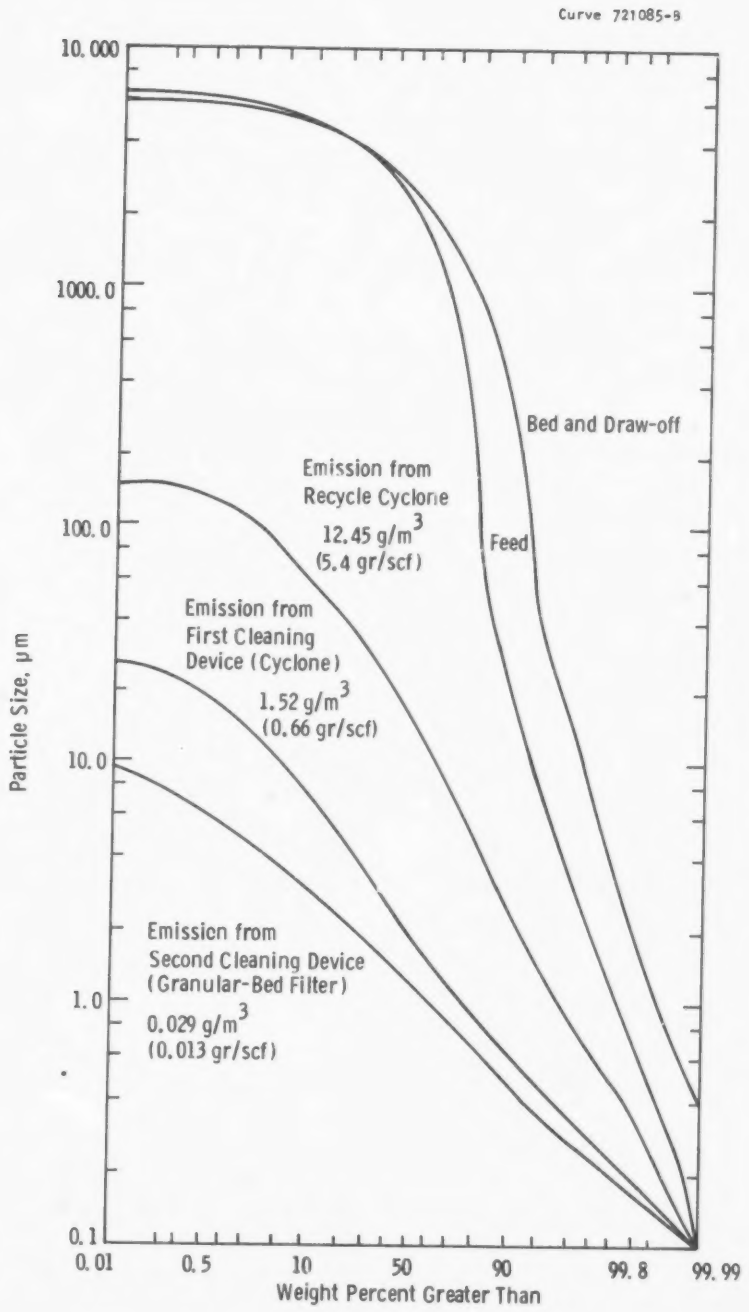

Figure 37 - Results with a Tenfold Reduction in Sorbent Attrition Rate

Table 21

RESULTS WITH DIFFERENT RATES OF SORBENT ATTRITION

Case	Fluidized-Bed Combustor							Particulate Control Train	
	Bed Draw-off		Overhead from Bed, g/s	Recycle Rate, g/s	Emission from Recycle Cyclone			Emission from Cyclone, g/m^3	Emission from Granular-Bed Filter g/m^3
	g/s	% Feed Rate			g/s	% Feed Rate	Loading, g/m^3		
Base Case (Attrition 6.2%/hr)	161.3	62.8	1367.9	1272.3	95.7	37.2	24.86	4.59	0.09
Attrition 3.1%/hr	187.8	73.1	1297.6	1228.4	69.2	26.9	17.97	2.89	0.056
Attrition 1.55%/hr	201.09	78.3	1263.5	1207.6	55.9	21.7	14.52	2.03	0.039
Attrition 0.62%/hr	209.3	81.4	1243.3	1195.4	47.9	18.6	14.45	1.52	0.29

6. REFERENCES

1. Kunii, D., and O. Levenspiel, Fluidization Engineering, New York John Wiley & Sons; 1969.

2. Yagi, S., and T. Aochi, Paper presented at the Society of Chemical Engineers (Japan), Spring Meeting, 1955.

3. Wen, C. Y., and R. F. Hashinger, AIChE Journal, 6: 220; 1960.

4. O'Connell, L., Personal communication to D. H. Archer, April 1979.

5. Wenglarz, R. A., et al., Hot Gas Cleaning for Pressurized Fluidized Bed Combustion Power Plants, Final Report prepared for EPRI by Westinghouse Research & Development Center, Pittsburgh, PA, 1980.

6. Merrick, D., and J. Highley, Particle Size Reduction and Elutriation in a Fluidized Bed Process, A.I.Ch.E. Symposium Series No. 137, Vol. 70; 1974: 366.

7. Lancaster, B. W., Granular Bed Filter Tests, Westinghouse R&D Research Memo 75 - 8 x 1 - PDUPS - M5, 1975.

8. Keairns, D. L. et al. Pressurized Fluid-Bed Combustor - Gas Cleaning/ Turbine Systems Integration for Economic Electric Energy Cost, Sixth International Conference on Fluidized Bed Combustion, Atlanta, GA, 1980.

9. Spagnola, H., Operating Experience and Performance at the Sunbury Baghouse. Symposium on Particulate Control in Energy Processes, 1976.

10. McCain, J. D., J. P. Gooch, W. B. Smith, Results of Field Measurements of Industrial Particulate Sources and Electrostatic Precipitator Performance, J. Air Pollution Control Association, 25 (2):117; 1975.

APPENDIX A

SOLUTION TECHNIQUES

Fundamental to the successful use of the formulation in Section 1 is the ability to solve the general performance equations (6) and (7) of the text for each species efficiently and accurately. Initially, we attempted a direct numerical integration using the technique of a Gaussian quadrature. This method ran into problems of numerical instability when parameters more typical of fluidized-bed processes were used. Subsequently, a couple of methods were developed that overcame this problem. In the first (henceforth referred to as method 1) the folded integrations in equation (6) are performed analytically by using suitable approximations for the integrand over relatively small size intervals. The second method (method 2) is the generalization of a computational procedure communicated to us by Prof. Octave Levenspiel.[A1] In this latter method a set of expressions for the solids balance is developed that precludes the troublesome exponential term (I integral) in the final questions. A description of all three methods follows.

1. NUMERICAL INTEGRATION BY GAUSSIAN QUADRATURE

This procedure involved breaking the particle size range into many small subintervals and integrating between points. In order that the description of the method used be kept simple, an example using 2-point quadrature is offered. Reference to Figure A1 is of use for visualizing the process. Having broken the size distribution range into intervals that were typically as follows:

0.1 - 0.2, 0.2 - 0.3 ··· 0.9 - 1.0μm
1 - 2, 2 - 3 ··· 9 - 10μm
10 - 20, 20 - 30 ··· 90 - 100μm
100 - 200, 200 - 300 ··· 900, 1000μm.

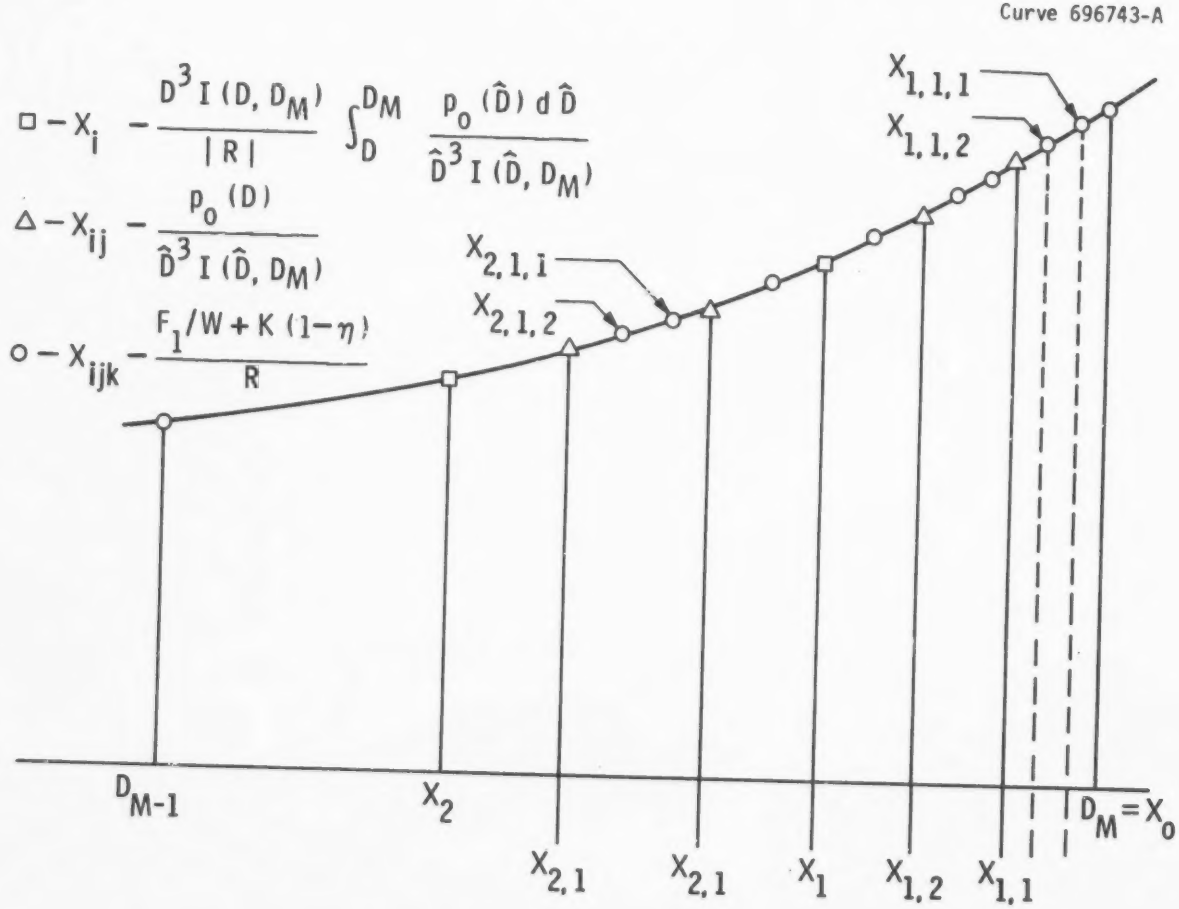

Figure A1 - Quadrature Points for Initial Integration Technique

we initiated integration from 900 to 1000μm. Using a 2-point Gaussian quadrature for the outer integral over this range requires that the integrand of equation (6) be evaluated at two points between 900 and 1000μm, labeled X_1, X_2. The integrand of interest, however, contains an integral from D to D_M = 1000μm. Therefore, a 2-point Gaussian quadrature was used to evaluate this second integral from X_1 to $X_o = D_M$ and X_2 to X_1, and this required evaluation of the integrand of the second or inner integral at two points on each of these intervals ($X_{1,1}$, $X_{1,2}$ and $X_{2,1}$, $X_{2,2}$). Finally, note that the second integrand contains the $I(D,D_M)$ function which is an integral itself, as defined by equation (7). This required evaluation of the I integral integrand at two points on the four subintervals ($X_{1,1}$ to X_o, $X_{1,2}$ to $X_{1,1}$, $X_{2,1}$ to $X_{1,2}$ and $X_{2,2}$ to $X_{2,1}$). These eight points are denoted as $X_{1,1,1}$, $X_{1,1,2}$, $X_{1,2,1}$ etc. in Figure A1. A FORTRAN program was written to carry out this procedure and was found to work well when compared to published examples.[A2] A numerical problem arose, however, when parameters more typical of fluidized-bed combustion processes were entered. The problem arose because the attrition rate expression used became very small for the smaller particle sizes. Since this term appeared in the denominator of the integrand of the I function, it caused the I function to become so small that underflow errors occurred. For example, typical parameters from 0.1 to 0.2 μm were:

$$F_1/W \doteq 3 \times 10^{-5} \text{ sec}^{-1}$$

$$K(1-\eta) \doteq 1 \times 10^{-3} \text{ sec}^{-1}$$

$$R \doteq 10^{-7} \text{ cm/sec}$$

$$\left[\frac{F_1/W + K(1-\eta)}{R}\right](\Delta D) \doteq 10^{3} \quad .$$

When these numbers were placed in the exponential of the I integral, the result was numbers smaller than 10^{-304}, which the Univac 1108 cannot handle.

Inspection of the general performance equation reveals that the troublesome I function appears in the denominator of the second integral and in the numerator of the outermost integral. These terms should, in fact, cancel each other to a large extent, and the quotient should remain well behaved. The problem with the method employed initially was that it required that the terms be calculated separately and only then could the division be performed.

The method that we developed subsequently resulted from an attempt to find suitable approximations that would allow the folded integrations to be performed analytically, incorporating the quotient of the I terms, and thereby avoiding the problem of calculating the individual terms.

2. METHOD 1

The technique was initiated by breaking the particle size distribution into small intervals over which several parameters could be considered to be of constant value equal to their average value over that particular interval. For example, if D_L were the maximum particle size, then over the interval from D_{L-1} to D_L the values of the elutriation rate constant, the cyclone efficiency, and the particle size distribution function were defined as follows:

$$K_{L-1} = (K(D_L) + K(D_{L-1}))/2 \tag{A1}$$

$$\eta_{L-1} = (\eta(D_L) + \eta(D_{L-1}))/2 \tag{A2}$$

$$P_{o,L-1} = (p_o(D_L) + p_o(D_{L-1}))/2 \quad . \tag{A3}$$

The rate of attrition expression was then forced to fit the form

$$R = - AD \quad . \tag{A4}$$

Commonly used[A2] expressions are of the following forms:

$$R = -k \tag{A5}$$

$$R = -kD \tag{A6}$$

$$R = -k(D - D_{MIN}) \quad . \tag{A7}$$

The form of equation (A4) could easily be fitted by the following definition for the constant A:

$$A_{L-1} = A(D_{L-1} \leq D \leq D_L) = \left(\frac{R(D_L)}{D_L} + \frac{R(D_{L-1})}{D_{L-1}} \right) \Big/ 2 \quad . \tag{A8}$$

These approximations allowed the general performance equation to be evaluated explicitly over each interval of interest by use of the following procedure.

The I integral function over the last interval can be written as follows:

$$I(D_{L-1} \leq D \leq D_L, D_L) = e^{-\int_{D_L}^{D} \left(\frac{\frac{F_1}{W} + K(1-\eta)}{R} \right) dD} \quad . \tag{A9}$$

If the approximations are inserted, and Q is defined as

$$Q_{L-1} = \frac{\frac{F_1}{W} + K_{L-1}(1-\eta_{L-1})}{A_{L-1}} \quad , \tag{A10}$$

then

$$I(D_{L-1} \leq D \leq D_L, D_L) = e^{-\int_{D}^{D_L} \frac{Q_{L-1} dD}{D}} = \left(\frac{D}{D_L} \right)^{Q_{L-1}} \quad . \tag{A11}$$

If the following notation is used,

$$I_{L-j} = \left(\frac{D_{L-j}}{D_{L-j+1}} \right)^{Q_{L-j}} \quad , \tag{A12}$$

it follows that in general,

$$I(D_{L-j-1} \leq D \leq D_{L-j}, D_L) = \left(\frac{D}{D_{L-j}}\right)^{Q_{L-j}} I_{L-j} \quad , \tag{A13}$$

where

$$I_L = 1 \quad .$$

Through this judicious choice of approximations, the I function has been expressed in a form readily amenable to the necessary subsequent integrations.

The next step of the process required that the I integral be inserted into the second integral of the triple integral and all explicitly executable operations be performed. Considering, again, the first interval back from D_{L-1} to D_L, one obtains the following:

$$S(D_{L-1} \leq D \leq D_L) = \int_D^{D_L} \frac{P_o dD}{D^3 I(D, D_L)} = \int_D^{D_L} \frac{P_{o,L-1} dD}{D^3 \left(\frac{D}{D_L}\right)^{Q_{L-1}} I_L} \tag{A14}$$

or

$$S(D_{L-1} \leq D \leq D_L) = \frac{(P_{o,L-1})}{(Q_{L-1} + 2)(D_L^2)(I_L)} \left[\left(\frac{D}{D_L}\right)^{-(Q_{L-1} + 2)} - 1\right] . \tag{A15}$$

Repeated substitutions of the appropriate terms for the I function over subsequent intervals led to the following general term for the S function:

$$S_{L-j}(D) = \frac{(p_{o,L-j})}{(Q_{L-j} + 2)(D^2_{L-j+1})(I_{L-j+1})} \left[\left(\frac{D}{D_{L-j+1}}\right)^{-(Q_{L-j} + 2)} - 1\right] + S_{L-j+1} \quad , \tag{A16}$$

with $S_L = 0$ and

$$S_{L-j}(D) = \int_{D_{L-j} \le D \le D_{L-j+1}}^{D_L} \frac{p_o dD}{D^3 I(D,D_L)} \quad . \tag{A17}$$

It then remained to insert this still readily integrable form into the outermost integral. The outer integral had been broken into sub-intervals as indicated:

$$\int_{D_{min}}^{D_L} \frac{\hat{D}^3 I(\hat{D},D_L) \int_{\hat{D}}^{D_L} \frac{p_o dD}{D^3 I(D,D_L)}}{|R|} d\hat{D} = \int_{D_1 - D_{min}}^{D_2} + \int_{D_2}^{D_3} + \int_{D_{L-1}}^{D_L} = \sum_{j=1}^{L-1} E_j \quad . \tag{A18}$$

Again, considering the first interval back from D_L, one obtains

$$E_{L-1} = \int_{D_{L-1}}^{D_L} \frac{\hat{D}^3 \left(\frac{\hat{D}}{D_L}\right)^{Q_{L-1}} I_L \left\{ \frac{(p_{o,L-1})}{(Q_{L-1}+2)(D_L^2)(I_L)} \left[\left(\frac{\hat{D}}{D_L}\right)^{-(Q_{L-1}+2)} - 1 \right] \right.}{(A_{L-1}\hat{D})}$$

$$\left. + S_L \right\} d\hat{D} \quad . \tag{A19}$$

Performing the indicated integrations, one obtains

$$E_{L-1} = \frac{(p_{o,L-1})}{(Q_{L-1}+2)(A_{L-1})} \left[\left(- \frac{D_{L-1}}{D_L} \right) - \frac{1 - \left(\frac{D_{L-1}}{D_L}\right)^{(Q_{L-1}+3)}}{Q_{L-1}+3} \right]$$

$$+ \frac{(S_L)(I_L)(D_L^3)}{(Q_{L-1}+2)(A_{L-1})} \left[1 - \frac{D_{L-1}}{D_L} \right]^{(Q_{L-1}+3)} \quad , \tag{A20}$$

or

$$E_{L-1} = B_{L-1} + C_{L-1} \quad . \tag{A21}$$

Repeated substitutions and integrations led to the following general forms:

$$B_{L-j} = \frac{(P_{o,L-j+1})}{(Q_{L-j}+2)(A_{L-j})}\left[\left(1-\left(\frac{D_{L-j}}{D_{L-j+1}}\right)\right) - \frac{1-\left(\frac{D_{L-j}}{D_{L-j+L}}\right)^{(Q_{L-j}+3)}}{Q_{L-j}+3}\right] \quad \text{(A22)}$$

$$C_{L-j} = \frac{(S_{L-j+1})(I_{L-j+1})(D^3_{L-j+1})}{(Q_{L-j}+3)(A_{L-j})}\left[1-\left(\frac{D_{L-j}}{D_{L-j+1}}\right)^{(Q_{L-j}+3)}\right] . \quad \text{(A23)}$$

In subsequent computations employing these formulations, we observed a numerical problem when calculating the values of the C_{L-j} terms. The problem was traced to the S_{L-j} term, and in fact it turned out to be a problem very similar in nature to the one experienced in the Gaussian quadrature method. For small values of D the rate was small and the Q term became very large (on the order of 10^3). This caused the term $\left(\frac{D_{L-j}}{D_{L-j+1}}\right)^{-(Q_{L-j}+2)}$ of S_{L-j} to become very large, since $D_{L-j} < D_{L-j+1}$. To avoid this problem we had to insert the recursion formula for S_{L-j} into the equation for C_{L-j} and cancel terms, thereby avoiding explicitly calculating S_{L-j}. Carrying out the algebraic manipulations led to the final expression for the C terms:

$$C_{L-j} = \left\{\left(\frac{D_{L-j+1}}{(Q_{L-j}+3)(A_{L-j})}\right)\left(1-\left(\frac{D_{L-j}}{D_{L-j+1}}\right)^{Q_{L-j}+3}\right)\right\}$$

$$\left\{\frac{P_{o,L-j+1}}{Q_{L-j+1}+2}\left(1-\left(\frac{D_{L-j+1}}{D_{L-j+2}}\right)^{(Q_{L-j+1}+2)}\right)\right. \quad \text{(A24)}$$

$$\left. + \frac{C_{L-j+1}\left(\frac{D_{L-j+1}}{D_{L-j+2}}\right)^{(Q_{L-j+1}+2)}}{\left(\frac{D_{L-j+2}}{(Q_{L-j+1}+3)(A_{L-j+1})}\right)\left(1-\left(\frac{D_{L-j+1}}{D_{L-j+2}}\right)^{(Q_{L-j+1}+3)}\right)}\right\},$$

where $C_{L-1} = 0$. As one can see, the troublesome terms have canceled out, and as Q becomes very large the C term approaches

$$C_{L-j} = \frac{(D_{L-j+1})(P_{o,L-j+1})}{(A_{L-j})(Q_{L-j})(Q_{L-j+1})} \tag{25}$$

in a well-behaved fashion.

To summarize what has been accomplished, then, the method of evaluating the triple integral of the general performance equations has been reduced to the following steps:

1. Divide the range of particle sizes into convenient intervals.
2. Calculate the average values of P_o, n, K, A, and Q for each interval.
3. Use equation (A24) to calculate the C_{L-j} terms.
4. Use equation (A22) to calculate the B_{L-j} terms.
5. Add B_{L-j} to C_{L-j} to get the E_{L-j} terms, and then sum the E_{L-j} terms to yield the value of the triple integral.

This value is compared with W/F_o, a new choice of F_1 is made, and the procedure is repeated until convergence is reached. A simple method of linear interpolation has been used to determine F_1 and has been found to converge rapidly in 4 to 6 iterations when the process is initiated with values of $F_1 = 0.1\ F_o$ and $F_1 = 0.9\ F_o$.

Having determined the value of F_1 that satisfies equation (6), we can determine the size distribution of the solids in the bed and in the draw-off, P_1, by applying equation (9) as shown in Reference 2. By inserting the proper expressions for I and R into equation (9), we can determine $P_1(D)$. Over the first interval, for example, the expression becomes

$$P_1(D_{L-1} \leq D \leq D_L) = \frac{(F_o)(P_{o,L-1})}{(W)(A_{L-1})(Q_{L-1}+2)} \left[1 - \left(\frac{D}{D_L}\right)^{(Q_{L-1}+2)}\right] . \tag{A26}$$

The following recursion formula for $P_{1,L-j}$ terms, in general, can be determined:

$$P_{1,L-j} = \left(\frac{F_o}{W(A_{L-j})}\right)\left(\frac{P_{o,L-j}}{Q_{L-j}+2}\right)\left(1 - \left(\frac{D_{L-j}}{D_{L-j+1}}\right)^{Q_{L-j}+2}\right) + \left(\frac{W}{F_o}\right)(A_{L-j+1})(p_{1,L-j+1})\left(\frac{D_{L-j}}{D_{L-j+1}}\right)^{Q_{L-j}+2} , \quad \text{(A27)}$$

with $p_{1,L} = 0$.

Once p_1 (D) has been calculated in this manner, it is possible to compute F_2 and A_2 by two different routes. From the defining equation for the elutriation rate constant (equation [1]) one can obtain F_2, as indicated by equation (10). Substituting the expression just developed for p_1 into this equation and performing the indicated integration over the size range leads to an expression for F_2 that is algebraically cumbersome enough to require the following coding:

$$\delta_{L-j} = Q_{L-j}+3$$

$$\gamma_{L-j} = Q_{L-j}+2$$

$$B_{L-j} = D_{L-j}/D_{L-j+1}$$

$$\alpha_{L-j} = P_{o,L-j}/\gamma_{L-j}$$

$$\tau_{L-j} = (1 - B_{L-j}^{\delta_{L-j}})/\delta_{L-j}$$

$$\phi_{L-j} = \frac{\dfrac{(T_{L-j})(A_{L-j})}{(F_o)(D_{L-j+1})(1-\eta_{L-j})(K_{L-j})} - \alpha_{L-j}(1 - B_{L-j} - \tau_{L-j})}{\tau_{L-j}} ,$$

where

$$T_{L-j} = \int_{D_{L-j-1}}^{D_{L-j}} (K)(1-\eta)(P_1)dD . \quad \text{(A28)}$$

The required recursion formula for the ϕ_{L-j} terms becomes

$$\phi_{L-j-1} = (\alpha_{L-j})(1 - B_{L-j}^{\gamma_{L-j}}) + B_{L-j}^{\gamma_{L-j}} \gamma_{L-j} \quad , \tag{A29}$$

with $\alpha_L = \phi_L = 0$.

The desired value of F_2 is simply obtained from the sum

$$F_2 = \sum_{j=1}^{L-1} T_{1-j} \quad . \tag{A30}$$

Having obtained F_2 in this fashion, we can obtain the mass of attrited material by an overall mass balance on the entire system, as shown here:

$$A_2 = F_o - F_1 - F_2 \quad . \tag{A31}$$

An alternate route to the determination of F_2 is simply to integrate the attrition rate expression, over the bed size distribution and get A_2 directly as follows:

$$A_2 = \int_{D_{min}}^{D_L} \frac{3\, Wp_1(\hat{D})R(\hat{D})d\hat{D}}{\hat{D}} \quad . \tag{A32}$$

As before, the integration is performed interval by interval back from D_L. Over the first interval from D_L, for example, one obtains the expression:

$$R_{L-1} = \int_{D_{L-1}}^{D_L} \frac{3\, W\left(\frac{F_o}{WA_{L-1}}\right)\left(\frac{P_{o,L-1}}{Q_{L-1}+2}\right)\left[1 - \left(\frac{\hat{D}}{D_L}\right)^{(Q_L+2)}\right](A_{L-1})\hat{D}d\hat{D}}{\hat{D}} \quad , \tag{A33}$$

or upon performing the integration and simplification,

$$R_{L-1} = 3\,F_o D_L \left\{ \left(\frac{P_{o,L-1}}{Q_{L-1}+2} \right) \left(1 - \frac{D_{L-1}}{D_L} \right) - \left(\frac{P_{o,L-1}}{Q_{L-1}+2} \right) \left[\frac{1 - \left(\frac{D_{L-1}}{D_L} \right)^{Q_{L-1}+3}}{Q_{L-1}+3} \right] \right\} . \quad \text{(A34)}$$

In general, using the previous notation, the following relations are developed:

$$\theta_{L-j} = (\alpha_{L-j} - \alpha_{L-j+1}) + B_{L-j+1}^{\gamma_{L-j+1}} \theta_{L-j+1} \quad , \quad \text{(A35)}$$

with $\alpha_L = \theta_L = 0$ and

$$R_{L-j} = 3\,F_o D_{L-j+1} \left[\alpha_{L-j}(1 - B_{L-j}) - \theta_{L-j} \left(\frac{1 - B_{L-j}^{\delta_{L-j}}}{\delta_{L-j}} \right) \right] . \quad \text{(A36)}$$

Finally, A_2 is determined as the sum of the R terms,

$$A_2 = \sum_{j=1}^{L-1} R_{L-j} \quad , \quad \text{(A37)}$$

and F_2 is then obtained through the mass balance of equation (A31). Agreement between the two methods in subsequent calculations has been shown to be satisfactory; one can obtain the flow of material into the recycle cyclone, however, by replacing the $(1-\eta)$ term in equation (A32) with unity and then the recycled stream flow by mass balance on the cyclone. Since knowing these terms is desirable, we prefer the method of integrating the elutriation rate expression.

The final carry-over parameter to be calculated is the size distribution of the elutriated material $p_2(D)$. This can be accomplished by direct application of equation (A32) as follows:

$$p_2(D) = (W/F_2)(1-\eta(D))(K(D))(p_1(D)) \quad .$$

3. METHOD 2

While the computer coding for implementing method 1 described above is relatively straightforward, the understanding and derivation of its various recursive formulas is undoubtedly tedious and cumbersome. Method 2 described here is the generalization of a computational procedure communicated to us by Prof. Octave Levenspiel.[1] It is based on the derivation of solid balance equations for a discrete particle size distribution such as the one shown in Figure A2.

For the flow scheme of Figure 2 of the text, the solids balance for the i^{th} size interval can be written for shrinking particles as:

$$\left(\begin{array}{l}\text{solids}\\ \text{entering}\\ \text{in feed}\end{array}\right) - \left(\begin{array}{l}\text{solids}\\ \text{leaving in}\\ \text{overflow}\end{array}\right) - \left(\begin{array}{l}\text{solids}\\ \text{leaving in}\\ \text{carry-over}\end{array}\right) + \left(\begin{array}{l}\text{solids}\\ \text{entering}\\ \text{from } (i+1)^{th}\\ \text{interval}\end{array}\right)$$
$$- \left(\begin{array}{l}\text{solids}\\ \text{leaving to}\\ (i-1)^{th} \text{ interval}\end{array}\right) - \left(\begin{array}{l}\text{solid depletion}\\ \text{due to attrition}\\ \text{within } i^{th}\\ \text{interval}\end{array}\right) = 0 \quad . \tag{A33}$$

With the usual nomenclature equation (A33) can be written as:

$$F_o p_o(D_i)\Delta D_i - F_i p_i(D_i)\Delta D_i - F_2 p_2(D_i)\Delta D_i + Wp_i(D_{i+1})R(D_{i+1})$$
$$- Wp_1(D_{i-1})R(D_{i-1}) - \frac{3Wp_b(D_i)R(D_i)\Delta D_i}{D_i} = 0 \quad . \tag{A34}$$

From equation (1) of the text, and with the assumption of backmix flow, becomes equation (A34)

$$F_o p_o(D_i)\Delta D_i - F_1 p_1(D_i)\Delta D_1 - K(D_i)Wp_1(D_i)\Delta D_i + Wp_1(D_{i+1})R(D_{i+1})$$
$$= Wp_1(D_{i-1})R(D_{i-1}) - \frac{3Wp_1(D_i)R(D_i)\Delta D_i}{D_i} = 0 \quad , \tag{A34}$$

which on simplifying gives:

$$p_1(D_i) = \frac{F_o p_o(D_i)\Delta D_i - WR(D_{i+1})p_1(D_{i+1})}{-WR(D_i) + F_1\Delta D_i + WK(D_i)\Delta D_i - \frac{3WR(D_i)\Delta D_i}{D_i}} \quad . \tag{A35}$$

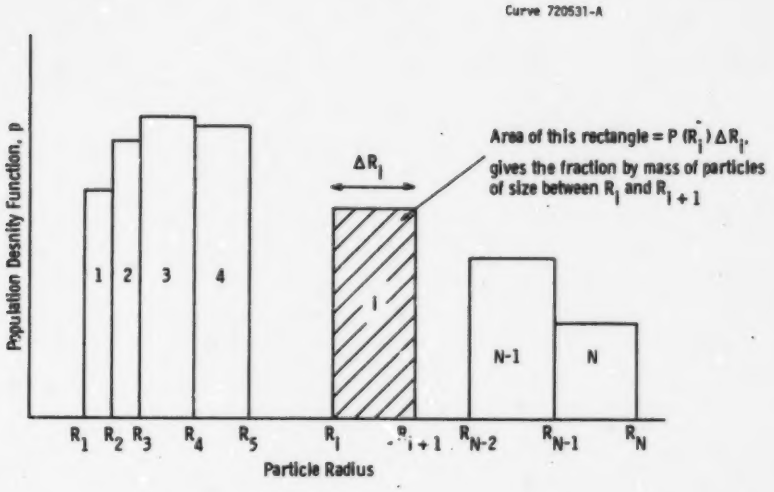

Figure A2 - Discrete Particle Size Distribution

The solution algorithm for a one-species system proceeds as follows:

1. Give F_o, W, a discrete feed particle size distribution of N size intervals, pick F_1.
2. Starting with $p_1(D_{N+1}) = 0$, recursively calculate the bed particle size distribution $p_1(D_i)$.
3. Check to see if $\sum_{i=1}^{N} p_1(D_i)\Delta D_i = 1$
4. If the constraint in step (3) is satisfied, stop. Otherwise update the value of F_1 and reiterate.

Once convergence has been obtained for F_1, the remainder of the computations do not require any iteration. The size distribution of the elutriated material is given by:

$$p_2(D_i) = \frac{K(D_i)Wp_1(D_i)}{F_2} \quad . \tag{A36}$$

The total mass rate of the attrited material is:

$$A_2 = \sum_{i=1}^{N} \frac{3Wp_1(D_i)R(D_i)\Delta D_i}{D_i} \quad . \qquad \text{(A37)}$$

REFERENCES

A1. Levenspiel O., Personal communication to D. F. Ciliberti, 1979.

A2. Kunii, D., and O. Levenspiel, Fluidization Engineering, New York, John Wiley & Sons; 1969.

APPENDIX B

PARTICULATE PROFILE PROGRAM MANUAL

PARTICULATE PROFILE PROGRAM MANUAL

TABLE OF CONTENTS

	Page
Introduction	90
1 Scope	90
2 Inputs to the Program	90
3 Elutriation Correlations	92
4 Attrition Parameters	92
5 Size Distributions	93
6 Particulate Control Devices	93
7 Data Cards	94
8 Program Subroutines	106
9 References	132

INTRODUCTION

The particulate profile program manual is comprised of two parts. The first part briefly discusses the scope of the program, details the choice of various parameters available to the user (elutriation correlations, particle removal devices, etc.), and provides card-by-card instructions in data formating. Reference to this part should generally be adequate for running the program.

The second part of the manual contains a detailed description of each subroutine in the program followed by the subroutine listing.

1. SCOPE

For a given combustor design and designated operating conditions the particulate profile program can be used to project the characteristics (particulate loading/mass rates and size distributions) of the carry-over and draw-off streams (Figure B1) from a fluidized bed, with particular regard to particle attrition and the recycle of fines to the primary bed. Additionally, it offers the means for evaluating the effectiveness of various configurations of particle removal devices. The program is useful, therefore, for gaining an understanding of the particulate loading and size distributions that might be emitted from a fluidized-bed combustor and how this is finally reflected in the gas fed to the turbine.

2. INPUTS TO THE PROGRAM

The inputs to the particulate profile program can be broadly classified into the three categories listed below:

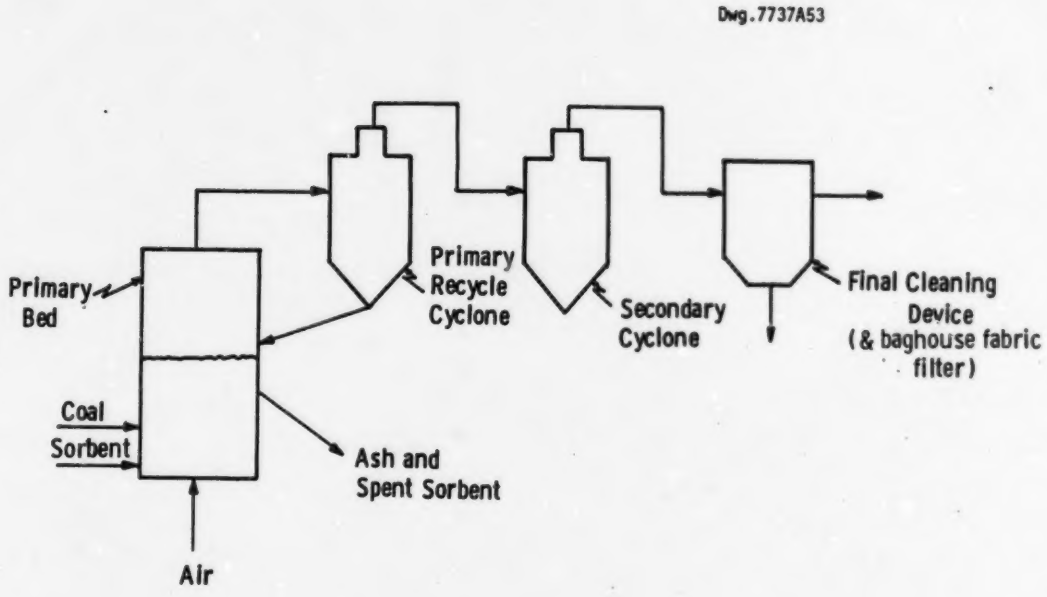

Figure B1 - Schematic of Solids Flow System

(I) Fluidizing Gas and Solid Parameters

- Gas density, viscosity, molecular weight, and superficial velocity
- Solid density and sphericity
- Solid feed size distributions

(II) Bed Parameters

- Area of cross section
- Expanded bed height
- Voidage

(III) Other Parameters

- Recycle cyclone, if any
- Elutriation correlation
- Attrition parameters
- Particulate removal train

The parameters in the first two categories are specified by the user, while the program offers a choice for those in the third. The latter are discussed in Sections 3 through 6.

3. ELUTRIATION CORRELATIONS

A choice of four empirical and/or semiempirical elutriation correlations from the literature[B1, B2] are available. These are listed below.

NAME OF ELUTRIATION CORRELATION	PROGRAM ELUTRIATION CORRELATION IDENTIFICATION NUMBER
Yagi and Aochi	1
Wen and Hashinger	2
Tanaka and Shinohara	3
Merrick and Highley	4

4. ATTRITION PARAMETERS

The attrition rate is described by an expression of the form:

$$R = k\ (D-D_{min}) \quad , \tag{B1}$$

where

R = attrition rate, cm

k = attrition rate constant, sec^{-1}

D_{min} = minimum attrited size, cm.

An estimate of the rate constant, k, may be obtained in the following manner. Assume that the experimentally reported attrition rate is on the order of 1% per hour. In other words,

$$\frac{dm/dt}{m} = \frac{0.01}{3600} = 2.7777 \times 10^{-6} \quad . \tag{B2}$$

The left-hand side of equation (2) can be expressed as:

$$\frac{dm/dt}{m} = \frac{\frac{\phi\pi D^2}{2}\frac{dD}{dt}}{\frac{\phi\pi D^3}{6}} = \frac{3}{d}\frac{dD}{dt} \quad . \tag{B3}$$

From equations (B2) and (B3),

$$R = \frac{dD}{dt} = (2.7777 \times 10^{-6}) \frac{D}{3} = 9.2593 \times 10^{-7} D \quad .$$

In general, for an attrition rate of x percent per hour, the rate expression will be $R = \frac{dD}{dt} = 9.2593 \times 10^{-7}$ Dx, which can be fitted to the form of equation (B1).

5. SIZE DISTRIBUTIONS

The particulate profile program requires particle diameter/size distribution data individually for the sorbent and ash in the feed and attrited streams. A typical sorbent feed size distribution is shown in Figure B2. The attrited sorbent size distribution also shown in Figure B2 has been taken from the UK National Coal Board's (NCB) experimental data on attrition. The ash feed size distribution is unknown. Since generally between 85 and 95% of the ash is elutriated, the assumption is made that the ash size distribution in both the feed and attrited material conforms to sizes measured by the NCB for coal-only runs. A typical distribution is shown in Figure B2.

6. PARTICULATE CONTROL DEVICES

Experimentally reported performance data in the form of size versus fractional penetration values for seven particulate control devices have been compiled in the subrouting DEVICE. These are listed below alongside the corresponding program device identification numbers.

Name/Description of Particulate Control Device	Program Device Identification Number
Ducon full-size cyclone at 871°C (1600°F)	1
Cold-side electrostatic precipator	2
Westinghouse bench-scale granular-bed filter	3
Sunbury fabric filter	4
The Argonne National Laboratory's CTIU primary (Ducon) cyclone	5
Medium efficiency cyclone	6
Tan Jet	7

The grade efficiency curves for the above devices can be seen in Figures B3 through B9.

7. DATA CARDS

This subsection contains card-by-card instructions on data formating. The general pattern followed is:

1. The format is specified (e.g., D10.4, F10.2) alongside the card number.
2. The parameters are specified in the correct order.
3. Values are assumed for the parameters, and the data card is written out in the form in which it should be punched.

Card 1 FORMAT (4D10.4)

Sorbent density g/cm^3, sorbent sphericity, ash density g/cm^3, ash sphericity.

If, for example, ρ_{sorb} = 2.5 g/cm^3, ϕ_{sorb} = 0.6, ρ_{ash} = 0.689/cm^3, ϕ_{ash} = 0.6,

the first data card will be:

2·5000D+000·6000D+000·6800D+000·6000D+00 .

Card 2 FORMAT (5D10.4)

Gas molecular weight g/g mole, gas temperature °C, gas density g/cm^3, gas viscosity g/cm-s, superficial velocity cm/s.

If, for example, M.W. gas = 28.84 g/gmole
gas temperature = 1000°C
ρ_{gas} = 3.05 x 10^{-3} g/cm^3
μ_{gas} = 4.5 x 10^{-4} g/cm-s
u = 150 cm/s.

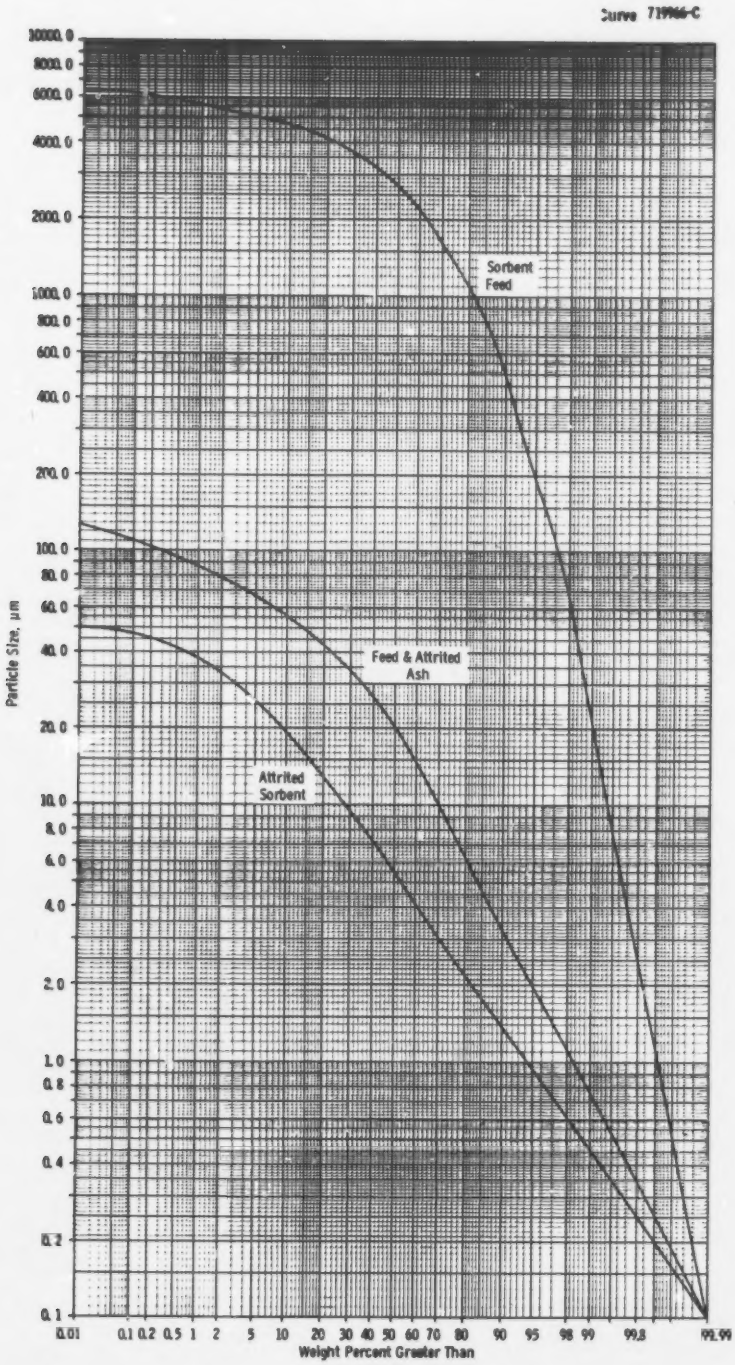

Figure B2 - Typical Feed and Attrited Size Distributions for the Sorbent and Ash

Reproduced from best available copy.

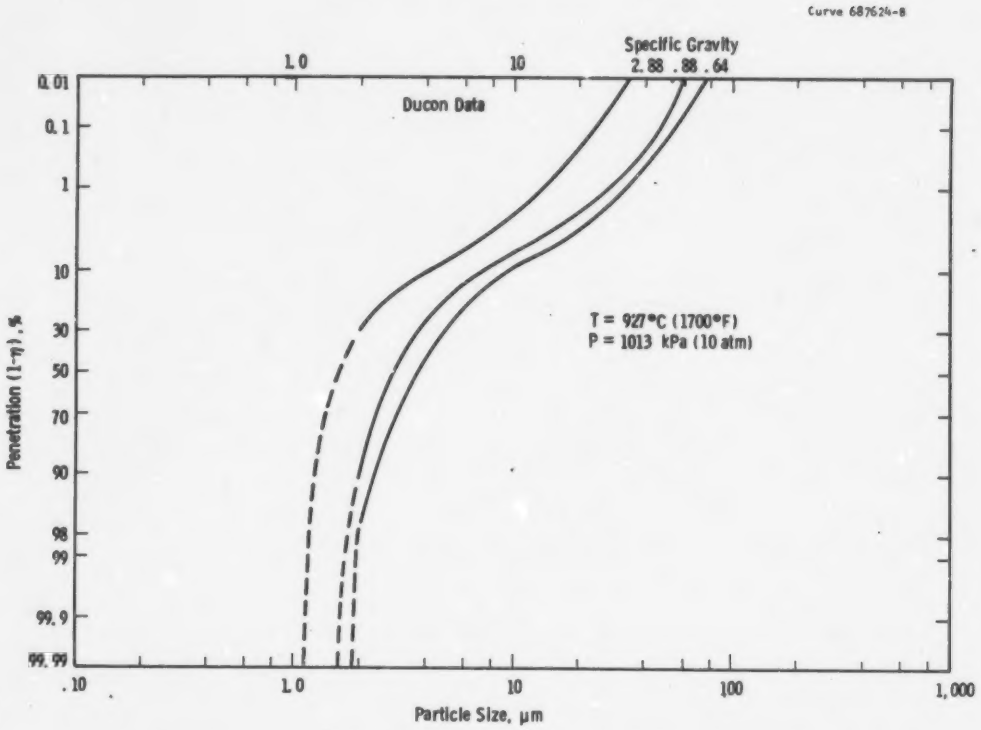

Figure B3 - Grade Efficiency for Ducon Cyclone

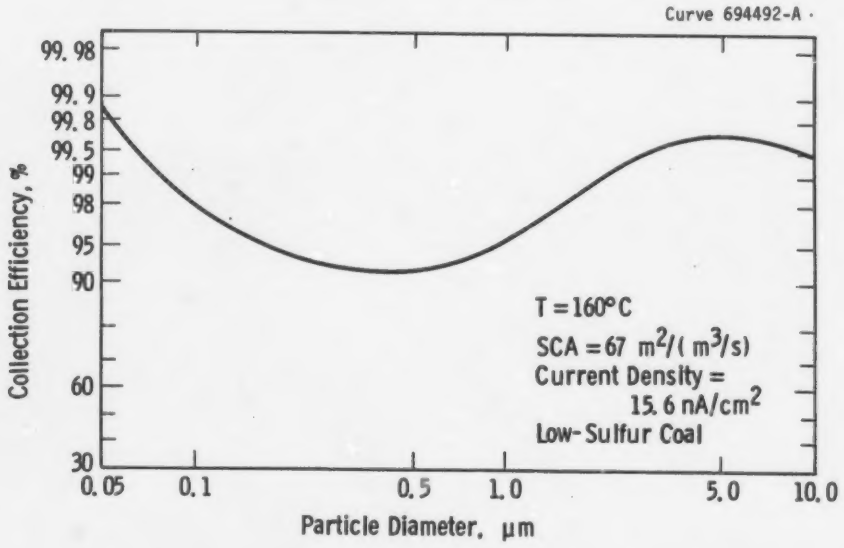

Figure B4 - Grade Efficiency for a Cold-Side Electrostatic Precipitator (10)

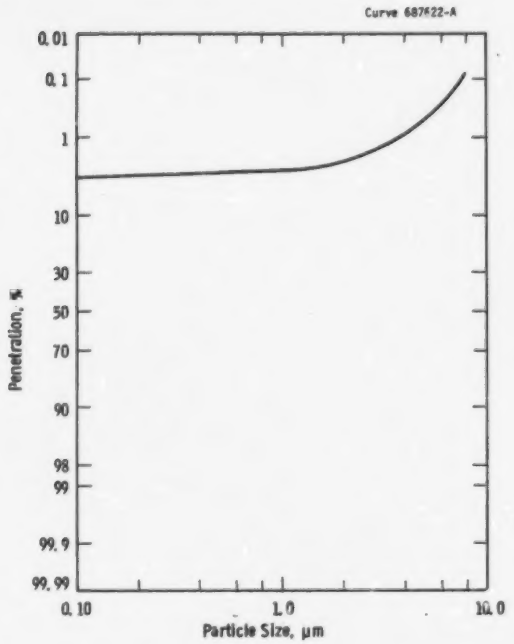

Figure B5 - Grade Efficiency for a Granular-Bed Filter

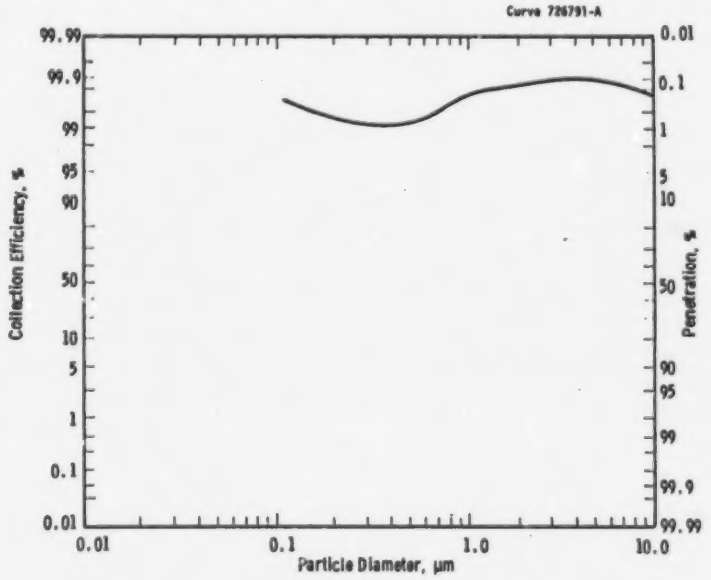

Figure B6 - Grade Efficiency Curve for Sunbury Fabric Filter

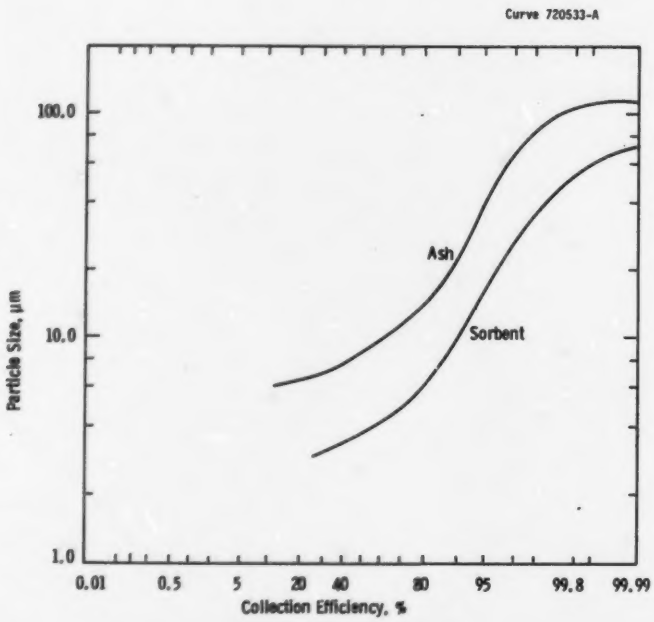

Figure B7 - Grade Efficiency Curve for Argonne National Laboratory's CTIU Ducon Primary Cyclone

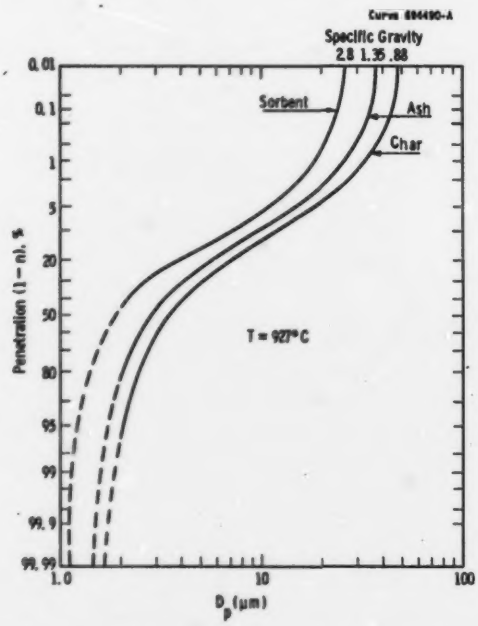

Figure B8 - Grade Efficiency Curve of a Medium Efficiency Cyclone

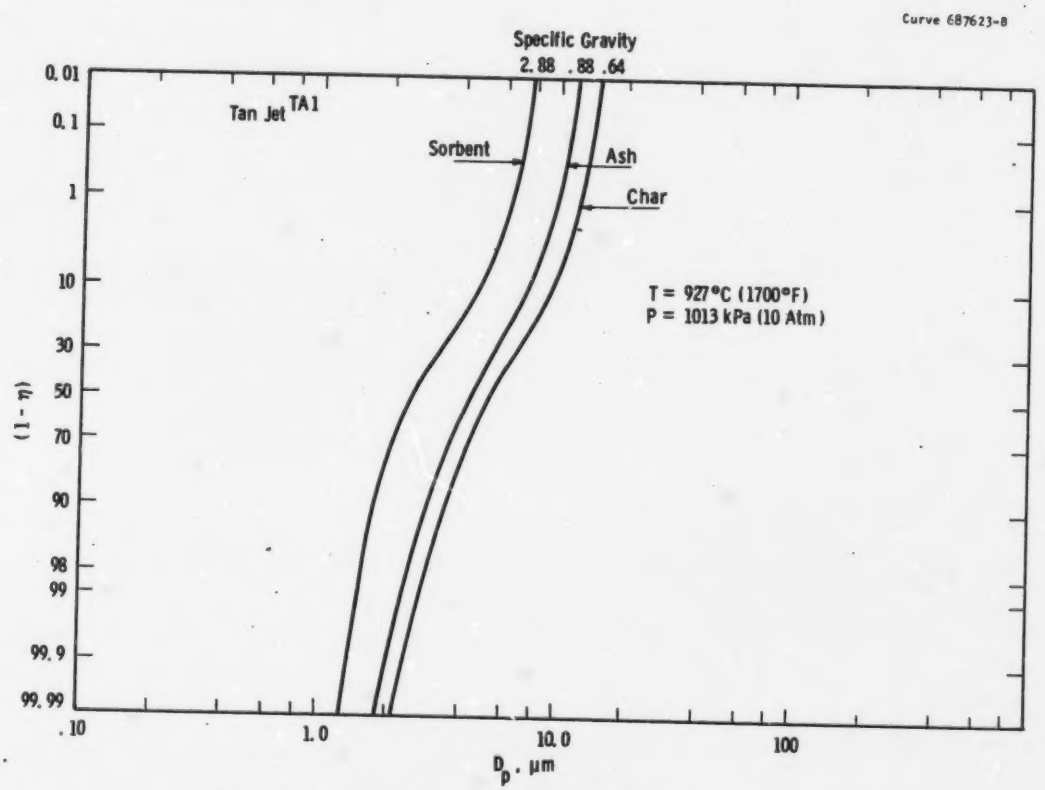

Figure B9 - Grade Efficiency Curve for Tan Jet

The second data card will be:

2·8840D+011·0000D+033·0500D-034·5000D-041·5000D+02 .

Card 3 FORMAT (3I2, 3D10.4)

Parameter for specifying recycle/nonrecycle mode, choice of recycle cyclone, if any, elutriation correlation number, constant in Merrick and Highley's correlation, mass median diameter of feed sorbent, mass median diameter of feed ash.

A value of one (1) is used to specify a recycle mode of operation. For the nonrecycle mode any positive integer other than 1 may be used (e.g., 2). The operator has a choice of the following recycle cyclones and correlations for the elutriation rate constant:

RECYCLE CYCLONE

Name/Type of Cyclone	Program Device Identification Number
Ducon full-size cyclone at 871°C (1600°F)	1
Argonne National Laboratory's CTIU primary (Ducon) cyclone	5
Medium efficiency cyclone	6
Tan Jet	7

See section 6 for the grade efficiencies of the above devices.

ELUTRIATION CORRELATIONS

Name of Correlation	Program Correlation Identification Number
Yagi and Aochi	1
Wen and Hashinger	2
Tanaka and Shinohar	3
Merrick and Highley	4

Thus, if we desire a medium-efficiency recycle cyclone, we choose Merrick and Highley's elutriation correlation with a value of 0.0015 for the constant, and if the mass median diameters of the feed sorbent and ash are 1000 and 20 μm respectively, the third data card will have the following form:

01 06 04·1500D-02 1·0000D+03 2·0000D+01 .

Card 4 FORMAT (3D10.4)

Bed cross-sectional area cm^2, expanded bed height cm, bed voidage.

If, for example, bed area = 7609 cm^2
expanded bed height = 256.8 cm
$\varepsilon = 0.4$,

the fourth data card will have the following form:

0·7609D+040·2568D+030·4000D+00 .

Card 5 FORMAT (I2)

Number of devices in the particulate removal train.

If two particulate removal devices are desired, the fifth data card will have the following form:

02 .

Card 6 FORMAT (5I2)

Sequence of particle removal devices.

Assume, for example, that a full-size Ducon cyclone followed by a granular-bed filter is desired. From Section 1 the sequence numbers of these devices are one and three, respectively. The sixth data card, therefore, has the form:

0103 .

Card 7 FORMAT (4D10.4)

Sorbent feed rate g/s, first guess for the sorbent mass fraction, ash feed rate g/s, second guess for the sorbent mass fraction.

In the two-species mode, the particle profile program is set up to do two different kinds of iterative calculations. In the first kind convergence is sought between the assumed and calculated values of the carry-over rate, $-F_1$. Based on these F_1 values (F_1 [ash] and F_1 [sorbent]), convergence is next sought for the mass fraction of the sorbent given by:

$$FG(\text{sorbent}) = \frac{F_1(\text{sorbent})}{F_1(\text{sorbent}) + F_1(\text{ash})} .$$

Recommended starting values for FG(sorbent) are 0.9 and 0.95. With this, and assuming that the sorbent and ash feed rates are given by 210 g/s and 47 g/s, the seventh data card will have the form:

0·2100D+030·9000D+000·4700D-020·9500D+00 .

Card 8 FORMAT (4D10.4)

First guess for $\left(\frac{F_1}{F_o}\right)_{\text{sorbent}}$, second guess for $\left(\frac{F_1}{F_o}\right)_{\text{sorbent}}$, first guess for $\left(\frac{F_1}{F_o}\right)_{\text{ash}}$, second guess for $\left(\frac{F_1}{F_o}\right)_{\text{ash}}$.

The explanation for this is given above (See data card 7). Recommended values are 0.1, 0.9, 0.1, and 0.5, respectively. With these values data card 8 will have the following form:

0·1000D+000·9000D+000·1000D+000·5000D+00 .

Card 9 FORMAT (4D10.4)

Sorbent attrition rate constant, minimum sorbent feed diameter, ash attrition rate constant, minimum ash feed diameter.

As explained in Section 1, the attrition rate may be given by an expression of the form:

$$\frac{dD}{dt} = \frac{k(D-D_{min})}{D} \quad ,$$

where

k = attrition constant
d_{min} = minimum attrited solid size (for convenience this may be taken as the minimum size in the solids feed distribution).

The parameters in the attrition rate expression may be evaluated on the basis of experimentally reported attrition rates (see Section 3). Typical values are:

$$R_{sorb} = 1.85 \times 10^{-7} \text{ sec}^{-1}$$
$$R_{ash} = 2 \times 10^{-5} \text{ sec}^{-1}$$
$$D_{min_{ash}} = D_{min_{sorb}} = 0.1 \text{ μm} \quad .$$

With these values card nine will have the following form:

1·8500D-070·1000D+002·0000D·050·1000D+00 .

Card 10

This card will have the form bl.

Card 10 FORMAT (I2)

Total number of points in the feed size distribution of the sorbent. A typical value might be 8, in which case this data card is simply

08 .

Cards 12 through 19 FORMAT (2F10.2)

Cards 12 through 19 will contain information on the sorbent feed size distribution, i.e., diameter versus values for the cumulative less-than function in a F10.2 format. Typically, these cards have the following form:

Card Number	Column 1 (diameter in μm)	Column 11 (cum. less-than function)
12	0.1	0.0001
13	10.0	0.011
14	60.0	0.058
15	430.0	0.29
16	1000.0	0.52
17	1700.0	0.745
18	2700.0	0.954
19	3150.0	0.9999

Card 20 FORMAT (I2)

Total number of points in the feed size distribution of the ash. A typical value might be 6, in which case this data card has the form:

b6

Cards 21 through 26 FORMAT (2F10.2)

Cards 21 through 26 will contain information on the ash feed size distribution, i.e., diameter versus values for the cumulative less-than function in a F10.2 format. Typically, these cards may have the following form:

Card Number	Column 1 (diameter in μm)	Column 11 (cum. less-than function)
21	0.1	0.0001
22	10.0	0.3
23	20.0	0.5
24	40.0	0.77
25	80.0	0.98
26	125.0	0.9999

Card 27 FORMAT (I2)

Total number of computational intervals over each of which the step size for the numerical integration pertaining to the sorbent computations is constant.

As seen from data cards 12 through 19, the sorbent feed size distribution is in the form of eight diameter-cumulative function data pairs, with the solid sizes varying from 0.1 to 3150 μm. The following step sizes are recommended:

From, μm	To, μm	Step size, μm
0.1	1.0	0.05
1.0	10.0	0.5
10.0	100.0	5.0
100.0	3150.0	50.0

Thus, the total number of computational intervals is 4, and data card 27 will be:

04 .

Note that the above are only suggested intervals, and the flexibility of choosing the step sizes rests with the user. Generally, the smaller the step sizes, the more accurate the computation, though with very fine step sizes the round-off error may become significant. Additionally, a very large number of intervals also means more core space and longer computer execution time.

Cards 28 through 31 FORMAT (2F10.2)

The upper limit of the computational interval and the (constant) step size within this interval are contained on each of these cards in a F10.2 format. Thus, based on the intervals and step sizes chosen above, data cards 28 through 31 will have the following form:

Card Number	Upper limit (1st column)	Step size (11th column)
28	1.0	0.05
29	10.0	0.5
30	100.0	5.0
31	3150.0	50.0

Card 32 FORMAT (I2)

Total number of computational intervals over each of which the step size for the numerical integration pertaining to the ash computations is constant.

See the explanation for card 27. If one assumes the same step sizes, i.e.,

a step size of: 0.05 μm from 0.1 to 1.0 μm
0.5 μm from 1.0 to 10.0 μm
5.0 μm from 10.0 to 125.0 μm ,

card 32 will be

03 .

Cards 33 through 35 FORMAT (2F10.2)

The upper limit of the computational interval and the (constant) step size within this interval are contained on each of these cards in a 2F10.2 format for the ash size distribution. Thus, based on the intervals and step sizes chosen above, data cards 33 through 35 will have the following form:

Card Number	Upper limit (1st column)	Step size (11th column)
33	1.0	0.05
34	10.0	0.5
35	125.0	5.0

Card 36 FORMAT (I2)

Total number of points in the size distribution of the attrited sorbent. A typical value may be 6, in which case this card is:

06 .

Cards 37 through 42 FORMAT (2F10.2)

Cards 37 through 42 will contain information on the size distribution of the attrited sorbent. As specified in card 36, there should be a total of six data pairs. Typically, these cards may have the following form:

Card Number	Column 1 (diameter in μm)	Column 11 (cum. less-than function)
37	0.1	0.0001
38	1.0	0.06
39	10.0	0.72
40	20.0	0.97
41	40.0	0.993
42	50.0	0.9999

Card 43 FORMAT (I2)

Total number of points in the size distribution of the attrited ash. A typical value may be six, in which case this card is:

06 .

Cards 44 through 49 FORMAT (2F10.2)

Cards 44 through 49 will contain information on the size distribution of the attrited ash. As specified on the preceding card, there should be a total of six data pairs. Typically, these cards may have the following form:

Card Number	Column 1 (diameter in μm)	Column 11 (cum. less-than function)
44	0.1	0.0001
45	10.0	0.3
46	20.0	0.5
47	40.0	0.77
48	80.0	0.98
49	125.0	0.9999

8. PROGRAM SUBROUTINES

This section of the manual contains a detailed description of all the subroutines in the particle profile program. The subroutines are discussed in the order in which they appear in the main program. The general pattern followed is as follows:

1. The arguments of the subroutine are identified.
2. The function the subroutine performs is explained.
3. The theoretical basis for the equations and computational procedure is explained, where appropriate.
4. A listing of the subroutine is provided.

SUBROUTINE FINDY (P, Y, IERR)

P = Array containing the values of the cumulative less-than function read by the main program.

Y = Array containing the corresponding values of the quantity $\frac{\text{Ln}(D/D_M)}{\sqrt{2}\ \text{Ln}(\sigma)}$,

where

D = particle diameter

D_M = mass mean diameter

σ = standard deviation.

IERR = Parameter to communicate a possible numerical problem in FINDY.

The subroutine FINDY is called a number of times by the main program as also by some of the other subroutines. It accepts a value P for the cumulative less-than function and returns a value for the quantity $Y = \frac{\text{Ln}(D/D_M)}{\sqrt{2}\ \text{Ln}(\sigma)}$.

FINDY is always used in conjunction with another subroutine SOLVEM to evaluate the mass median diameter and the standard deviation between points. The explanation follows:

For log-normally distributed dusts

$$P = \frac{1}{2}\ 1\left\{+\ \text{erf}\left[\frac{\text{Ln}(D/D_m)}{\sqrt{2}\ \text{Ln}\ (\sigma)}\right]\right\} \tag{B4}$$

$$Y = \frac{\text{Ln}(D/D_m)}{\sqrt{2}\ \text{Ln}\ (\sigma)}\ . \tag{B5}$$

Then, from (B4) and (B5),

$$P = \frac{1}{2}\left[1 + \text{erf}(Y)\right]\ . \tag{B6}$$

For any particular P, starting with Y = -5.0 (note that erf(-5) = -1) and incrementing Y by 0.1 for every pass, FINDY calculates the quantity 2P-1-erf(Y). It stores successive values of this quantity in variables A and B and checks for the condition.

Is $$|(A+B)| < |A| + |B| \quad ?$$

When this condition is met, we are clearly near Y, since the quantity 2P-1-erf(Y) has undergone a sign change.

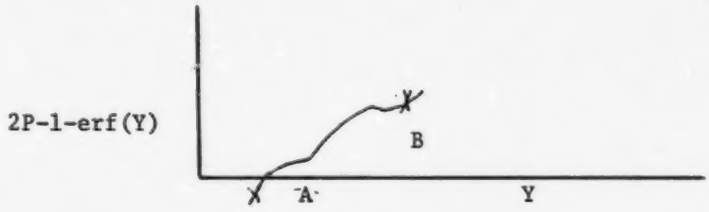

FINDY next applies Newton's method to converge to an accurate Y:

$$Y_{n+1} = Y_n - \frac{f(Y)}{f'(Y)} \qquad \text{(B7)}$$

$$f(Y) = 2P\text{-}1\text{-}erf(Y) \qquad \text{(B8)}$$

$$f'(Y) = \frac{-2}{\sqrt{\pi}} e^{-Y2} \quad . \qquad \text{(B9)}$$

In other words, the next guess for Y is:

$$Y_{n+1} = Y_n + \frac{2P\text{-}1\text{-}erf(Y_n)}{1.1287 \exp(-Y_n^2)} \quad .$$

SUBROUTINE SOLVEM (Y, D, DM, S)

Y = Array containing the values of the quantity $\frac{\text{Ln}(D/Dm)}{\sqrt{\pi}\text{Ln}(\sigma)}$ returned by the subroutine FINDY

D = Array of particle diameters

DM = Array containing the values of the mass median diameter between pairs of particle diameters

S = Array containing the values of the standard deviation between pairs of particle diameters.

The subroutine SOLVEM is called a number of times by the main program as also by some of the other subroutines. It is called always and immediately after the subroutine FINDY has been called. SOLVEM uses pairs of values from the Y and D arrays and solves for the standard deviation S and the mass median diameter DM between these pairs by using the following equations:

$$\text{Ln}(S) = \frac{\text{Ln}\ (D1/D2)}{\sqrt{2}\ (Y_1 - Y_2)} \qquad \text{(B10)}$$

$$\text{Ln}(DM) = \text{Ln}D_1 - Y_2\ \sqrt{2}\ \text{Ln}S \quad . \qquad \text{(B11)}$$

```
 FILE PARTICLE*PROFILE            **** SOLVEM ****

PARTICLE*PROFILE(1).SOLVEM
     1              SUBROUTINE SOLVEM(Y,D,DM,S)
     2              IMPLICIT DOUBLE PRECISION(A-H,O-Z)
     3              DIMENSION Y(50),S(50),DM(50),D(50)
     4              COMMON/B1/NPT,NPTM,ROTWO,ROTWPI
     5              CONST = 1.414213562
     6              DO 10  I=1,NPTM
     7              S(I) = DEXP(DLOG(D(I)/D(I+1))/(CONST*(Y(I) - Y(I+1))))
     8              DM(I) = DEXP(DLOG(D(I))- Y(I)*CONST*DLOG(S(I)))
     9          10 CONTINUE
    10              RETURN
    11              END
```

Reproduced from best available copy.

SUBROUTINE SIZE [X(I), D, DM, S, PO(I)]

X(I) = Particle diameter

D = Array of particle diameters

DM = Array of mass median diameters

S = Array of standard deviations

PO(I) = Value of the population density function

Subroutine SIZE is called a number of times by the main program as also by some of the other subroutines. SIZE places the incoming value of the particle diameter X(I) in the appropriate size interval of the particle diameter array D and evaluates the population density function using equation (B12) below:

$$PO(I) = \frac{1}{D\sqrt{2\pi}\ \mathrm{Ln}S} \exp\left[-\frac{\mathrm{Ln}(D/Dm)}{\sqrt{2}\ \mathrm{Ln}(\sigma)}\right]. \qquad \text{(B12)}$$

Note that for log-normal distributions the cumulative less-than function p is given by:

$$p = \frac{1}{2}\left\{1 + \mathrm{erf}\ \frac{\mathrm{Ln}(D/Dm)}{2\ \mathrm{Ln}(\sigma)}\right\}. \qquad \text{(B13)}$$

The population density function as given by equation (B12) is the derivative $\frac{dp}{dD}$ of the cumulative less-than function given by equation (B13).

```
 FILE PARTICLE*PROFILE              **** SIZE ****

PARTICLE*PROFILE(1).SIZE
     1              SUBROUTINE SIZE(EX,D,DM,S,VAL)
     2              IMPLICIT DOUBLE PRECISION(A-H,O-Z)
     3              DIMENSION D(50),DM(50),S(50)
     4              COMMON/B1/NPT,NPTM,ROTWO,ROTWPI
     5              DO 10  I=1,NPTM
     6              IF(EX - D(I+1)  .LE.  0.0) GO TO 20
     7         10   CONTINUE
     8         20   CONTINUE
     9              A = DLOG(S(I))
    10              CON = (DLOG(EX/DM(I))/(ROTWO*A))**2
    11              VAL = DEXP(-CON)/(EX*ROTWPI*A)
    12              RETURN
    13              END
```

Reproduced from best available copy.

SUBROUTINE PENECY (X(I), N, PE(I))

X(I) = Particle diameter

N = Species number, e.g., for the sorbent N = 1, for the ash N = 2

PE(I) = Penetration (1-efficiency) of a particle of size X(I) through the recycle cyclone

The parameters lMODE AND IRECYC are input to PENECY via a common block with the main program. lMODE specifies the mode of operation; lMODE equal to one (1) indicates a recycle mode of operation, while any other value for lMODE signifies a nonrecycle mode. IRECYC specifies the type of recycle cyclone. If a recycle cyclone is desired, PENECY calls the subroutine DEVICE. Based on the device number (IRECYC) and the species number (N), DEVICE returns a value of the penetration corresponding to a size X(I). See the explanation for DEVICE for more details.

```
 FILE PARTICLE*PROFILE              **** PENECY ****

PARTICLE*PROFILE(1).PENECY
     1              SUBROUTINE PENECY(PS,N,PEN)
     2              IMPLICIT DOUBLE PRECISION(A-H,O-Z)
     3              COMMON/B42/IMODE,IRECYC
     4              IF(IMODE.EQ.1) GO TO 10
     5              PEN=1.
     6              RETURN
     7        10    CALL DEVICE(PS,IRECYC,1,N,PEN)
     8              RETURN
     9              END
```

SUBROUTINE ELUTK (DP, ISPEC, EK, FRACT)

DP = Particle diameter
ISPEC = Species number, e.g. ISPEC=1 for sorbent, ISPEC=2 for ash
EK = Elutriation constant
FRACT = Fraction of sorbent in the bed

The subroutine ELUTK is called by the main program; it returns a value for the elutriation rate constant EK. The information containing the gas and solid properties and the choice of the elutriation correlation desired is input to ELUTK via a COMMON block with the main program. Currently ELUTK offers a choice of four empirical or semiempirical elutriation correlations from the published literature, namely, Yagi and Aochi, Wen and Hashinger, Tanaka and Shinshara, and Merrick and Highley. Since most of the correlations contain a terminal velocity term(s), ELUTK calls the subroutine UTERM for this information. The minimum fluidizing velocity required for using the Merrick and Highley correlation is calculated internally within ELUTK.

If the two-species particle profile program is being used, ELUTK multiplies the calculated value of the elutriation rate constant EK by the appropriate mass fraction for the species of interest.

SUBROUTINE UTERM (WTMOL, GASTMP, D, RHOG, RHOS, SMU, SPH, UT)

WTMOL = Molecular weight of the fluidizing gas
GASTMP = Gas temperature
D = Particle diameter
RHOG = Gas density
RHOS = Solid density
SMU = Gas viscosity
SPH = Sphericity of solids
UT = Particle terminal setting velocity.

The subroutine UTERM is called by the subroutine ELUTK. UTERM accepts values for the gas and solid properties, and for a particle of a given size it returns the terminal settling velocity.

UTERM contains a set of equations for the particle Reynolds number at terminal setting Re_t as a function of the Galileo number Ga. These equations obtained by curve fitting Log (Re) versus Log ($C_D Re^2$) data for spherical particles from the literature[B3,B4] are :

$$Ga = \frac{4}{3} g \frac{(RHOS-RHOG)(RHOG)(D^3)}{(SMU)^2} \quad (B14)$$

$$Re_t = \frac{(D)(UT)(RHOG)}{SMU} \quad (B15)$$

$2.438 < Ga < 76.913$, $Re_t = 0.04483(Ga)^{0.9375}$

$76.913 < Ga < 1496.236$, $Re_t = 0.08991(Ga)^{0.7738}$ (B16)

$1496.236 < Ga < 10939.564$, $Re_t = 0.15812(Ga)^{0.6943}$

$Ga < 2.438$, $Re_t < 0.1$ is the Stokes' Law range given by

$$Re_t = \frac{Ga}{24} \quad . \quad (B17)$$

UTERM first calculates the Galileo number Ga from equation (B14) and then the particle Reynolds number at terminal settling from equations (B16)

and (B17) as appropriate. For particles in the Stokes' Law range less than 8 μm in size, the Cunningham correction is applied. UTERM then uses equation (B15) to back out the terminal settling velocity UT. This correction for sphericity is made as follows:

$$UT = UT\ (0.843)\ \text{Log}\ \left(\frac{SPH}{0.065}\right) . \qquad \text{(B18)}$$

For Ga > 707945.784, UTERM evaluates the terminal velocity directly using equation (B19) below:

$$UT = \left\{\frac{4}{3}\ \frac{(D)(RHOS-RHOG)(981)}{(CR)(RHOG)}\right\}^{\frac{1}{2}} , \qquad \text{(B19)}$$

where

$$CR = 5.31 - (4.88XSPH) . \qquad \text{(B20)}$$

```
FILE PARTICLE*PROFILE          **** UTERM ****

PARTICLE*PROFILE(1).UTERM
      1               SUBROUTINE UTERM(WTMOL,GASTMP,D,RHOG,RHOS,SMU,SPH,UT)
      2               IMPLICIT DOUBLE PRECISION (A-H,O-Z)
      3               DRHO=RHOS-RHOG
      4               EK1=0.843*DLOG10(SPH/0.065)
      5               GA=(4./3.)*(980.*DRHO*RHOG)*(D**3.)/(SMU**2.)
      6               ALFA=(SMU)/(RHOG*D)
      7               IF(SPH.EQ.1.) GO TO 10
      8               IF(SPH.EQ..6) GO TO 20
      9               IF(SPH.EQ..125) GO TO 30
     10               IF(SPH.LT.1..AND.SPH.GT..6) GO TO 40
     11               IF(SPH.LT..6.AND.SPH.GT..125) GO TO 50
     12        10     IF(GA.LT.2.438) GO TO 101
     13               IF(GA.LT.76.913) GO TO 102
     14               IF(GA.LT.1496.236) GO TO 103
     15               IF(GA.LT.10939.564) GO TO 104
     16               IF(GA.LT.707945.784) GO TO 105
     17               REP=1.81104*(GA**0.4898)
     18               GO TO 106
     19        101    REP=GA/24.
     20               GO TO 106
     21        102    REP=0.04483*(GA**0.9375)
     22               GO TO 106
     23        103    REP=0.08991*(GA**0.7738)
     24               GO TO 106
     25        104    REP=0.15812*(GA**0.6943)
     26               GO TO 106
     27        105    REP=0.3634*(GA**0.6076)
     28        106    CONTINUE
     29               IF(SPH.LT.1.) GO TO 401
     30               UT=REP*ALFA
     31               RETURN
     32        20     IF(GA.LT.5.7) GO TO 201
     33               IF(GA.LT.100.) GO TO 202
     34               IF(GA.LT.1000.) GO TO 203
     35               IF(GA.LT.10000.) GO TO 204
     36               IF(GA.LT.60000.) GO TO 205
     37               IF(GA.LT.100000000.) GO TO 206
     38               REP=0.9968*(GA**0.46825)
     39               GO TO 207
     40        201    REP=GA/24.
     41               REP=REP*EK1
     42        202    REP=0.02156*(GA**0.8817)
     43               GO TO 207
     44        203    REP=0.01305*(GA**0.8062)
     45               GO TO 207
     46        204    REP=0.07767*(GA**0.6709)
     47               GO TO 207
     48        205    REP=0.2423*(GA**0.5474)
     49               GO TO 207
     50        206    REP=0.22588*(GA**0.553795)
     51        207    CONTINUE
     52               IF(SPH.GT..6.AND.SPH.LT.1.) GO TO 402
     53               IF(SPH.LT..6.AND.SPH.GT..125) GO TO 501
     54               UT=REP*ALFA
     55               RETURN
     56        30     IF(GA.LT.7.1) GO TO 301
     57               IF(GA.LT.100.) GO TO 302
     58               IF(GA.LT.1000.) GO TO 303
     59               IF(GA.LT.10000.) GO TO 304
     60               IF(GA.LT.100000.) GO TO 305
     61               IF(GA.LT.20003000.) GO TO 306
     62               REP=0.3934*(GA**0.4664)
     63               GO TO 307
     64        301    REP=GA/24.
     65               REP=REP*EK1
     66               GO TO 307
     67        302    REP=0.92048*(GA**0.809076)
     68               GO TO 307
     69        303    REP=0.03033*(GA**0.72379)
     70               GO TO 307
     71        304    REP=0.051258*(GA**0.64762)
     72               GO TO 307
     73        305    REP=0.13328*(GA**0.54407)
     74               GO TO 307
     75        306    REP=0.21655*(GA**0.5019)
     76               GO TO 307
     77        307    CONTINUE
     78               IF(SPH.GT..125) GO TO 502
     79               UT=ALFA*REP
     80               RETURN
     81        40     CONTINUE
     82               GO TO 10
     83        401    CONTINUE
     84               REP1=REP
     85               GO TO 20
     86        402    CONTINUE
     87               REP2=REP
     88               REP=REP2+((REP1-REP2)*((SPH-0.6)/0.4))
     89               UT=REP*ALFA
     90               RETURN
     91        50     CONTINUE
     92               GO TO 20
     93        501    CONTINUE
     94               REP1=REP
     95               GO TO 30
     96        502    CONTINUE
     97               REP2=REP
     98               REP=REP2+((REP1-REP2)*((SPH-0.125)/0.475))
     99               UT=ALFA*REP
    100               RETURN
    101               END
```

Reproduced from best available copy.

SUBROUTINE ATRATE (X(I), N, A(I))

X(I) = Particle diameter

N = Species number, e.g., N=1 for sorbent and N=2 for ash

A(I) = Attrition rate calculated by ATRATE

The subroutine ATRATE calculates the shrinkage rate of a given sized particle. The rate of attrition can be described by an expression of the form:

$$\frac{dD}{dt} = C(D-D_{min}) \quad , \tag{B21}$$

where

t = time

D_{min} = some minimum diameter

t = a rate constant for each species.

The values of C and D_{min} for each species are available to ATRATE via a common block with the main program. Since the main program requires the attrition term in the form $\frac{1}{D}\left(\frac{dD}{dt}\right)$, the value returned by A[I] is given by:

$$A(I) = \frac{C(D-D_{min})}{D} \quad . \tag{B22}$$

```
 FILE PARTICLE*PROFILE              **** ATRATE ****

PARTICLE*PROFILE(1).ATRATE
     1              SUBROUTINE ATRATE(D,I,A)
     2              IMPLICIT DOUBLE PRECISION(A-H,O-Z)
     3              COMMON/SUBATR/ C1(2),DL(2)
     4              A=C1(I)*(D-DL(I))/D
     5              RETURN
     6              END

$CPU
DIFF=1.109 SEC =.001(CPU)+.604(CCER)+.504(IO) .. AVG SIZE=10804

$nDG,P  FILE PARTICLE*PROFILE              **** CLEAN ****

$PRI,S  SF$.CLEAN/
FORPUR 28R1 U1 E35 S74T11 02/19/81 14:41:38
```

Reproduced from best available copy.

SUBROUTINE ZOFIND (X(I), D, DM, S, CUMO(I))

X(I) = Particle diameter

D = Array of particle diameters

DM = Array containing values of the mass median diameter

S = Array containing values of the standard deviation

CUMO(I) = Value calculated by ZOFIND for the cumulative less-than function

The subroutine ZOFIND places the incoming value of the particle diameter X(I) into the appropriate interval of the particle diameter array D and uses the available values of the mass median diameters DM(I) and the standard deviation S(I) for this interval to evaluate the value of the cumulative less-than function from the following equation which applies to a log-normal distribution:

$$CUMO(I) = \frac{1}{2}\left\{1 + \text{erf}\left[\frac{\text{Ln}\ (D/D_m)}{2\ \text{Ln}(\sigma)}\right]\right\} \quad . \qquad \text{(B23)}$$

```
 FILE PARTICLE*PROFILE              **** ZOFIND ****

PARTICLE*PROFILE(1).ZOFIND
      1              SUBROUTINE ZOFIND(EX,D,DM,S,Z)
      2              IMPLICIT DOUBLE PRECISION(A-H,O-Z)
      3              DIMENSION D(50),DM(50),S(50)
      4              COMMON/B1/NPT,NPTM,ROTWO,ROTWPI
      5              DO 10  I=1,NPTM
      6              IF(EX - D(I+1)  .LE.  0.0) GO TO 20
      7           10 CONTINUE
      8           20 CONTINUE
      9              A = DLOG(EX/DM(I)) /(ROTWO*DLOG(S(I)))
     10              Z = .5*(1. + DERF(A))
     11              RETURN
     12              END
```

SUBROUTINE ATIN (DA, DMA, SA, KA)

DA = Array of (attrited) particle diameters read in by ATIN

DMA = Array containing the values of the mass median diameters between successive points of the array DA

SA = Array containing the values of the standard deviation between successive points of the array DA

KA = Total number of particle diameters in the array DA

The subroutine ATIN reads in the size distribution of the attrited material. The total number of points read in is KA. DA(I) and PA(I) refer to the particle diameter and cumulative less-than value, respectively, of the distribution read in.

ATIN takes in these data points in pairs and, by calling subroutines FINDY and SOLVEM, evaluates the mass median diameter and the standard deviation for a log-normal form between these pairs.

```
 FILE PARTICLE*PROFILE                **** ATIN ****

PARTICLE*PROFILE(1).ATIN
     1              SUBROUTINE ATIN(DA,DMA,SA,KA)
     2              IMPLICIT DOUBLE PRECISION(A-H,O-Z)
     3              DIMENSION DMA(100),SA(100),DA(100),PA(100),Y(100)
     4              COMMON/B1/NPT,NPTM,ROTWO,ROTWPI
     5              READ(5,1000) NPT
     6         1000 FORMAT(I2)
     7              KA = NPT
     8              NPTM = NPT - 1
     9              DO 10  I=1,NPT
    10              READ(5,2000) DA(I),PA(I)
    11         2000 FORMAT(2F10.2)
    12           10 CONTINUE
    13              CALL FINDY(PA,Y,IERR)
    14              CALL SOLVEM(Y,DA,DMA,SA)
    15              RETURN
    16              END
```

SUBROUTINE A2P2 (X, CUM2, DM, S, D, K1)

X = Array of particle diameters created by the main program

CUM2 = Array containing values of the cumulative greater-than function for the size distribution of the carry-over solids corresponding to the diameters in the X array

DM = Array containing values of the mass median diameters for the carry-over solids

S = Array containing the values of the standard deviation for the carry-over solids

D = Array of particle diameters created by subroutine A2p2

K1 = Total number of elements in the D array

The subroutine A2P2 scans the contents of the incoming X and CUM2 arrays and does the following:

- The X array is condensed, e.g., if the X-array initially has the form 0.1, 0.105, 0.110, 0.115..., it is condensed to the form 0.1, 0.2, 0.3, ... The condensed array so created is stored in an array D.
- The values of the cumulative greater-than function that constitutes the elements of CUM2 are converted to a cumulative less-than form. The values of the cumulative less-than function that correspond to the elements of the D array are stored in an array labeled P.
- The subroutines FINDY and SOLVEM are called to create the mass median diameter array DM and the standard deviation array S for pairs of points taken from D and P. Thus, corresponding to the pair of points [D(1), P(1)] and [D(2), P(2)] will be a mass median diameter DM(1) and a standard deviation S(1).

SUBROUTINE ADDF2A (DA, DMA, SA, D, DM, S, A_2, F_2, K_1, KA)

DA = Array created by subroutine ATIN that contains the diameters of the attrited solids

DMA = Array containing the values of the mass median diameter for pairs of particle diameters from the DA array; DMA is also created by subroutine ATIN

SA = Array containing the values of the standard deviation for pairs of particle diameters from the DA array; SA is created by the subroutine ATIN

D, DM, S = These three arrays are created by the subroutine A2P2, and they contain the diameters, mass median diameter values, and the standard deviation values pertaining to the size distribution of the carry-over solids.

A2 = Mass flow rate of attrited material

F2 = Mass flow rate of solids in carry-over

K1 = Number of elements in array D above

KA = Number of elements in array DA above

The subroutine ADDF2A adds the size distribution assumed for the attrited solids (and read in through subroutine ATIN) to the calculated size distribution of the elutriated solids to obtain the total distribution of the carry-over material. The following equation is used:

$$p_c = \int_{D_{min}}^{D_{max}} \frac{A_2 p_A(dp) + F_2 p_2(dp)}{A_2 + F_2} \, ddp \qquad \text{(B24)}$$

$$A_T = A_2 + F_2 \quad , \qquad \text{(B25)}$$

where

A_2 = Mass flow rate of attrited material

p_A = Population density function of attrited material

p_2 = Population density function of elutriated material

F_2 = Mass flow of elutriated material

p_c = Population density function of the combined attrited and elutriated material

A_T = Total (attrited & elutriated) mass flow rate of carry-over.

The subroutine SIZE is called twice, to obtain the p_2 and p_A arrays required in equation (B24).

FILE PARTICLE*PROFILE **** ADDF2A ****

PARTICLE*PROFILE(1).ADDF2A

```
      1              SUBROUTINE ADDF2A(DA,DMA,SA,D,DM,S,A2,F2,K1,KA)
      2              IMPLICIT DOUBLE PRECISION(A-H,O-Z)
      3              DIMENSION DA(100),DMA(100),SA(100),D(100),DM(100),S(100)
      4              DIMENSION Y(100),X(100), T(4),WT(4),SUM(100)
      5              COMMON/B1/NPT,NPTM,ROTWO,ROTWPI
      6              DATA(T(J),J=1,4)/-.8611363100,-.3399810400,.3399810400,.8611363100
      7             +/
      8              DATA(WT(J),J=1,4)/.3478548500,.6521451500,.6521451500,.3478548500/
      9              IF(DA(1) - D(1)) 10,10,20
     10           10 X(1) = DA(1)
     11              GO TO 30
     12           20 X(1) = D(1)
     13           30 CONTINUE
     14              SS = .01
     15              IF(X(1)  .LE.  .09999) GO TO 40
     16              SS = .1
     17              IF(X(1)  .LE.  .9999) GO TO 40
     18              SS = 1.0
     19              IF(X(1)  .LE.  9.999) GO TO 40
     20              SS = 10.0
     21           40 CONTINUE
     22              UL = 10.*SS
     23              UUL = .999*UL
     24              IPRINT = 1
     25              FA2 = A2/(A2 + F2)
     26              IF(DA(KA) - D(K1))50,50,60
     27           50 CONTINUE
     28              TOP = D(K1)
     29              GO TO 70
     30           60 CONTINUE
     31              TOP = DA(KA)
     32           70 CONTINUE
     33              TIP = .999*TOP
     34              M = 1
     35              SUM(1) = .000001
     36              A = X(1)
     37              DO 110  JJ=1,10
     38              DO 90  I=1,100
     39              ADD = 0.0
     40              M = M + 1
     41              B = A + SS
     42              IF(B  .GE.  UUL)  B = UL
     43              IF(B  .GE.  TIP) B = TOP
     44              X(M) = B
     45              PRE = (B - A)/2.
     46              DO 80  J=1,4
     47              EX = ((B-A)*T(J) + A + B)/2.
     48              PA = 0.0
     49              IF(EX  .GT.  DA(KA)) GO TO 75
     50              IF(EX  .LT.  DA(1)) GO TO 75
     51              CALL SIZE(EX,DA,DMA,SA,PA)
     52           75 CONTINUE
     53              P = 0.0
     54              IF(EX  .LT.  D(1)) GO TO 76
     55              CALL SIZE(EX,D,DM,S,P)
     56           76 CONTINUE
     57              ADD = ADD + WT(J)*PRE*(FA2*PA + (1.- FA2)*P)
     58           77 CONTINUE
     59           80 CONTINUE
     60              SUM(M) = ADD
     61              A = B
     62              IF(B  .GE.  UL) GO TO 100
     63              IF(B  .GE.  TIP) GO TO 120
     64           90 CONTINUE
     65          100 CONTINUE
     66              SS = 10.*SS
     67              UL = 10.*UL
     68              UUL = .999*UL
     69          110 CONTINUE
     70          120 CONTINUE
     71              MM = M - 1
     72              DO 130  I=1,MM
     73              SUM(I+1) = SUM(I) + SUM(I+1)
     74          130 CONTINUE
     75              NPT = M
     76              NPTM = M - 1
     77              CALL FINDY(SUM,Y,IERR)
     78              CALL SOLVEM(Y,X,DM,S)
     79              DO 150  I=1,M
     80          150 D(I) = X(I)
     81              K1 = M
     82              RETURN
     83              END
```

SUBROUTINE CLEAN (D, DM, S, WT, T, A2, F2, NP)

D = Array of particle diameters

DM = Array containing values of the mass median diameter to characterize the log-normal segment between pairs of points from the array above

S = Array containing values of the standard deviation to characterize the log-normal segment between pairs of points from the D array above

WT = Array containing values of the weights required for performing a Gaussian quadrature-type numerical integration

T = Array containing the T values required for performing a Gaussian quadrature-type numerical integration

A2 = Mass flow rate of the attrited solids

F2 = Mass flow rate of the elutriated solids

NP = Total number of elements of the D array.

The subroutine CLEAN allows the study of the effect of various particulate control devices on the solids loading and particle size distribution of the material escaping the recycle cyclone. CLEAN calls the subroutine DEVICE to obtain the device penetration values over the spectrum of particle diameters for all the devices specified by the user for the particle removal train. It then uses this information to compute the loading and distribution escaping each device. The equations for this computation are discussed below.

Let η_i be the grade efficiency corresponding to a particle size of dp_i for any given particulate removal device. Then, the cumulative size distribution of the solids escaping this device is given by:

$$Z_i(D) = \int_{D_{min}}^{D_{max}} p_c(D)(1-\eta_i)dD \qquad \text{(B26)}$$

where $p_c(D)$ is the population density function of the solids entering the device, i.e., escaping the recycle cyclone.

Equation (B26) may also be expressed as

$$Z_i(D) = \int_{D_{min}}^{D_{max}} p_c(D) p_1 dD \quad , \tag{B27}$$

where $p_1 = (1-\eta_i)$ is the device penetration.

In general, for a train of N particle removal devices,

$$Z_i(D) = \int_{D_{min}}^{D_{max}} p_c(D) p_1 p_2 \; p_N \; dD \quad , \tag{B28}$$

where

Zi(D) = Cumulative less-than function

$P_i = (1-\eta_i)$ = Penetration of the i^{th} device

$P_c(D)$ = Population density function of the solids entering the first device of the cleanup train.

CLEAN uses a four-point Gaussian quadrature to perform the integration indicated in equation (B28).

SUBROUTINE DEVICE (EX, IDEV, NDEV, ISPEC, PEN)

EX = Particle diameter

IDEV = Device number that ranges from one to seven, e.g., for a Ducon full-size cyclone IDEV=1, etc.

NDEV = Total number of devices used in the cleanup train excluding the recycle cyclone

PEN = Device penetration

The subroutine DEVICE that is called by subroutine CLEAN calculates the fractional penetration of particles of a given size and species (i.e., sorbent or ash) through a specified device. DEVICE currently contains performance data on seven particle removal devices. These data are in the form of size-versus-penetration values with the species (i.e., ash or sorbent) as parameter.

The data are stored in the arrays D(I, J, K) and P[I, J, K], where the J refers to the species number and the K to the device number; I is the data point number. The incoming particle diameter is placed in the appropriate interval of the size-penetration data for the required species and device. The device penetration is assumed to have the form:

$$P = Ae^{BX} \quad , \tag{B29}$$

where

P = Device penetration

X = Particle size

A,B = Device constants.

For any given particle diameter X, $X_1 \leq X \leq X_2$, the constants A and B are given by

$$B = \frac{\mathrm{Ln}(P_1/P_2)}{X_1 - X_2} \tag{B30}$$

$$A = P_1 \exp(-BX_1) \quad . \tag{B31}$$

```
FILE PARTICLE*PROFILE          **** DEVICE ****
PARTICLE*PROFILE(1).DEVICE
      1             SUBROUTINE DEVICE(EX,IDEV,NDEV,ISPEC,PEN)
      2             IMPLICIT DOUBLE PRECISION(A-H,O-Z)
      3             DIMENSION P(15,3,10),D(15,3,10),IDEV(10),IP(10),PEN(3)
      4             J = ISPEC
      5             DATA (IP(I),I=1,10)/7,10,8,8,10,9,9,11,7,8/
      6       CCCC  DUCON FULL SIZE CYCLONE AT 1600 DCS FAN
      7             DATA((P(I,J,1),I=1,7)/.10-3,.10-2,.80-2,.640-1,.19500,.4500,1.00/
      8             DATA((P(I,J,1),I=1,7)/.10-3,.10-2,.80-2,.640-1,.19500,.4500,1.00/
      9             DATA((P(I,J,1),I=1,7)/.10-3,.10-2,.80-2,.640-1,.19500,.4500,1.00/
     10             DATA((D(I,J,1),I=1,7)/26.00,25.00,22.00,9.00,4.200,2.00,1.00/
     11             DATA  ((D(I,J,2),I=1,7)/55.00,53.00,47.00,19.100,8.900,4.200,2.100/
     12       CCCC  COLD STOE ELECTROSTATIC PRECIPITATOR
     13             DATA((P(I,J,2),I=1,10)/.10-4,.150-2,.50-2,.30-2,.10-1,.50-1,.80-1,.
     14            +100,.30-1,.20-2/
     15             DATA((P(I,J,2),I=1,10)/.10-4,.150-2,.50-2,.30-2,.10-1,.50-1,.80-1,.
     16            +100,.30-1,.20-2/
     17             DATA((P(I,J,2),I=1,10)/.10-4,.150-2,.50-2,.30-2,.10-1,.50-1,.80-1,.
     18            +100,.30-1,.20-2/
     19             DATA((D(I,J,2),I=1,10)/15.00,10.00,7.00,5.00,2.00,1.00,.500,
     20            *.300,.100,.0500/
     21             DATA((D(I,J,2),I=1,10)/15.00,10.00,7.00,5.00,2.00,1.00,.500,
     22            *.300,.100,.0500/
     23             DATA((D(I,J,2),I=1,10)/15.00,10.00,7.00,5.00,2.00,1.00,.500,
     24            *.300,.100,.0500/
     25       CCCCC WESTINGHOUSE BENCH SCALE GRANULAR BED FILTER
     26             DATA((P(I,J,3),I=1,8)/.10-3,.150-2 ,.520-2,.210-1,.30-1,.350-1,.40-
     27            +1,.45C-1/
     28             DATA((P(I,J,3),I=1,8)/.10-3,.150-2 ,.520-2,.210-1,.30-1,.350-1,.40-
     29            +1,.45C-1/
     30             DATA((P(I,J,3),I=1,8)/.10-3,.150-2 ,.520-2,.210-1,.30-1,.350-1,.40-
     31            +1,.45C-1/
     32             DATA((D(I,J,3),I=1,8)/10.00,7.00,5.00,2.00,1.00,.200,.100,.0500/
     33             DATA((D(I,J,3),I=1,8)/10.00,7.00,5.00,2.00,1.00,.200,.100,.0500/
     34             DATA((D(I,J,3),I=1,8)/10.00,7.00,5.00,2.00,1.00,.200,.100,.0500/
     35       CCCCC SUNBURY FABRIC FILTER DATA
     36             DATA((P(I,J,4),I=1,8)/.10-3,.10-2,.20-2,.10-2,.20-2,.01100,.30-2,.1
     37            +D-3/
     38             DATA((P(I,J,4),I=1,8)/.10-3,.10-2,.20-2,.10-2,.20-2,.01100,.30-2,.1
     39            +D-3/
     40             DATA((P(I,J,4),I=1,8)/.10-3,.10-2,.20-2,.10-2,.20-2,.01100,.30-2,.1
     41            +D-3/
     42             DATA((D(I,J,4),I=1,8)/20.00,15.00,10.00,4.00,1.00,.500,.100,.0500/
     43             DATA((D(I,J,4),I=1,8)/20.00,15.00,10.00,4.00,1.00,.500,.100,.0500/
     44             DATA((D(I,J,4),I=1,8)/20.00,15.00,10.00,4.00,1.00,.500,.100,.0500/
     45       CCCCC DUCON PRIMARY CYCLONE CITY #48-#2A
     46             DATA((P(I,J,5),I=1,10)/.10-3,.10-2,.60-2,.350-1,.100,.1300,.2100,.3
     47            1800,.7400,1.55/
     48             DATA((D(I,J,5),I=1,10)/7.201,6.01,4.01,2.01,10.00,8.00,6.00,4.500,3
     49            1.00,1.800/
     50             DATA((D(I,J,5),I=1,10)/115.00,10.01,80.00,50.00,30.00,20.00,15.00,
     51            +8.00,6.00,4.600/
     52             DATA((P(I,J,5),I=1,10)/.10-2,.40-2,.120-1,.320-1,.70-1,.1200,.1800,
     53            +5800,.6800,1.00/
     54       CCCCC PSRI (UNCORRECTED FOR LOADING)
     55             DATA((P(I,J,6),I=1,9)/.10-2,.60-2,.40-1,.840-1,.1700,.3300,.4800,.6
     56            1800,1.00/
     57             DATA((D(I,J,6),I=1,9)/150.00,120.00,90.00,70.00,40.00,20.00,15.00,1
     58            10.00,6.00/
     59             DATA((D(I,J,6),I=1,9)/.10-2,.70-1,.100,.1500,.1800,.3300,.5700,
     60            +.830C,1.62/
     61             DATA((D(I,J,6),I=1,9)/175.00,130.00,120.00,90.00,70.00,40.00,20.00,
     62            +10.00,4.600/
     63       CCCCC FAN JET
     64             DATA (P(I,J,7),I=1,6)/.000100,.0700,.3300,.7300,.98700,.9999000/
     65             DATA((P(I,J,7),I=1,6)/7.00,5.00,3.00,2.00,1.500,1.2500/
     66             DATA (P(I,J,7),I=1,6)/.000100,.0700,.3300,.7300,.98700,.9999000/
     67             DATA (P(I,J,7),I=1,6)/15.100,9.900,6.400,4.100,2.700,2.200/
     68             DATA((P(I,J,7),I=1,6)/.000100,.0700,.3300,.7300,.98700,.9999000/
     69       CCCCC RECYCLE CYCLONE FROM KUNNI AND LEVENSPILL EXAMPLE
     70             DATA(P(I,J,8),I=1,11)/0.0604400,.001500,.002800,.005500,.009600,.0
     71            1600,.02000,.0360,.06200,.0800,.300/
     72             DATA((D(I,J,8),I=1,11)/60.00,50.00,45.00,40.00,36.00,32.00,28.00,26
     73            +.00,24.00,20.00,10.00/
     74             DATA(P(I,J,8),I=1,11)/0.0004400,.001500,.002800,.005500,.009600,.0
     75            1600,.02000,.0360,.06200,.0800,.300/
     76             DATA((D(I,J,8),I=1,11)/60.00,50.00,45.00,40.00,36.00,32.00,28.00,26
     77            +.00,24.00,20.00,10.00/
     78       CCCCC DUCON FULL SIZE CYCLONE WITH SAME PERFORMANCE FOR ASH & SOOBENT
     79             DATA((P(I,J,9),I=1,7)/.10-3,.10-2,.80-2,.640-1,.19500,.4500,1.00/
     80             DATA (P(I,J,9),I=1,7)/.10-3,.10-2,.80-2,.640-1,.19500,.4500,1.00/
     81             DATA((D(I,J,9),I=1,7)/26.00,25.00,22.00,9.00,4.200,2.00,1.00/
     82             DATA((D(I,J,9),I=1,7)/26.00,25.00,22.00,9.00,4.200,2.00,1.00/
     83       CCCCC EXXON SIX INCH MEASURED PERFORMANCE
     84             DATA((P(I,J,10),I=1,8)/5.00,4.00,3.00,2.00,1.00,.750C,.500,.340C/
     85             DATA((D(I,J,10),I=1,8)/5.00,4.00,3.00,2.00,1.00,.750C,.500,.340C/
     86             DATA((P(I,J,10),I=1,8)/.10-3,1.0-2,4.0-2,.1300,.3400,.4600,.6600,1.
     87            10C/
     88             DATA(P(I,J,10),I=1,8)/.10-3,1.0-2,4.0-2,.1300,.3400,.4600,.6600,1.
     89            10C/
     90             DO 50 M=1,NDEV
     91             M = IDEV(M)
     92             IMAX = IP(M)
     93             IF(EX  .GT.  D(1,J,M)) GO TO 30
     94             IF(EX  .LT.  D(IMAX,J,M)) GO TO 40
     95             IPM = IMAX - 1
     96             DO 10  I=1,IPM
     97             IF(EX - D(I+1,J,M)  .GE.  0.0) GO TO 20
     98          10 CONTINUE
     99             RETURN
    100          20 CONTINUE
    101             B = DLOG(P(I,J,M)/P(I+1,J,M))/(D(I,J,M) - D(I+1,J,M))
    102             A = P(I,J,M)*DEXP(-B*D(I,J,M))
    103             PEN(M) = A*DEXP(B*EX)
    104             GO TO 50
    105          30 PEN(M) = 0.0
    106             GO TO 50
    107          40 PEN(M) = 1.0
    108          50 CONTINUE
    109             RETURN
    110             END
```

Reproduced from best available copy.

9. REFERENCES

B1. Yagi, S., and T. Aochi, Presented at the Society of Chemical Engineers (Japan), Spring Meeting, 1955.

B2. Wen, C. Y., and R. F. Hashinger, A.I.Ch.E.J., 6: 220; 1960.

B3. Fuchs, N. A., Mechanics of Aerosols, Trans., C. N. Davies, ed. New York: Pergamon; 1964.

B4. Lapple, C. E., Fluid and Particle Mechanics, Newark, DE: University of Delaware; 1956.